

https://dspace.org/

Adding value and confidence in Mineral Resource Estimation through exploratory data analysis: a case study

Cloete, Elsabe Maria

2022
https://hdl.handle.net/10539/34958

Downloaded from a DSpace repository. https://dspace.org/

School of Mining Engineering



UNIVERSITY OF THE
WITWATERSRAND,
JOHANNESBURG

ADDING VALUE AND CONFIDENCE IN MINERAL RESOURCE ESTIMATION THROUGH EXPLORATORY DATA ANALYSIS: A CASE STUDY

Elsabe Maria Cloete

A research report is submitted to the Faculty of Engineering and the Built Environment, University of the Witwatersrand, Johannesburg, in partial fulfilment of the requirements for the degree of Master of Science in Mining Engineering.

2022

DECLARATION

I declare that this project is my own, unaided work. I have read the University Policy on Plagiarism and hereby confirm that no Plagiarism exists in this report. I also confirm that there is no copying nor is there any copyright infringement. I willingly submit to any investigation in this regard by the School of Mining Engineering and I undertake to abide by the decision of any such investigation.



12 September 2022

Signature Date

ABSTRACT

The unexploited Gamsberg East deposit in the Northern Cape Province of South Africa, has been the subject of renewed interest as exploration target. This research study examined the available exploration drill hole data using a variety of data validation and analysis techniques. This was done to gain a sound understanding of the spatial and statistical characteristics of the data, which contributes to the confidence in the Mineral Resource Estimate.

All information in the drill hole database was compiled and summarised into a validated dataset. This dataset was subjected to Exploratory Data Analysis, using a variety of graphical and statistical techniques to describe the distributions of grade within the deposit. An implicit geological model was created in Leapfrog Geo. The final model was used as the basis for variography and Mineral Resource Estimation through Ordinary Kriging.

Exploratory Data Analysis resulted in the identification of the underlying grade probability distributions as CGLN. It was also found that outliers may represent a separate domain. A variety of methods was used in Leapfrog Geo and the outputs compared to produce a valid geological model for the deposit. Indicator Kriging and the refined model approach in Leapfrog Geo were used in an attempt to create subdomains. This did not yield the expected results, with subdomains still showing mixed populations. In the course of this work, the existence of a core and fringe zone was observed when displaying indicator values in 3D. These were modelled and used as domains in the Mineral Resource Estimate.

Variography was conducted for the variable of interest within these domains and variograms showed geometric anisotropy, typical of base metal deposits. Inconclusive results from a Quantitative Kriging Neighbourhood Analysis resulted in the adaption of a kriging plan from a previous study over the deposit in question. The resultant Mineral Resource Estimate had low slope of regression indicating conditional bias. However, histograms and swath plots showed that the Mineral Resource Estimate fairly reproduced grade distributions within domains. Given the findings, it is recommended that simulation be considered to reduce conditional bias. Further work is also necessary to locate missing data and improve the Mineral Resource Estimate through unfolding.

The use of simple statistical and graphical techniques in this study helped the practitioner achieve a thorough understanding of the data and its limitations. This increases the confidence in the final results of such a study.

TABLE OF CONTENT

DECLARATION i
ABSTRACT ii
LIST OF TABLES vi
LIST OF FIGURES vii
LIST OF UNIT SYMBOLS xi
LIST OF ABBREVIATIONS xii
1. INTRODUCTION 1
1.1. Research Background 1
1.2. Research Motivation 2
1.3. Problem Statement 2
1.4. Research Hypothesis 2
1.5. Assumptions 3
1.6. Research Objectives 3
1.7. Research Methodology 3
1.8. Research Study Report Layout 4
2. LITERATURE REVIEW 6
2.1. The Geology of Gamsberg 6
2.2. Exploratory Data Analysis 7
2.3. Geological Modelling 11
2.4. Variography 12
2.5. Ordinary Kriging 13
2.6. Indicator Kriging 14
2.7. Multivariate Estimation 14
2.8. Validation of Resource Models and Estimates 15
2.9. Summary 17
3. FIRST STAGE DATA VALIDATION 18
3.1. Assumptions 18
3.2. Data Compilation and Summary 18
3.2.1. Drill Type and Hole Diameter 19
3.2.2. Assay Method 20

3.2.3. Sample Type 20
3.2.4. Comments 21
3.2.5. Excluded drill holes 21
3.3. Overlaps in interval data 21
3.4. QA-QC and duplicates 23
3.5. Samples without assay 24
3.6. Samples with negative assays 25
3.7. Checking and Validation 25
3.8. Desurveying 25
3.9. Summary and Conclusion 25
4. EXPLORATORY DATA ANALYSIS 27
4.1. Statistically Defining Zones of Interest. 27
4.2. Determining Data Support and Composite length 31
4.3. Comparison of Drill Type 34
4.4. Comparison of Assay Method 35
4.5. Correlations and Bivariate Scatterplots 39
4.6. Analysis of Outliers 42
4.7. Statistics and Histograms for Zn % grade 44
4.8. Models for Distributions 46
4.9. Cumulative Probability Graphs 52
4.10. Summary and Conclusion 55
5. GEOLOGICAL MODELLING 57
5.1. Properties to be modelled 57
5.2. Data Validation 57
5.3. Geological Modelling Methodology 57
5.3.1. Intrusive model (from Base Lithology) 59
5.3.2. Deposit model (from Contacts) 60
5.3.3. Vein Model 61
5.4. Model Validation 63
5.5. Use of Indicator Kriging (IK) to model subdomains 65
5.6. Use of indicators to refine models 72

5.7. Use of grade to define domains. 76
5.8. Summary and Conclusion 80
6. MINERAL RESOURCE ESTIMATION 83
6.1. Selection of variable to be estimated 83
6.2. Variography 84
6.3. Kriging Plan 86
6.3.1. Quantitative Kriging Neighbourhood Analysis (QKNA) 86
6.3.2. Boundaries 88
6.3.3. Grade Capping 89
6.4. Validation 90
6.5. Resource Classification 93
6.6. Grade Tonnage Curves 93
6.7. Summary and Conclusion 95
7. OVERVIEW AND SUMMARY 97
8. CONCLUSIONS AND RECOMMENDATIONS 100
REFERENCES 102
APPENDIX A: Indicator variograms for MPO and PEO 105
APPENDIX B: Variograms for core and fringe zone 107
APPENDIX C: Estimation parameters for core and fringe zone 113
APPENDIX D: Swath Plots 114

LIST OF TABLES

Table 4.1: Description of Rock Types (Anglo American Exploration, 2010) with mean Zn % > 3.6 % Zn..... 29

Table 4.2: Summary Statistics for Rock Types with mean Zn % > 3.6 % Zn.... 29

Table 4.3: MPO and PEO: Summary of statistics for Zn % for variable length composites and 1m composites. 33

Table 4.4 Summary Statistics per drill type. 35

Table 4.5: Summary Statistics per assay method. 37

Table 4.6 Correlation Matrix for all rock types. 39

Table 4.7 Correlation matrix for composite combined MPO and PEO..... 39

Table 4.8 Logged mineral percentages per rock type for MPO and PEO..... 40

Table 4.9: Outliers for MPO and PEO. 42

Table 4.10: Summary Zn % Statistics of1 m composites in the MPO and PEO. 44

Table 5.1: Grouped Lithologies in Gamsberg East Leapfrog Geo project. 58

Table 5.2: Summary Statistics of Inter Ore units in Leapfrog Geo Deposit model. 60

Table 5.3: Summary Statistics for % Zn grade in the modelled domains. 64

Table 5.4: Summary Statistics for Zn % in MPO subdomains. 68

Table 5.5: Summary Statistics for Zn % in PEO subdomains..... 69

Table 5.6: Summary Statistics for Zn % in MPO Refined Volumes. 73

Table 5.7 Summary Statistics for Zn % in PEO Refined Volumes..... 74

Table 5.8: Summary statistics for Zn % in Core and Fringe Zones. 77

Table 6.1 Outlier values for SG and Zn in core and fringe zones..... 84

Table 6.2: Adapted QKNA after Reid & Harley (2009). 87

Table 6.3 Summary Statistics for the Zn % block estimates in the core and fringe zones and corresponding samples..... 90

LIST OF FIGURES

Figure 2.1 The Black Mountain Complex in the Namaqualand Terrane, Northern Cape, South Africa. 6

Figure 3.1 Collar positions at Gamsberg- October 2019. Gamsberg East is circled in red. 19

Figure 3.2 Ranked Half Absolute Relative Difference Plot for Zn duplicates in Gamsberg East. 24

Figure 4.1 Gamsberg East CPD for the entire Zn % data set. 27

Figure 4.2 Gamsberg East CPD for Zn below 10 %. 28

Figure 4.3 Gamsberg East Distribution of rock types. 28

Figure 4.4 Spatial Plot of Rock Types with mean Zn % > 3.6 % Zn. 30

Figure 4.5 Distribution of Sample Length across Gamsberg East. 31

Figure 4.6 Gamsberg East MPO and PEO variable Sample Length Distribution. 32

Figure 4.7 Gamsberg East MPO and PEO Sample Length Distribution after compositing to 1 m. 33

Figure 4.8 Gamsberg East Distribution of drill methods. 34

Figure 4.9 Gamsberg East MPO and PEO Distribution of Drill Types 1 m composites. 34

Figure 4.10 Gamsberg East Distribution of assay methods. 36

Figure 4.11 Zn % CPD plots comparing different assay methods. 36

Figure 4.12 Gamsberg East 3D spatial plot of all assay methods (left) and 4AROG_UN method (right). 38

Figure 4.13 Distribution of Zn grade with that of 4AOG_UN samples 38

Figure 4.14 Bivariate scatterplots for Zn vs. Cd for the MPO and PEO units combined(left), MPO (centre) and PEO (right). 40

Figure 4.15 Bivariate scatterplots for Pb vs. Ag for the MPO and PEO units combined(left), MPO (centre) and PEO (right). 41

Figure 4.16 Bivariate scatterplots for Cu vs. Fe for the MPO and PEO units combined(left), MPO (centre) and PEO (right). 41

Figure 4.17 Spatial plot of outliers in MPO. 43

Figure 4.18 Spatial plot of outliers in PEO. 43

Figure 4.19 MPO Histogram of Zn % grades..... 46
Figure 4.20 PEO Histogram of Zn % grades. 46
Figure 4.21 MPO Histogram for Zn % grade with modelled normal distribution. 47
Figure 4.22 PEO Histogram for Zn % grade with modelled lognormal distribution. 47
Figure 4.23 MPO Histogram for Zn % grade modelled with a mixture of three normal distributions overlain..... 48
Figure 4.24 PEO Histogram for Zn % grade modelled with a mixture two normal distributions. 48
Figure 4.25 MPO Histogram for log transformed Zn (ln (Zn %))..... 49
Figure 4.26 PEO Histogram for log transformed Zn (ln (Zn %)). 49
Figure 4.27 MPO Cumulative Normal Probability plot for %Zn grade..... 50
Figure 4.28 PEO Cumulative Normal Probability plot for %Zn grade. 50
Figure 4.29 MPO ln(observed frequency) vs. class midpoint of x = ln(%Zn). ... 51
Figure 4.30 PEO ln(observed frequency) vs. class midpoint of x = ln(%Zn)..... 51
Figure 4.31 MPO CPD plot for Zn %. 52
Figure 4.32 MPO CPD plot for Zn % below 15%..... 53
Figure 4.33 PEO CPD plot for Zn %..... 54
Figure 4.34 PEO CPD plot for Zn % below 5%. 54
Figure 5.1 Section looking North to view intersection of interest on GAMD061. 58
Figure 5.2 PEO Intrusive Leapfrog Geo models from base lithology with no trend (left) and a non-decaying structural trend (right)..... 59
Figure 5.3 Deposit model in Leapfrog Geo for MPO (left) and PEO (right). 61
Figure 5.4 PEO in plan-view, without the pinch out option (left) and with the pinch out option (right). 62
Figure 5.5 Vein model with drill hole intersections and traces for MPO (left) and PEO (right). 63
Figure 5.6 MPO heat- scaled indicator kriged block values..... 66
Figure 5.7 PEO heat- scaled indicator kriged block values. 67

Figure 5.8 MPO (left) and PEO (right) subdomains based on IK probability cut-offs. 67

Figure 5.9 MPO Domain 1 Relative Frequency Distribution for Zn %..... 68

Figure 5.10 Box Plot for Zn % in MPO Domain 2. 69

Figure 5.11 Relative Frequency Distribution for Zn % in PEO Domain 1. 70

Figure 5.12 Box Plot for Zn % in PEO Domain 2. 70

Figure 5.13 Cross section showing core and fringe and barcoding of grades in PEO. 71

Figure 5.14 MPO (left) and PEO (right) refined volumes based on indicator values. 72

Figure 5.15 Boxplot for Zn % in MPO Refined Volume 0. 73

Figure 5.16 Relative Frequency Distribution for Zn % in MPO Refined Volume 1. 74

Figure 5.17 Histogram for Zn % in PEO Refined Volume 0. 75

Figure 5.18 Relative Frequency Distribution for Zn % in PEO Refined Volume 1. 75

Figure 5.19 Drill holes showing Zn % values above (orange) and below (green) the 3.6 % Zn indicator threshold. 76

Figure 5.20 Cross section of Core and Fringe Zone. 77

Figure 5.21 Histogram for Zn % in Fringe Zone. 78

Figure 5.22 Histogram for Zn % in Core Zone. 78

Figure 5.23 Cross section showing mixing of grades in Core Zone. 79

Figure 5.24 Cross section showing geometry including low grades into Core Zone. 79

Figure 6.1 Experimental Semi-variogram for Zn with fitted model in core zone. 86

Figure 6.2 Plot of declustered mean vs cell size for Zn in core zone. 88

Figure 6.3 Contact Profile for Zn across Core/Fringe Boundary. 89

Figure 6.4 Relative frequency distribution for Zn in the core zone of the block model (50% transparency) and the database. 91

Figure 6.5: Swath Plot for Zn in core zone. 91

Figure 6.6 SLOR for Zn estimate in core zone. 92

Figure 6.7 KV (left) and drill hole spacing (right) in Gamsberg East. 93

Figure 6.8 Grade Tonnage curve for Gamsberg East, with tabulated grade and tonnage at incremental cut-off values. 94

LIST OF UNIT SYMBOLS

UNIT	SYMBOL
Ag	Silver
Ba	Barium
Cd	Cadmium
Co	Cobalt
Cu	Copper
Fe	Iron
g/cm^3	gram per cubic centimetre
Mn	Manganese
Mt	Million tonnes
Pb	Lead
S	Sulphur
Tl	Thallium
Zn	Zinc

LIST OF ABBREVIATIONS

ABBREVIATION	DEFINITION
2D	Two dimensional
3D	Three dimensional
4AOG_UN	4 Acid digest with unknown finish
AR_ICPES	Aqua Regia digest with ICP-ES finish
AROG_UN	Aqua Regia Digest with unknown finish
BMM	Black Mountain Mining
CPD	Cumulative Probability Distribution
GCLN	Generalised Compound Lognormal
CLT	Chlorite Fels
CV	Coefficient of Variation
EDA	Exploratory Data Analysis
GPM	Garnet Pyroxene Magnetite
HARD	Half Absolute Relative Distance
ICP-OES	Inductively Coupled Plasma – optical emission spectrometry
IDs	Unique identifiers used for drillholes or samples
IK	Indicator Kriging
IQR	Inter Quartile Range
KE	Kriging Efficiency
KV	Kriging Variance
ln	Natural logarithm
LOM	Life of Mine
MPO	Pyroxene-Amphibole-Garnet-Magnetite hosted ore
NQ	Diamond drill core with diameter of 60.0 mm.
NR	Not recorded
OCC	Okiep Copper Company
OK	Ordinary Kriging
PEO	Quartz-Sillimanite pelite hosted ore
QA-QC	Quality Assurance and Quality Control
QKNA	Quantitative Kriging Neighbourhood Analysis
R^2	Coefficient of determination
RBF	Radial Basis Function
SAMREC	The South African Code for the Reporting of Exploration Results, Mineral Resources and Mineral Reserves
SEDEX	Sedimentary Exhalative
SG	Specific Gravity
SLOR	Slope of Regression

1. INTRODUCTION

The unexploited Gamsberg East deposit lies approximately 16 km east of the town of Aggeneys in the Northern Cape Province of South Africa and forms part of the larger Gamsberg Zn deposit. Black Mountain Mining (BMM) holds the Mining Right in South Africa. The Gamsberg deposit was initially investigated by surface diamond drilling in 1972. Limited underground development took place from 1975. Goldfields of South Africa re-evaluated the deposit in 1975. Additional drilling led to the delineation of 160 Mt grading at 6.5 % Zn and 0.5 % Pb (du Toit, 1998b)

BMM has been operating in Aggeneys since 1980 and produces Cu, Pb, Zn and Ag from its Deeps and Swartberg underground operations, and Zn from its Gamsberg open pit. Black Mountain Mining was acquired from Anglo American by the Vedanta Group in 2011 (Vedanta Zinc International, 2018). The Gamsberg East project's current resource is 240 Mt with a grade of 6 – 6.5 % Zn, with an estimate LOM of 30 years. The first phase aims to produce 4 Mt of Zn from the open pit and has a LOM of 13 years (Vedanta Zinc International, 2018).

This research study was prompted by a renewed interest in Gamsberg East as exploration target. Prior to the addition of drill hole data not previously used, the existing historic dataset was studied to determine the quality, quantity, and confidence of the data as well as to gain an understanding of the previous resource estimations.

1.1. Research Background

Gamsberg East Exploration drilling ceased prior to 2009. A preliminary Mineral Resource assessment of the deposit was produced using Ordinary Kriging (OK) by Anglo American in 2009 (Reid & Harley, 2009) and reviewed by SRK for BMM in 2011 (Potgieter, 2016).

The drilling information is stored in a database which contains all drill hole data including, but not limited to, drill hole identification (ID), collar positions, downhole azimuths, and dips, logged lithologies, logged mineral percentages, measured specific gravity (SG) values and lab assays for elements of interest, most importantly – Zn grades. In addition to these attribute fields, the database also contains metadata, such as information on survey instruments, drill types and assay techniques.

This research study examines the existing Gamsberg East database in detail using a variety of data validation and analysis techniques. The aim of this is to improve the quality and confidence in the Gamsberg East Mineral Resource Estimate, by gaining a sound understanding of the spatial and statistical

characteristics of the data, particularly grade data for Zn, through an extensive and detailed Exploratory Data Analysis (EDA). This resulted in the identification of distinct geological domains, to be used during geological modelling and resource estimation.

1.2. Research Motivation

As BMM aims to expand its greenfield operations, this research study could add value in establishing a best-practice guideline for data handling, validation and analysis and geological modelling of Broken Hill-type Zinc deposits. The understanding of the data could also aid the Resource Geologist in making informed decisions regarding, for example, the variogram model and kriging neighbourhood to be used in order to produce a reliable Mineral Resource Estimate.

1.3. Problem Statement

A number of years has passed since the Gamsberg deposit changed hands and, in that time, BMM's focus has been on developing Gamsberg North and maintaining production from the underground operations at the Black Mountain Deeps and Swartberg mining operations. Due to this, much the deposit knowledge and understanding of the Gamsberg East dataset has been lost.

In recent years there has been renewed interest in the Gamsberg East deposit. This has brought about the need to assess existing data and methods used previously during Mineral Resource Estimation. New advances in software and modelling techniques also present the opportunity to relook at the deposit using techniques such as implicit modelling, a methodology not previously applied.

1.4. Research Hypothesis

The hypothesis of this research study is that the systematic application of basic data validation and statistical techniques, will improve the knowledge and understanding of the Gamsberg East Deposit. It is envisaged that such a rigorous process will improve the quality and confidence of the Mineral Resource Estimate.

The understanding that this investigative process brings will help inform the delineation of ore for wireframes and estimation domains. Domains based on these statistical principles, should lead to improved Mineral Resource Estimates. Leading to increased confidence in the resource estimation as reflected by kriging estimation metrics, such as Slope of Regression (SLOR) and Kriging Efficiency (KE).

This research study aims to address the following questions:

- Which data validation techniques can be implemented on a historical data set, to ensure a reasonable level of confidence in the data?
- What is the best way to define domains for wireframing and estimation, based on grade and/or geological characteristics?
- Once a Mineral Resource has been estimated, how can the researcher test and confirm the quality of the estimate?

1.5. Assumptions

Since the focus of this research study is a sound understanding of the existing drill hole database through EDA, the theory of kriging and variography, as applied in Mineral Resource Estimation, is considered to be out of scope for this research study but are however discussed at a high level in the literature review section of this research study report.

1.6. Research Objectives

The objective of this research is to investigate a variety of data validation and analysis techniques to:

- Understand and describe the Gamsberg East database in terms of the statistical and spatial characteristics of Zn grades.
- Identify errors and correct these where possible.
- Identify distinct geological domains which will be considered separately during geological modelling and estimation.

By applying these techniques this research study aims to add value to the drill hole database by establishing an EDA workflow that can be followed as a guideline on future studies. As part of the literature review, implicit modelling and multivariate geostatistics are also covered, as these topics are considered relevant to the research study.

1.7. Research Methodology

The planned and executed methodology followed in this research study is presented below and covers 3 broad stages namely data validation and analysis, geological modelling, followed by grade estimation and validation. The research study is concluded with interpretation and discussion of results as well as recommendations for future work.

Stage 1: Data Validation and Analyses

In this stage, relevant resource data had been extracted from the Gamsberg database and then subjected to extensive data analysis and data validation following guidelines identified in the literature review. The focus at this stage was to extract as much useable information as possible from the dataset. As the database does include historic information this stage comprises some fact-finding regarding logging, data collection and Quality Assurance and Quality Control (QA-QC) practices used when the dataset was created.

Exploratory Data Analysis is performed on the entire dataset. The purpose of this is to identify geological domains and systemic spatial variation. Editing of existing data is applied only in cases where deemed necessary, motivated and sound to do so. The objective of this stage is to end up with a “clean” validated dataset, in which the researcher can have a reasonable amount of confidence with the domains to be modelled in the next stage.

Stage 2: Geological Modelling

Using the dataset produced in stage 1, the geological modelling takes place. For this, use is made of various 3D modelling software packages (SEEQUENT Leapfrog Geo and Maptek Vulcan) to investigate the best methodology of delineating ore packages or grade envelopes within the Gamsberg East orebody. After modelling is completed, the model is validated. Drill hole data are intersected with wireframes and a second phase of EDA carried out, to ensure that the domaining was effective in producing second-order stationarity in the spatial grade distribution of the Zn.

Stage 3: Grade Estimation and Validation of Results

In this stage, intersected data is used to construct experimental variograms per domain for each element of interest. QKNA is conducted, a kriging plan devised and the Mineral Resource is estimated using the modelled variograms. Results are validated through swath analyses, cross-validation or jack-knifing and confidence in the estimation is assessed by considering conditional bias measures such as KE and SLOR.

Finally, on completion of the three broad stages, a discussion and interpretation of the work is presented. This is followed by recommendations for future work based on these findings.

1.8. Research Study Report Layout

There are eight chapters, followed by a list of references and appendices of supplementary information. A high-level summary of the chapters follows.

Chapter 1 offers background information to the research study and introduces the study area and the motivation behind the research study. The chapter also states the problem and objectives, and addresses assumptions made in the research study. The research methodology followed is also described.

In Chapter 2, literature relevant to this research study is reviewed and presented. This is an important part of the research study, as it creates the theoretical and practical framework within which the study takes place. The literature review covers the geology of the deposit and area to provide background and context to the research study. It also covers EDA, Geological modelling, and some aspects of resource estimation, such as multivariate estimation and validation of resource models and briefly, kriging and variography.

Chapter 3 covers the first stage data analysis in which the Gamsberg East drill hole database is interrogated, validated, summarised, and cleaned up. The output of this process is a desurveyed validated sample dataset. All findings and assumptions are discussed. This validated sample dataset is the input data to the EDA process.

EDA is covered in Chapter 4. As part of this process the sample dataset is examined statistically to establish the zones of interest and an appropriate composite length. Then composites within the zones of interest are interrogated using a variety of techniques with the aim of identifying the grade probability density distributions.

Chapter 5 covers the geological modelling conducted in Leapfrog Geo. Different techniques are used to create wireframes, outputs are examined, and the validity of each method discussed. Methods for grade domaining are also discussed, specifically Indicator Kriging, refined models, and grade domaining for estimation.

Chapter 6 describes the Mineral Resource Estimation process, the variography and the determination of the kriging plan to meet the objectives of the estimate. The resultant block model is validated, a classification method is discussed, and a grade tonnage curve presented.

In Chapter 7, the previous chapters are summarised, and the findings are discussed within the context of the aims and objectives of the research study.

Finally, Chapter 8 presents the research study’s conclusions based on the findings. This chapter also contains recommendations for further work to be considered.

2. LITERATURE REVIEW

2.1. The Geology of Gamsberg

The Mokolian Bushmanland terrane of the Namaqualand Tectonometamorphic Province, host 4 major stratiform exhalative sediment-hosted deposits, of which Gamsberg is the most easterly. Figure 2.1 adapted from Google (2018) shows from West to East, Swartberg, Broken Hill, Big Syncline and Gamsberg. All occur at a similar stratigraphic position within the metapelitic sequence and in close spatial correlation to major quartzite units. These deposits form what is known as the Black Mountain Complex.

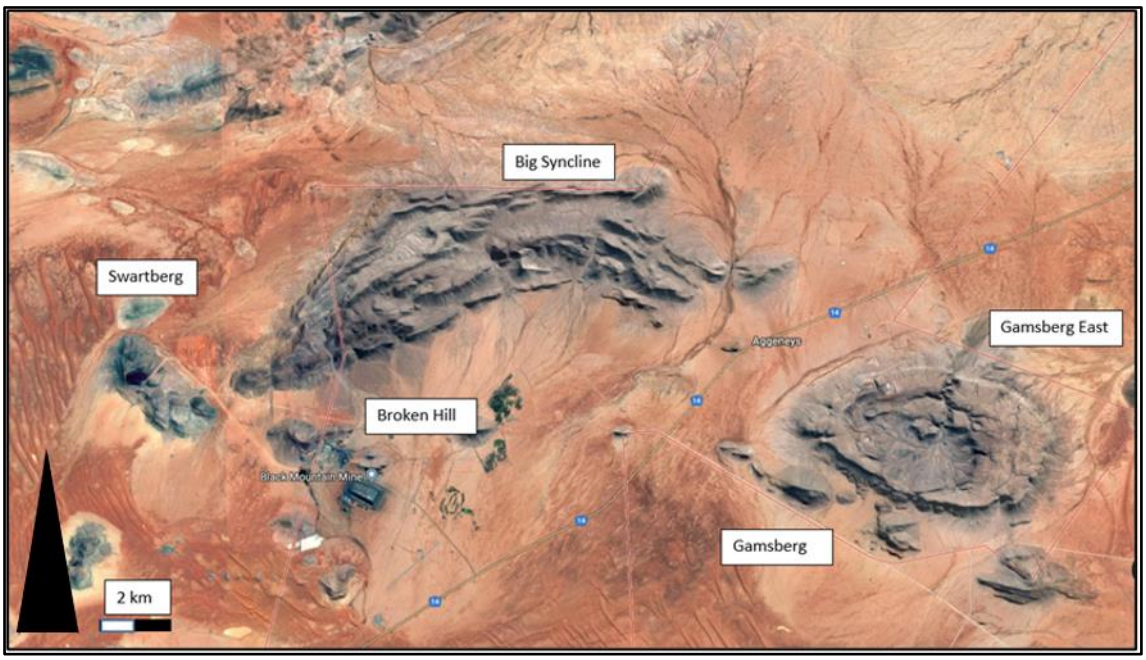


Figure 2.1 The Black Mountain Complex in the Namaqualand Terrane, Northern Cape, South Africa.
(Google, 2018)

The ore at Gamsberg is hosted in the Gams Iron formation, which consist of a quartz-sillimanite schist, metapelite and quartz-garnet-magnetite-pyroxenoid-amphibole iron formation. The formation has been subjected to polyphase deformation and medium to high-grade metamorphism (Anglo Base Metals, 2009).

The Pb and Zn mineralisation is confined to the middle of the Gams formation, a metamorphosed fine-grained siliceous and aluminous sediment with precipitates of iron, manganese, barium, sulphur, and base metals. The sulphide content of this package varies between 5 and 14% by volume, with pyrite, pyrrhotite and sphalerite as dominant sulphides. The most important mineral is sphalerite which

occur as small disseminated, honey-coloured grains or massive aggregates associated with pyrrhotite, marcasite and pyrite (du Toit, 1998a).

From surface diamond drilling it is known that the Gamsberg East deposit is an east-dipping, gently folded tabular body. The geometry of the deposit is controlled by a mega-scale recumbent sheath fold closing towards the east. The deposit is developed down-dip of Gams Iron Formation outcropping on the eastern side of the Gamsberg basin, where stratiform barite was mined historically (Anglo Base Metals, 2009).

To date, only the upper, overturned limb of the sheath fold has been drill-tested. The shallowest ore was intersected at 300m and the deepest at 760m. Drill data indicates a north-south striking body, that dips eastward, between 30 – 90°, with dips steepening eastwards, approaching the fold closure (Anglo Base Metals, 2009).

The four deposits in Figure 2.1 that make up the Black Mountain Complex, has a spatial association with Banded Iron Formations which suggests a well-established SEDEX stratiform massive sulphide ore genesis model. This model is thought to be closely related to Mokolian marine sedimentary accumulations in the intracratonic, fault-controlled basins that developed due to continental rifting. The three western deposits are Pb-dominated with minor Zn, whereas Gamsberg is Zn-dominated (du Toit, 1998b).

2.2. Exploratory Data Analysis

EDA is a vital part of every good Mineral Resource Estimate. Organising and analysing data can take up to half the total time needed to conduct a Mineral Resource Estimate. The main purpose of EDA is to improve the quality of the estimate by gaining insight into the data. Specific goals of an EDA study can be to familiarise oneself with the statistical characteristics of the variable of interest, to recognize the spatial variation of elements of interest or geological domains, to identify outliers or errors, or to evaluate differences between different kinds of raw data. (Sinclair, 1998)

According to Abzalov (2016), EDA can provide insights into domaining and wireframing, which could lead to the revisiting of these. Making EDA a reiterative process, that is done using a combination of traditional statistical and specialised data analysis methods.

Which methods are used often depends on the complexity of the deposit in question, and the sources of error and risks. The effectiveness of the EDA process is largely dependent on the experience and intuition of the person conducting it. Sinclair (1998) suggests using a structured approach for EDA,

stating that it contributes to efficiency and gives assurance that the data under consideration is understood as far as it can be understood.

The literature review conducted on EDA suggests consideration of the following aspects:

Data Storage Design

The design of the database should be such that it is easy to store and access the data. The data fields to be collected and stored depend on the type of deposit under consideration (Sinclair, 1998).

Database Management

Data that resides in databases form the basis of the evaluation of deposits. This data may be lost or corrupted – intentionally or unintentionally. To guard against that, the database administrator should ensure that all users have the correct permissions (Abzalov, 2014). The database should also be backed up regularly and back-ups kept off-site, and hard copies should be stored in a safe, fire-proof location (Abzalov, 2016).

Data Validation

Data validation can lead to recognising anomalous entries or errors within a dataset and should take place once a database is constructed and at every subsequent addition of data. An important check to be done is the checking assayed grades of duplicate assays and standards arising from the QA-QC program (Sketchley, 1998; Long, 1998; cited in Sinclair, 1998). These data can be helpful in quantifying error and data variability between sampling and assaying procedures (Sinclair, 1998).

Blank samples, which contain negligible concentrations of the element of interest, are used to monitor contamination (Abzalov, 2016).

Data Support and Compositing

Support is the size, shape and orientation of samples and can have a great effect on the variability of grades (Sinclair, 1998). Compositing is the process whereby data is regularised for Mineral Resource Estimation purposes (Abzalov, 2016). Most commonly, composites are weighted averages of adjoining analytical data (Sinclair, 1998). Composite length is usually fixed throughout the deposit but can be different for different domains based on the geometry of the deposit (Abzalov, 2016).

According to Abzalov (2016) composites should be larger or equal to the average sample length, approximately half the kriging block size in the downhole direction, i.e., the z dimension, and should not change the mean grade or metal content.

Declustering

Clustered data, which commonly occur where high grades are sampled preferentially, especially during exploration (Sinclair, 1998; Abzalov, 2016) can complicate statistical analyses. The influence of data clusters can be overcome by assigning weights that reflect the degree to which data is clustered. Samples in sparsely sampled areas will receive more weight and vice versa. This acts to temper the influence of clustered data (Abzalov, 2016).

Two methods commonly used in Mineral Resource Estimation resource estimation to decluster data is polygonal declustering and cell declustering (Isaaks & Srivastava, 1989). In polygonal declustering, a polygonal area of influence around each sample is used to assign a declustering weight to that sample. Cell declustering involves the area under consideration being divided into rectangular cells, and each sample within the cell receiving a weight inversely proportional to the total number of samples in the same cell. Generally, this results in more clustered samples receiving lower weights. The choice of cell size and the origin of the grid used to assign cells are important considerations.

Outliers

An outlier is a value that appears inconsistent with the majority of the other data points (Sinclair, 1998). Outliers can cause large variability in estimates of statistical parameters and can result in unusually high values in block estimation or even negative grade where it coincides with negative kriging weight (Sinclair, 1998).

Outliers may represent a geological domain with very different properties and continuity, which might need separate consideration during estimation. An outlier population could be as the result of a material handling or data error or it could be a legitimate sub-population based on geology. One of the purposes of data evaluation is to distinguish the latter type of outliers. The implementation of QA-QC protocols increases the likelihood that outliers are a separate geological population (Sinclair, 1998).

Univariate Statistics

Summary Statistics. These everyday statistics, such as mean, range and standard deviation can be used to summarise data and compare data from subgroups (Sinclair, 1998).

Histograms and Continuous Distribution Models. Histograms display information about numerical variables and can be used to visualise properties such as spread, skewness and range. Histograms are especially useful for data of equal support. Unbiased histograms can be fitted with continuous distribution models, which describe the data (Sinclair, 1998).

Probability Graphs. Using probability graphs is a simple visual technique that can be applied to find and describe multiple populations in applied geochemistry (Sinclair 1974,1976,1991 cited in Sinclair, 1998). This method can be used for determining fundamentally different geological domains for resource estimation (Sinclair, 1998).

Bivariate Statistics

Scatter plots. Scatter plots are a simple and useful way to check bivariate data and can provide a quick way of checking the correlation between variables or for outliers in duplicate data (Sinclair, 1998).

Correlation. Coefficients for linear correlations range from -1 to 1, indicating how similar two variables are. High correlation values could indicate linear trends but could also be affected by outliers and non-linear trends. These correlation coefficients can be examined in matrix form or on scatter plots (Sinclair, 1998).

Multivariate Statistics

Multivariate statistics is the consideration of multiple elements at one time and allow for the consideration of changes in several properties simultaneously (Davis, 2002). It allows for the identification of groups of variables that behave similarly but are not widely used in Mineral Resource Estimation, as data transformations are often necessary to make statistical assumptions and can be mathematically complex (Sinclair, 1998).

Triangular Diagrams. These are often used in earth sciences to display relative variations of three variables. Triangular diagrams display ratios between variables but not absolute abundances (Sinclair, 1998).

Multiple Regression. This involves the expression of a dependent variable in terms of two or more independent variables (Sinclair, 1998; Davis, 2002).

Spatial characteristics of data.

It is important to examine data spatially, since it could help with recognition of systematic spatial distribution patterns such as metal zoning and geological domains. A good starting point for this is plotting data in plan and section (Sinclair, 1998).

Moving window statistics can be used to inspect spatial variations (Isaaks & Srivastava, 1989 cited in Sinclair, 1998). Once the size, shape and overlap of windows have been established, means and standard deviations are mapped for all windows and can be used in recognizing a relationship that might be useful in studying autocorrelation.

The methods described above will be used to analyse and describe the Gamsberg East dataset and identify any errors, outliers, element correlation and specifically sub-populations within the data, which will inform the delineation of

domains for geological modelling and estimation. These domains are often referred to as stationary domains (Rossi & Deutsch, 2014).

Strict stationarity occurs when a phenomenon is homogenous in space (Chilès & Delfiner, 2012a). Strict stationarity hardly ever occurs in nature and is very hard to confirm from experimental data (Abzalov, 2016).

Second Order Stationarity, also known as weak stationarity or wide-sense stationarity, occur when for the first two moments of a random function, namely the mean and covariance, it is assumed that the former is constant, and that the latter exists and depends on the separation distance between sample locations in space (Chilès & Delfiner, 2012a; Abzalov, 2016).

2.3. Geological Modelling

Geological models are subsurface interpretations based on limited data that simplify the complexity of natural phenomena (Birch, 2014) such as mineral deposits. Abzalov (2016) identifies some key steps in creating geological models, referred to as wireframes. These include:

- Establishing what domains should represent, a certain geological unit, ore package or estimation domain.
- Identifying the properties to be modelled for example grade, geology, weathering, alteration. These should represent mineralisation controls (Rossi & Deutsch, 2014).
- Studying the internal structure of the variable of interest, as ore bodies are usually heterogenous.
- Defining the domaining criteria, which could be grade, geology or a combination of properties.
- Studying the nature of contacts; whether these are sharp, gradational, straight, or irregular.
- Coding data according to chosen domains
- Taking into consideration the selected properties, create the domains.
- Test the subsequent domains, to confirm that these fulfil the purpose of the exercise and are geologically robust.

Interpretation of geological variables along sections and extending these to 3D is a traditional approach to geological modelling. This approach uses data and general geologic knowledge of the deposit, or similar types, as well as a plausible theory of genesis (Rossi & Deutsch, 2014).

It is often tedious and time-consuming and because of its repetitive nature, often left to junior staff. This kind of modelling relies on interpretation in areas of uncertainty (Birch, 2014). Using the same principles, implicit modelling is a technique that uses radial basis functions (RBF) to rapidly and efficiently generate

models from various data sources, such as drill holes, outcrop and structures (Birch, 2014).

The RBF describes scattered data points with a single mathematical function. It is particularly good for interpolating data that are not on a regular grid. Data input can be coded data such as lithology and alteration captured in drill hole logs or assays (Hodkiewicz, 2013).

Structural trends, as well as mineralisation trend and deformation style, can be introduced through mathematical applications such as anisotropic interpolation, adjustable search ellipsoids or idealised trends. These inputs provide greater control over modelled surfaces, so that the resultant wireframe represents the modelled orebody (Stoch, et al., 2018).

Mineral Resource evaluation takes place within block models that are constrained by wireframes. The process of modelling geology is key to defining stationary domains that allows for dependable estimation (Chanderman, et al., 2017).

Since the area under consideration was last modelled in 2009, these guidelines were followed in creating and modelling domains. The new model has been created in Leapfrog Geo software, through a combination of implicit and explicit methods. The output from the modelling process is compared to previous models and reviewed to ensure that it is geologically sound and representative.

2.4. Variography

A sound understanding of theory of variography is assumed for this research study - only salient points follow. The variogram is the most widely used tool for quantitatively defining spatial continuity in geological properties and is used to identify the optimum weights to be assigned to the samples in the estimation (Journel and Huijbregts, 1978, Goovaerts, 1998 cited in Abzalov, 2016), Most geostatistical methods, including estimation and simulation require a variogram model (Rossi & Deutsch, 2014).

An experimental semi variogram (commonly referred to simply as the variogram), γ(h) is half the average squared difference between the paired data values $Z(x_i)$ and $Z(x_i + h)$ at a distance h apart, where $Z(x_i)$ is the data value at location x_i. The equation for calculating an experimental variogram is shown in Equation 1

$$\gamma^*(h) = \frac{1}{2N}\sum_{i=1}^{N}\{[Z(x_i + h) - Z(x_i)]^2\}$$

Equation 1

where N is the number of data pairs separated by a vector h. The variogram values are calculated in a specific direction and plotted against the distance h

(Abzalov, 2016). Points on the experimental variogram represent only certain distances and directions, geostatistical calculations, such as kriging, require variogram values in all directions and at all locations. By fitting these experimental points with a parametric function γ(h), a 3D model for the variogram is acquired (Armstrong, 1984 cited in Rossi & Deutsch, 2014). This γ(h) function for all h values, includes all "*geological information derived from the experimental model, including anisotropies, trends, nugget effects etc*" (Rossi & Deutsch, 2014).

2.5. Ordinary Kriging

OK is based on a "*minimum error variance of a linear estimate at a location where the true value is unknown*" (Rossi & Deutsch, 2014) and is the most widely used estimation method for Mineral Resource Estimation (Journel & Huijbregts, 1978 cited in Abzalov, 2016). OK is a weighted average method that inter-and/or extrapolates sampled values at known locations to the unknown target location (Abzalov, 2016). The variogram model is used as an input to calculate kriging weights for each sample used. The method also minimises the estimation variance, by setting a constraint that the sum of the kriging weights assigned to the grades considered in the estimate, has to be equal to 1. The OK kriging estimate is shown below in Equation 2 (Wackernagel, 2003)

$$Z^*_{OK}(x) = \sum_i \left[\lambda_i^{OK} Z(x_i)\right] \;\; subject\ to \sum_i \lambda_i^{OK} = 1$$

Equation 2

where the estimated value of the variable at an unknown location x is $Z^*_{OK}(x)$, $Z(x_i)$ is the sample value at location x_i and λ_i^{OK} the kriging weight for that specific sample $Z(x_i)$.

The minimised estimation variance, also known as the kriging variance (KV) is shown in Equation 3 (Rossi & Deutsch, 2014)

$$\sigma^2_{OK}(x) = \sigma_0^2 - \sum_\alpha \lambda_\alpha^{OK} \gamma(x_0 - x_\alpha) - \mu_{OK}$$

Equation 3

where $\sigma^2_{OK}(x)$ is the KV at unknown location x, σ_o^2 is the sill of the variogram, $\gamma(x_0 - x_\alpha)$ is the spatial variance between the known data locations x_α and the unknown location x_o, and μ_{OK} is the Lagrange multiplier.

Equation 3 shows that the KV is independent of sample values, therefore it follows that it can be calculated before the estimation is performed (Rossi & Deutsch, 2014). The KV can be used to evaluate uncertainties in the model and

also identify areas of high risk such as where high KV values are associated with high grade values (Abzalov, 2016).

2.6. Indicator Kriging

Indicator based estimation methods can be used to relate discrete distributions by assigning indicator values to each geological attribute. Indicator Kriging (IK) furnishes a probability of the attribute being present (Rossi & Deutsch, 2014). With IK no prior assumptions are made about the distribution being estimated (Rossi & Deutsch, 2014). The objective of IK is to estimate the distribution itself and not the parameters of the distribution (Journel, 1983 cited in Rossi & Deutsch, 2014). This non-parametric property of IK is one of the method's appeals (Glacken & Blackney, 1998).

Multiple Indicator Kriging (MIK) can also be used to estimate mixed data populations. MIK divides the overall sample distribution using a number of thresholds, which makes it unnecessary to find a distribution model for each division. If thresholds are chosen carefully with respect to the input grade distribution, the distribution within most divisions will be nearly linear, with the exception of the highest and lowest grade classes. These require special consideration and a method for this was introduced by Deutsch & Journel (1998, cited in Glacken & Blackney).

Categorical Kriging is an application of IK, where the probability of a categorical variable occurring at a certain location is produced. The results can be presented as a probability map (Glacken & Blackney, 1998).

2.7. Multivariate Estimation

Resource data sets usually consist of more than one variable. Often these data could occur at other locations from the variable of interest (Chilès & Delfiner, 2012b). These secondary variables may provide valuable information on the element of interest and should be taken into account. If a spatial correlation exists and can be inferred from available data, the two variables can be co-kriged. Co-kriging is an estimation technique that uses data from one variable to estimate another, if a spatial correlation can be inferred from available data (Rossi & Deutsch, 2014).

The theory of co-kriging is similar to that of kriging, but notations and geometries of datasets can be challenging. Due to the problem of establishing a multivariate model, a simplified implementation known a collocated co-kriging is often used (Chilès & Delfiner, 2012a). Collocated co-kriging makes use of two simplifications. Firstly – that only one secondary variable is under consideration and secondly, it assumes that the cross variance is a linear scaling of the

variance. This assumption ensures that the collocated values are more significant than other values in the neighbourhood and screens the influence of those (Rossi & Deutsch, 2014).

However, there are circumstances under which co-kriging will not improve an OK estimate (Minnitt & Deutsch, 2014). These, according to Isaaks and Srivastava (1989) are instances in which the primary and the secondary variable is equally sampled (collocated) meaning that no one variable is under sampled with respect to the other.

Preliminary work indicated that within the Gamsberg East dataset, lead (Pb) and zinc (Zn); both economic elements of interest within the deposit are sampled in the same locations; every sample that has a Zn assay also has a Pb assay. Therefore, it was considered that co-kriging will not improve the estimate.

2.8. Validation of Resource Models and Estimates

Resource models should always be checked and validated. The main reasons for this are to make sure of the internal consistency of models and, where possible, to supply an estimate of the accuracy of predicted variables (Rossi & Deutsch, 2014). In practice, many decisions are made when kriging an estimate; these include which type of kriging to use, search parameters and data selection (Deutsch, et al., 2014). Since the modelling and estimation of a resource model has a large number of steps, each of these steps should be checked to ensure the integrity of the final model (Rossi & Deutsch, 2014).

In addition to that, conditional bias occurs in most kriged estimates. Conditional bias occurs when the expected value of the true grade is not equal to the estimated grade (Rossi & Deutsch, 2014). One of the major causes of conditional bias is the smoothing effect of kriging, which reduces variability. This results in high grades being underestimated and low grades being overestimated (Abzalov, 2016).

When considering conditional bias, it is important to consider what type of estimate is required. According to Deutsch *.et al,* (2014) there are three types of estimates, each of which requires a different strategy and criteria for assessing results. These are:

- estimates for "*visualisation and geological understanding*",
- interim estimates for long term planning and
- final estimates to be used for reserve classification.

Using many samples in an estimate decreases the conditional bias (Deutsch, et al., 2014; Rossi & Deutsch, 2014). This approach would be appropriate for final estimates, where decisions on ore vs. waste are made. Ore vs. waste decisions

should be made on an estimate where the squared error and the conditional bias has been minimised (Deutsch, et al., 2014).

The approach of using many samples would not be appropriate for other types of estimation. Interim estimates are used for long term planning. For these kinds of estimates, restricting the search and so increasing the variance would reflect the information effect and increase understanding of variability to be expected in future (Deutsch, et al., 2014).

A geological model can be checked by comparing the proportion of each geological unit in the database with the modelled volumes of wireframes or block models. A 90 % co-occurrence is suggested as a target by Rossi and Deutsch (2014), although complex geology might result in a lower score.

Leuangthong *et al.,* (2004) recommends that resource estimates be validated both graphically and statistically. Graphical validation can be done in software or on paper, plotting cross sections or plan views of estimated block model grades and composite grades (Rossi & Deutsch, 2014).

Leuangthong *et al.,* (2004) recommends the following minimum criteria be met for a resource estimate produced though geostatistical simulation to be valid:

- Variable values must be reproduced at sampled locations
- Reproduction of the target histogram
- Reproduction of summary statistics.
- Reproduction of the variogram.

Other commonly accepted checks and validations include:

Swath analyses, in which declustered drill holes are plotted against block model averages in x, y and z directions. On a swath plots estimated blocks should show the same grade trends as composited, declustered grades (Rossi & Deutsch, 2014).

Cross-Validation, where a sample value is removed and then re-estimated using surrounding data. This process is repeated for each location throughout the domain and an error value between the sampled and estimated value is then calculated. Usually, this method is used to compare alternative kriging plans, variogram models or types of kriging. Rossi and Deutsch (2014) states that although the validity of this method has been questioned, it remains useful when comparing two very different variogram models. Ideally, the estimated value and the true value should be strongly correlated, but in practice the lower variance of estimated values lead to under estimation at high grades and vice versa. Jack-knifing, in which a subset of data is removed from the start and the estimation process repeated without it, is considered to be more robust (Deutsch, et al., 2014).

For unsampled locations, the following kriging metrics can be used:

The slope of regression (SLOR), which indicates conditional bias, by plotting true, but unknown values, against estimated values. Unbiased, accurate estimates would plot along the bisect of the diagram (Abzalov, 2016). True values are usually unknown, unless the values are estimated using conditional simulation techniques (Rossi & Deutsch, 2014). However, it still possible to estimate the SLOR for a block, using kriging weights, covariance between samples and covariance between samples and the block (Nowak & Leuangthong, 2016). The regression of estimated values from the true values gives an indication of conditional bias in the estimate (Rivoirard, 1987).

Kriging Efficiency (KE) measures the efficiency of block estimates. It is calculated by normalising the kriging variance (σ^2_K) by the variance of the true blocks (σ^2). KE is expressed as a percentage and a high KE indicates a low kriging variance i.e., that the variance of the block estimates is comparable to the variance of the true block values. For perfect valuations, the efficiency is 100% (Deutsch, et al., 2014). As part of this research study, Mineral Resource Estimates will be validated, to ensure that the final estimated grades are a reasonable reflection of the data available in the study area.

2.9. Summary

This chapter reviewed all the topics relevant to this research study. Firstly, an overview of the geological setting was given to provide geological context to this research study. The regional geology, mineralogical and physical characteristics of the deposit and the larger Gamsberg deposit was described. EDA was reviewed at length, discussing various aspects of the EDA process, such as data storage design and validation, as well as univariate and bivariate methods to summarise and describe data. Next, the steps involved in geological modelling is discussed, as well as the benefit of new implicit modelling methods over the traditional approach of joining up sections in 3D. Variography and OK was covered in brief, by reviewing only to most relevant theory, since a sound knowledge of these are assumed for this research study. The implementation of IK was reviewed, discussing the use of IK for grade estimation and estimating probability of categorical variables, also known as categorical kriging. Co-kriging, as multivariate method, was discussed, but since preliminary work indicated that co-kriging would not improve the estimate, it was only reviewed in brief. Lastly, a variety of methods was reviewed which can be used to validate resource models.

3. FIRST STAGE DATA VALIDATION

This chapter is dedicated to data validation, a necessary first step to ensure the input dataset is of a good quality and valid before further work is done. The dataset in question had been studied previously as part of *MINN7043 (2018) – Practical Implementation of Geostatistical Mineral Resource Evaluation Techniques*. However, for use in this research study, the data was extracted to a Microsoft Excel spreadsheet from the Gamsberg database hosted in Maxwell DataShed on the 5th of November 2019, over an ODBC link.

Data validation can lead to recognising anomalous entries or errors within a dataset and should take place once a database is constructed and at every subsequent addition of data. An important check to be done is the checking of duplicate assays and duplicates arising from the QA-QC program (Sketchley, 1998; Long, 1998; cited in Sinclair, 1998). These data can be helpful in quantifying error and data variability between sampling and assaying procedures (Sinclair, 1998).

3.1. Assumptions

For the purposes of this research study, it is assumed that three essential assumptions can be made, namely:

- Assays are precise.
- Assays are accurate.
- Samples are representative of the deposit under consideration.

3.2. Data Compilation and Summary

Since all of exploration drilling over the Gamsberg tenement is stored in a single database, the first step was identifying the collars of holes drilled in the Gamsberg East deposit area. To do this, collar coordinates were plotted in plan-view (Figure 3.1) below. Holes covering the deposit under consideration were identified and marked as "*East*" in a new column in the collar file. These holes were then flagged in the rest of the database, using the VLOOKUP function in Microsoft Excel.

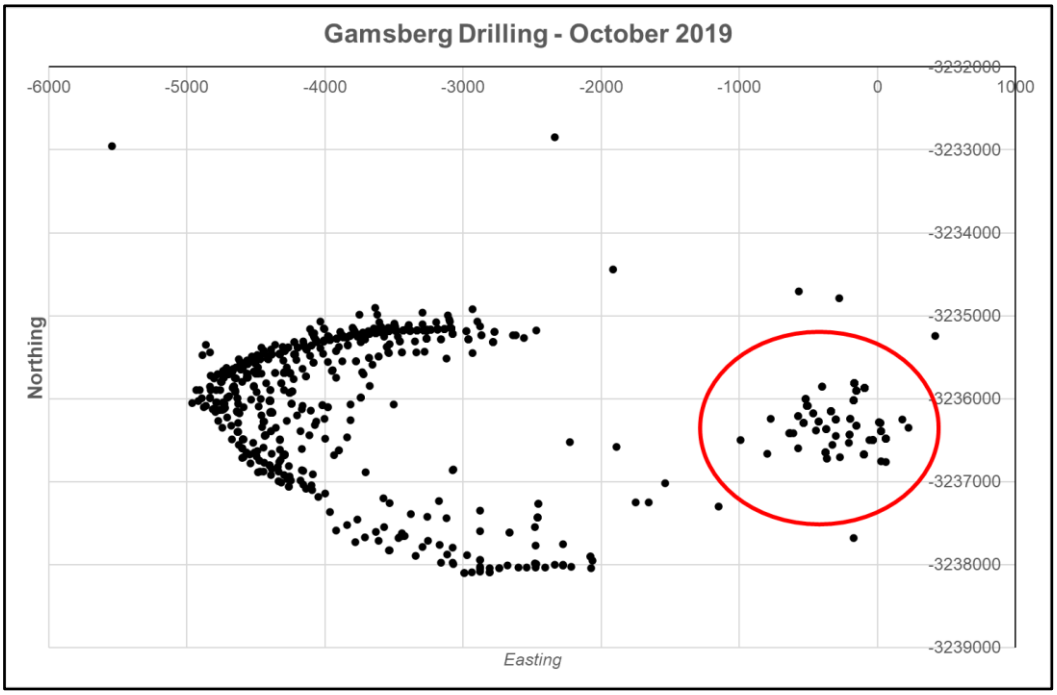


Figure 3.1 Collar positions at Gamsberg- October 2019. Gamsberg East is circled in red.

To further ease data handling, all columns with no captured data were removed, as well as all columns that only had the default value *NR (not recorded*). Next, a spreadsheet was compiled summarising the data available for each hole. The purpose of this was to assess the completeness of data, as well as serve as a reference when making a decision about the suitability of holes for specific purposes, such as geological modelling or resource estimation. Data summarised in this spreadsheet includes, but is not limited to, whether a hole has a downhole survey, assays, re-assays, check samples, and textural logging.

3.2.1. Drill Type and Hole Diameter

Some information was captured in more than one place – for instance, information about the drill hole diameter was captured in the Hole_Diameter column in the Drilling spreadsheet as well as in the Core_Size_Info column in the Collar spreadsheet. Similarly, hole diameter also occurred in two separate columns. The two columns of data were compared, to decide which column to consider and which not to consider.

For drill type, information was captured in the Hole_Type column in the Collar spreadsheet as well as in the Hole_Type column in the Drilling spreadsheet. In this case, there were 17 holes that were captured under the Collar spreadsheet, but not under the Drilling spreadsheet. From this it was decided to use the drill type information from the Collar spreadsheet, since the Collar spreadsheet is more complete.

For hole diameter, information was captured in the Hole_Diameter column in the Drilling spreadsheet, as well as in the Core_Size_Info column in the Collar spreadsheet. In this instance, the same 17 drill holes as with drill type, had no information recorded in either column. Two other holes (GAMD054-2-0 and GAMD054-3-0) had hole diameter information in the Collar spreadsheet, but not in the Drilling Spreadsheet. In addition to that, one drill hole (GAMD024-1-0) had information in the Drilling spreadsheet, but not in the Collar spreadsheet. In this case, the information was transferred to the Collar spreadsheet.

The information present in the *Gamsberg East Competent Person's Statement Mineral Resources* (Potgieter, 2016), states that all drilling was NQ. Therefore the 21 drill holes with blank size entries were populated with NQ Core_Size_Info.

Four drill holes drilled by OCC, has "Percussion" as hole diameter under the Collar spreadsheet but no information captured under the Drilling spreadsheet. Two diamond core holes drilled by Okiep Copper Company (OCC) have core diameters recorded for the first couple of meters as a text comment with depths in Collar spreadsheet. This information is broken down into intervals in the Drilling spreadsheet. These entries were left as is.

Based on the information contained in each column, the Core_Size_Info column on the Collar Spreadsheet was retained, with the addition of the information populated as described above. This column was renamed to Hole_Diameter, which was considered more appropriate.

3.2.2. Assay Method

For 63 batches, two different assay methods were recorded, namely AROG_UN and AR_ICPES. AROG_UN is an Aqua Regia digest on ore-grade material with an unknown finish. AR_ICPES is an Aqua Regia digest with an ICPES finish.

In all of these batches, sample numbers and batch numbers were verified to confirm that the samples all occurred within the same batch. Since the *Gamsberg East Competent Person's Statement Mineral Resources* (Potgieter, 2016) states that all samples were assayed with an Aqua Regia Digest with ICP-OES finish, it was therefore assumed that all samples with assay method recorded as AROG_UN is actually AR_ICPES. All changes were recorded.

3.2.3. Sample Type

In the "Sample Type" column, information was captured as CHIPS for four historical percussion drill holes. Company reports state all other drilling to be diamond core (Reid & Harley, 2009; Potgieter, 2016). That information is also evident from drill diameters captured in the database. Based on that, an assumption was made that CORE drill type was not recorded and, in the spreadsheets, NR was replaced with CORE for all other samples. All changes

mentioned above was recorded in an additional spreadsheet, along with the old value, the new value, as well as the source of the new value.

3.2.4. Comments

The “Comments” field contains valuable information, mostly on the purpose and nature of the drill holes. These were simplified into a query-able column with standardised descriptions.

3.2.5. Excluded drill holes

Reid & Harley (2009) include a drill hole data inventory, in which 13 drill holes are noted to be excluded from both modelling and estimation. The authors cite an internal report by Neufeld (Neufeld, 2009 cited in Reid & Harley, 2009) which indicates a number of metallurgical deflections that were not considered suitable for modelling and estimation, as a result of not having survey data.

In the Collar spreadsheet, 18 holes had “Metallurgical Deflection” indicated as the drill purpose. It was assumed that these drill holes were the excluded holes referred to above. Further investigation of these drill holes showed that seven of these drill holes do not have assay data although they do have lithological data. However, the other 11 drill holes do have survey data in the dataset. Based on that, it was decided to include these 11 drill holes in modelling and estimation for this research study.

3.3. Overlaps in interval data

Overlapping and gaps in interval data checking is a crucial step of the data validation process, since overlapping intervals cause conflicts in geological software packages such as Vulcan and Leapfrog Geo - especially when compiling composites. Because of the relatively small number of entries in the Gamsberg East database, intervals were checked and corrected manually in Microsoft Excel.

To check for overlaps, the following method was used:

- Two blank columns were added to the spreadsheets containing interval data namely lithology and assay.
- These sheets were then sorted on two levels, first by hole_ID and then by the start depth (from) of the interval.
- In the first check column, end depth (to) of the previous interval was subtracted from the start depth of the interval under consideration. Wherever this value is negative, it indicates a potential overlap. Where this value is positive, it indicates a gap. However, since data was sorted according to hole_ID, a negative value would also occur at the start of each new hole.

- In the second check column, an IF statement was used, to check whether or not the entry was a new hole. The start of new holes was flagged with the entry “Start” in this column.
- The combination of these two conditions (check column 1 < 0 and check column 2 ≠ “Start”) indicated a true overlap.

No overlaps occurred for intervals in the Rock_Type or Final_SG columns of the Lithology and SG sheets, respectively. The Assay sheet did have 267 overlaps.

These overlaps are due to re-assays or second phases of sampling. A study of historical company reports led to awareness of the existence of re-assays, as well as holes for which re-assays were not available at the time of the previous preliminary resource assessment (Reid & Harley, 2009). Of the seven holes for which re-assays were outstanding, one hole (GAMD040 – 1- 0) now has re-assay data and one hole (GAMD035-5-0) has no assays available in the current database, although it does have lithology and survey data that can be used for geological modelling. As such, GAMD035-5-0 was considered for the purposes of geological modelling.

To identify re-assays, the batch number was used. Any hole where more than one batch number occurred was assumed to have been re-assayed. Since no data rankings or priorities on re-assays are available in the current database, all holes with more than one set of assays were considered separately. Re-assay intervals differed from original assays. This caused some confusion, as logged interval corresponded to the original batch sample intervals.

In the absence of additional information, a systematic approach was adopted using batch numbers and sample number sequences.

- In cases where intervals for batches had no overlap, it was considered as two separate batches - possibly a second phase of sampling. In such cases, both batches were considered valid and retained in the dataset.
- In cases where the batches fully or mostly overlapped, the second one, with a higher batch number and sample number sequence, was considered the re-assay and retained.

In one instance (GAMD037-1-2) the two batches were present in the holes, but the batches contained different mineralised intersections. In the unmineralized samples, there was some overlap between the two batches. In this case, the mineralised intersections on both batches were retained and five unmineralised samples causing overlap were removed.

For GAM091 and GAM092, two historical holes drilled by OCC, a second phase of sampling occurred, along intervals that differed from the original sampling. The second phase of samples only had assays for S, Ba, Mn, and Tl and were ignored for this research study.

One potential pitfall of this approach is the loss of SG information. SG intervals correspond to the logged intervals, and therefore also the original assays. The decision was taken not to transfer SG to re-assayed samples, since the SG interval would not correspond to the assay interval. Since SG is known to correlate strongly to mineral content, especially Pb, this decision can be justified.

SG sample information were stored separately from assays. Because SG intervals mostly correspond to assay intervals, a unique sample number was created by concatenating the drill hole number with the start depth value of the interval – for example the sample in GAMD027-0-0 starting at 730.29m would have a unique sample number of GAMD027-0-0_730.29. This unique sample number was then used as the primary field in a VLOOKUP function, which linked each SG to the corresponding assay.

3.4. QA-QC and duplicates

Although company reports refer to the implementation and results of QA-QC procedures (Reid & Harley, 2009; Potgieter, 2016), no check samples, apart from lab duplicates, exist for Gamsberg East in the current database. The discussion on QA-QC from Reid & Harley (2009) reveals that approximately 6 % of sample assays, equating to seven drill holes, within the orebody failed QA-QC. These samples were submitted for re-assay, but results had not been received in time for their final data cut-off. However, the failed assays were included in the estimation on request of Anglo American Exploration Division. These samples are listed in Appendix 1 of the Reid & Harley (2009) report.

As part of this research study these samples were identified in the summary sheet discussed in section 3.2. The seven drill holes are discussed in section 3.3. Considering that there are at present only five drill holes that failed QA-QC and that Reid & Harley stated that these only failed marginally, it was decided to include these samples in the study.

Another anomaly in the QA-QC for Gamsberg East noted by Reid & Harley (2009) was the performance of pulp duplicates vs. coarse duplicates. Half absolute relative difference (HARD) was calculated by halving the absolute difference between the two values divided by the mean of the two values. The formula is shown below as Equation 4

$$HARD = \frac{1}{2} \times \left[\frac{ABS\,(Assay\,1 - Assay\,2\,)}{\frac{(Assay\,1 + Assay\,2)}{2}} \right] \times 100\,\%$$

Equation 4

If the cumulative assays exceed a HARD limit of 10%, the observed error may be considered unacceptably high. In the Figure 3.2, the HARD plot for Zn is shown. In this plot the coarse duplicates had lower HARD values in comparison to the pulp duplicates.

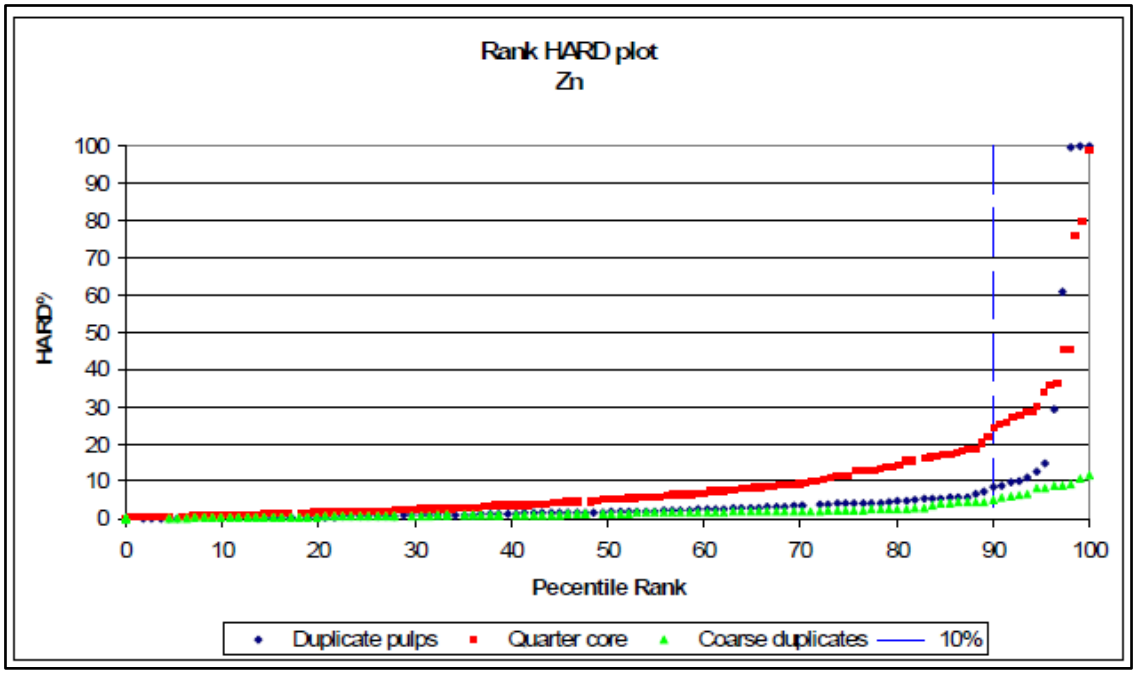


Figure 3.2 Ranked Half Absolute Relative Difference Plot for Zn duplicates in Gamsberg East.
(Reid & Harley, 2009)

Usually pulp duplicates would have lower HARD values due to greater homogenisation introduced by milling. This anomaly cannot fully be explained by poor splitting practices of pulps. The coarse reject duplicates are also milled and then split. Therefore, errors associated with pulp splitting practices should be accumulated within the coarse reject duplicate results. (Reid & Harley, 2009)

3.5. Samples without assay

For two drill holes, samples occur without assays. One of these holes (GAMSD061) is a new hole, drilled since the last evaluation of the deposit. On this hole, a different sampling methodology is used, where samples are created over unmineralised intersections, in order to capture SG measurements for waste material. These samples are marked with an N and not sent for assay. These 11 samples were removed.

- Another hole, GAMD014-0-0, has 25 samples without assays. These samples were removed.
- On GAMD35-0-1, the samples from 655.08 m to 657.08 m that is for 2 m are blank and were removed.

All removed samples were listed in two separate Microsoft Excel spreadsheets – one for blank samples and another for overlapping samples.

3.6. Samples with negative assays

During work conducted for *MINN7043* (Cloete, 2018) two samples were identified, with negative assays for Ag. Since the other values for these samples were considered valid, the samples were included, and the negative Ag values ignored.

3.7. Checking and Validation

From the above work, a shortened collar, survey, assay, and lithology sheet was compiled and imported into Leapfrog Geo to check for errors. This checking and validation are iterative. Validation issues flagged in Leapfrog Geo were noted down and addressed in Microsoft Excel. All changes were noted and captured in separate spreadsheets for record keeping purposes. The shortened versions were again imported into Leapfrog Geo and validated until database was fully validated and considered acceptable for further usage in this research study.

3.8. Desurveying

To create samples for EDA, drill holes were imported into Vulcan using a custom database design that accommodates all relevant fields in the collar, survey, assay, and lithology sheets. Data was desurveyed in Vulcan. In Vulcan this is done through a method called Straight Compositing. All assays, SG, logged mineral percentage, textural information and rock type was recorded for each sample.

Executing the composite function, no conflicts were identified; this is a good indication that the database is valid. It is very important to keep in mind that different software packages use different default methods for desurveying. Leapfrog Geo uses a spherical arc method and Vulcan a tangential method. The default method has to be considered and appropriately changed to ensure compatibility between the software packages.

3.9. Summary and Conclusion

In this chapter, the essential data assumptions were discussed. Drill hole data relevant to the study area was identified from a larger dataset and compiled into a subset. A summary was made to serve as an indication of the completeness of the subset. The drill hole data was then validated, checking specifically for

overlaps in interval data, samples without assays and samples with negative assays. In addition to that, the historical QA-QC results presented by Reid & Harley (2009) were reviewed and the information presented was incorporated into the summary of the drill hole data. Finally, data was desurveyed to create a sample dataset of variable composites for the next stage.

First Stage Data Analysis is a time-consuming and often frustrating, iterative process; especially where record keeping is spurious or a project has changed ownership, such as is the case for Gamsberg East. However, it serves the purpose of familiarising the resource estimation practitioner with the dataset being studied – what it contains but also what it does not contain. This knowledge should be used as inputs when considering a Mineral Resource classification scheme. The product of this kind of process is a validated dataset, which is familiar to the practitioner.

4. EXPLORATORY DATA ANALYSIS

The main purpose of EDA is to improve the quality of the estimate by gaining insight into the data. Specific goals of an EDA study can be to familiarise oneself with the statistical characteristics of the variable of interest, to recognize the spatial variation of elements of interest or geological domains, to identify outliers or errors, or to evaluate differences between different kinds of raw data. (Sinclair, 1998). According to Abzalov (2016), EDA can provide insights into domaining and wireframing, which could lead to the revisiting of these.

For this research study, EDA was conducted mostly in Microsoft Excel but with some additional specialist work, specifically fitting continuous distributions in JMP13 software. Composites were transferred as .txt files into JMP13.

4.1. Statistically Defining Zones of Interest.

To define the areas of interest to be modelled, the following steps were followed: Firstly, a cumulative probability distribution (CPD) was plotted for Zn % for the entire dataset see Figure 4.1.

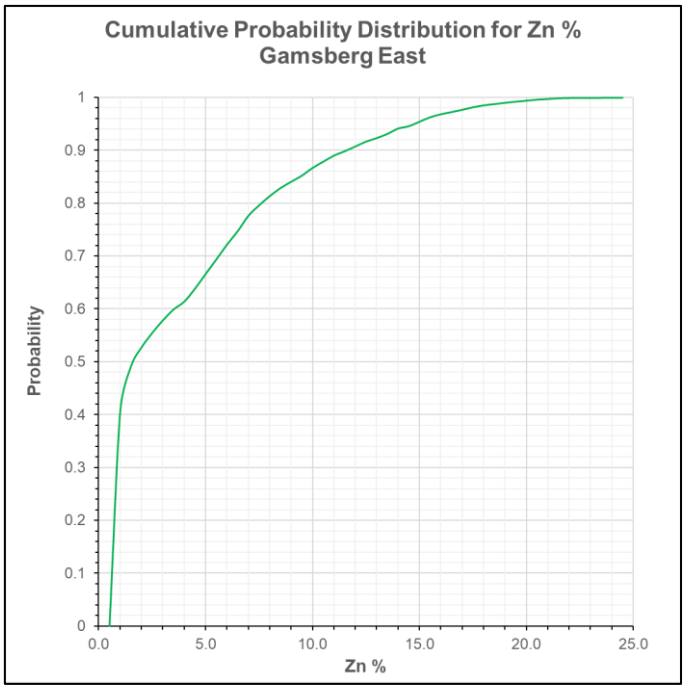


Figure 4.1 Gamsberg East CPD for the entire Zn % data set.

The CPD plot is repeated but focussing on grades below 10 Zn % and shown in Figure 4.2. Two inflextion points can be observed at 3.6 Zn% and approximately 7 Zn %, indicating the possibility of two Zn % populations.

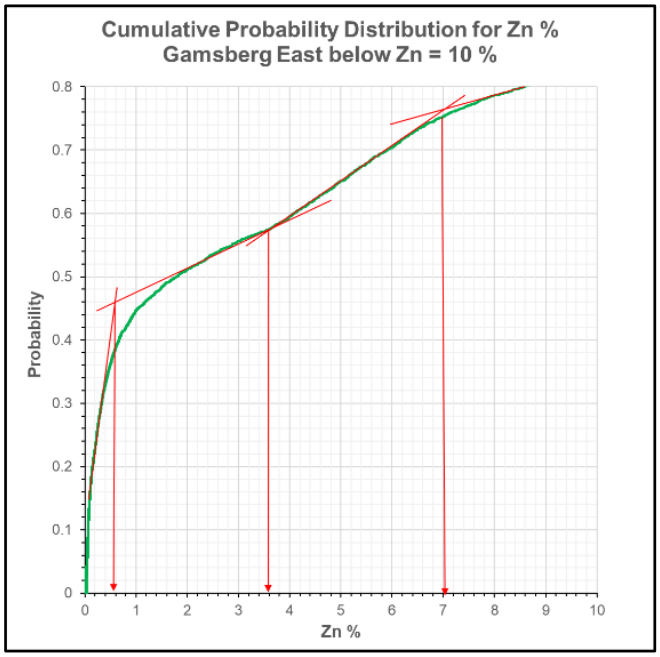


Figure 4.2 Gamsberg East CPD for Zn below 10 %.

Next, a bar chart of rock types was plotted (Figure 4.3), to find the majority of lithologies that represented by the samples. Considering common exploration sampling procedures, these can be assumed to be the ore lithologies. Since the dataset contains 49 unique lithological codes, only 19 rock types that each represents 1% or more of the total population were plotted. The remaining 30 rock types combined represent 11.4% of the total population. From Figure 4.3, it can be seen that PEO and MPO represent 29% and 11% of the total population, respectively.

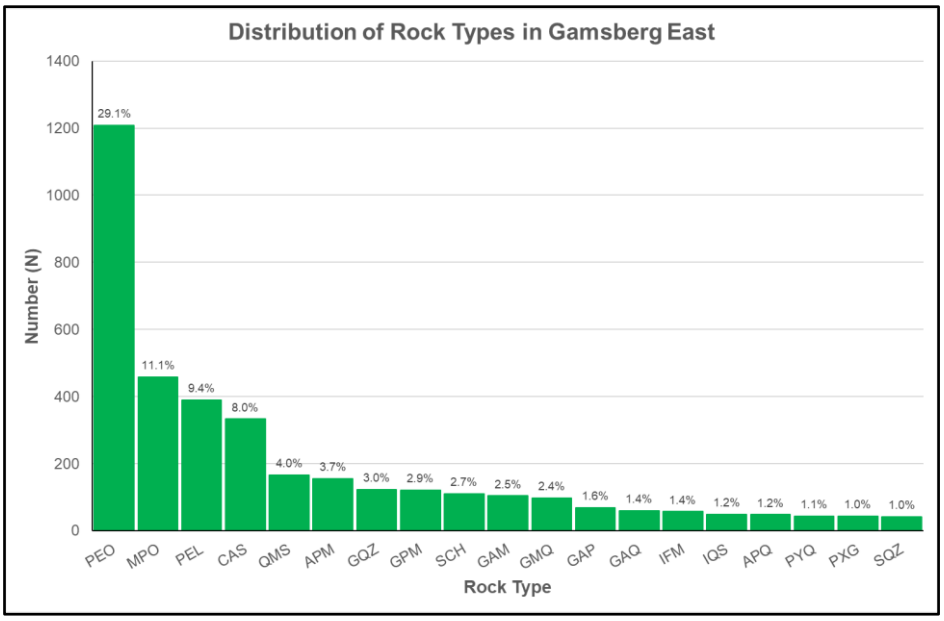


Figure 4.3 Gamsberg East Distribution of rock types.

A table of average Zn % grades was compiled in Microsoft Excel to get an overview of grades per rock type. From this summary, six rock types with mean Zn % > 3.6 % Zn were identified. These are SBO, MPO, PEO, PEO_Po, CLT and ORE. A description of rock types is provided below in Table 4.1.

Table 4.1: Description of Rock Types (Anglo American Exploration, 2010) with mean Zn % > 3.6 % Zn.

Rock Type	Description
SBO	Sulphide Breccia
MPO	Pyroxene-Amphibole-Garnet-Magnetite hosted ore
PEO	Quartz-Sillimanite pelite hosted ore
PEO_Po	Quartz-Sillimanite pelite hosted ore with dominant pyrrhotite
ORE	Historically logged, unspecified mineralisation
CLT	Chlorite Fels

To complete the descriptive statistical analysis for these rock types summary statistics were calculated in Microsoft Excel, and these appear in Table 4.2**.** Which reveals that SBO has the highest mean grade at 10.437 % Zn as well as the highest variance. It is however necessary to note that there only 11 samples of this rock type.

Table 4.2: Summary Statistics for Rock Types with mean Zn % > 3.6 % Zn.

	Rock Type	Variable Composites					
		SBO	MPO	PEO	PEO_Po	CLT	ORE
Zn	N	11	459	1208	10	5	10
	Mean (%)	10.437	10.207	7.148	7.099	4.742	3.923
	Standard Devation (%)	5.942	5.212	3.824	2.618	5.193	1.828
	Variance (% ^{2})	35.313	27.167	14.621	6.852	26.972	3.343
	Median (%)	12.300	10.250	6.165	5.970	2.150	3.280
	Mode (%)	12.750	10.200	4.860			
	CV	0.569	0.511	0.535	0.369	1.095	0.466
	Kurtosis	2.795	2.259	2.259	3.414	8.413	- 1.257
	Skewness	- 0.700	- 0.036	1.214	0.878	2.267	0.579
	Maximum (%)	18.900	25.100	24.500	11.800	17.400	7.400
	Minimum (%)	0.348	0.230	0.049	2.870	0.460	1.830
	IQR (%)	4.890	7.980	4.205	3.500	3.188	3.443
	Range (%)	18.552	24.870	24.451	8.930	16.940	5.570

To investigate the spatial relationships between these rock types, rock types were plotted in 3D using Leapfrog Geo (Figure 4.4). From this, it can be seen that PEO occur above MPO. From company reports, it is known that MPO occurs above PEO stratigraphically (Anglo American Exploration, 2010), but also that Gamsberg East is over-turned (Reid & Harley, 2009; Potgieter, 2016), hence the reversal of the sequence.

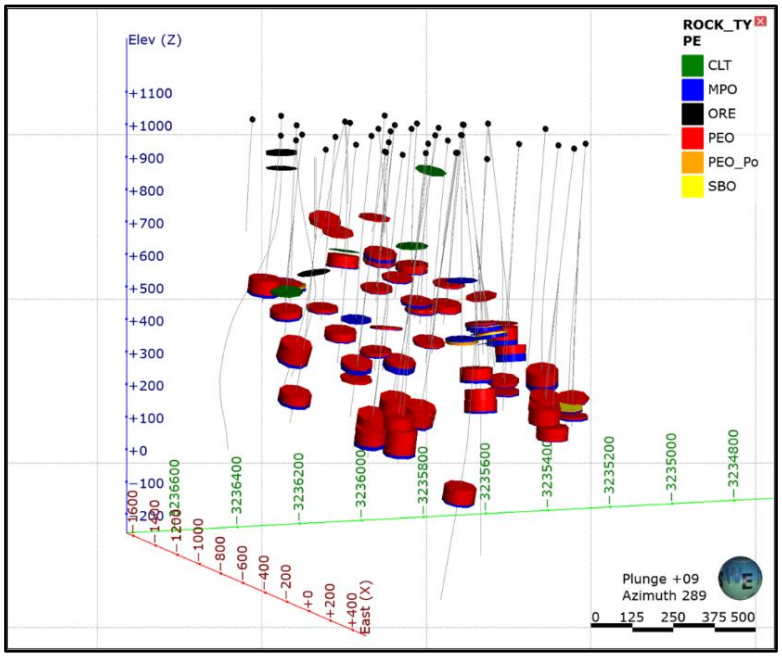


Figure 4.4 Spatial Plot of Rock Types with mean Zn % > 3.6 % Zn.

In the case of ORE, one hole (GAM092) intersects the main body of drilling. The other hole in which this rock type occurs (GAM091) is far removed and up-dip of the main drilled zone. Since there is precedence for excluding these intersections in the literature (Reid & Harley, 2009) and due the large spacing between GAM091 and the main body of drilling, this rock type was not considered.

A massive chlorite fels (CLT), occur in 4 drill holes and at two distinct stratigraphic positions. In the sample dataset, there is only a single logged interval of CLT, consisting of 5.7 m occurring in GAMD26-0-0. The other occurrences of CLT had not been sampled and therefore do not occur within the sample dataset. The interval in GAMD26-0-0 was sampled at approximately 1m intervals to produce 5 samples. In the original exported dataset, a summary column of the primary lithology code column (Lith1_Sum) categorised CLT as “Other”. Due to the low sample number and the wide spatial distribution of CLT, the rock type was not considered.

From the spatial plot in Figure 4.4, PEO_Po appear analogous to PEO in space. A stratigraphic column in the *Gamsberg Project Manual* has PEO and PEO_Po

grouped as a single unit and described as quartz sillimanite pelite hosted ore and quartz-sillimanite pelite hosted ore with dominant pyrrhotite, respectively (Anglo American Exploration, 2010). PEO and PEO_Po also show very similar grades (Table 4.2). Based on this information, PEO_Po was considered part of PEO.

Although it has the highest mean Zn % grade, SBO has very few samples and occurs mostly within PEO. Based on that and historical reports (Reid & Harley, 2009; Anglo American Exploration, 2010), SBO was considered as part of that unit.

Based on the above, a new column of simplified rock types was created in Microsoft Excel. In this column, MPO and PEO were retained and PEO_Po and SBO were recoded as PEO. ORE and CLT, totalling 15 samples, were not considered for this research study. MPO and the recoded PEO was combined to form a dataset of 1688 variable composite lengths.

4.2. Determining Data Support and Composite length

Support is the size, shape and orientation of samples and can have a great effect on the variability of grades (Sinclair, 1998). To determine the correct composite length for the Gamsberg East deposit, a distribution was plotted for all sample lengths across the entire deposit. The results are shown in Figure 4.5. Sample length shows a bimodal distribution with the highest peak at 1 m (59.7 % of data) and a second peak at 2 m (22 %).

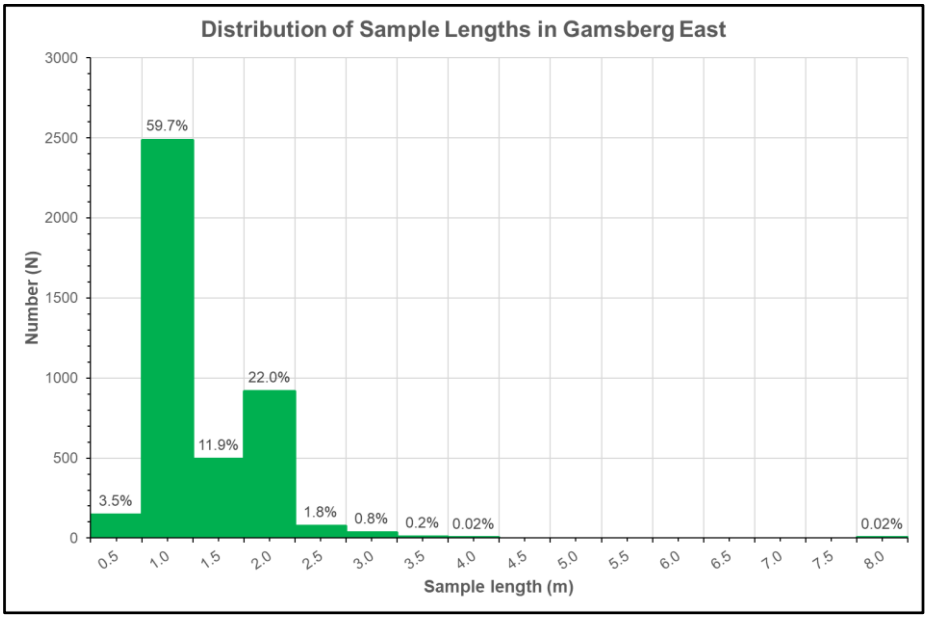


Figure 4.5 Distribution of Sample Length across Gamsberg East.

Sample length distributions were also plotted for the MPO and PEO subset (Figure 4.6). This distribution showed the same bimodal distribution, with 72.2% of the samples falling in the 1 m interval and 13.4% of samples falling in the 2 m interval.

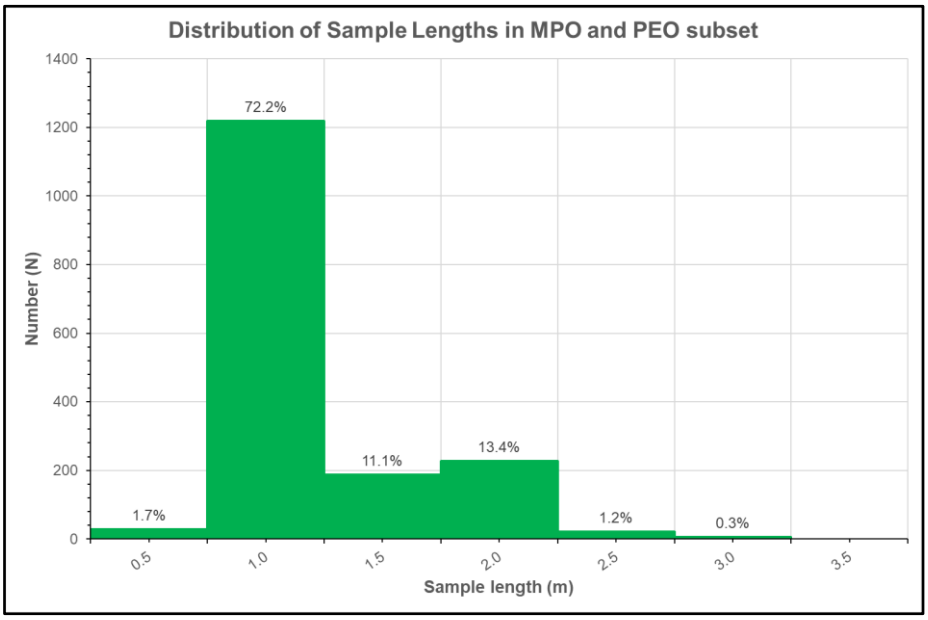


Figure 4.6 Gamsberg East MPO and PEO variable Sample Length Distribution.

Decompositing longer samples down to 1 m intervals, will decrease the variance at short range. When a 2 m sample is decomposited to two 1 m samples with the same value, the variance between them would be zero. This will result in a lowered nugget effect when considering variograms. Therefore decompositing is generally not advised. Nonetheless, since the majority of data is sampled at 1 m, it was decided to use 1 m as the composite length of choice for the research study.

A run length composite was done in Maptek Vulcan, compositing all assay values, and recording lithology, mineral, structural, drill, and assay type. Drill holes were composited to 1m controlled by geology, meaning that if the recorded lithology changes a new sample would be created.

Drill holes were composited downhole starting from the top of the hole, with intervals < 0.5 m merged to the previous interval. The resulting sample length distribution after composting appears in Figure 4.7 below, 94 % of samples now has a sample length of approximately 1 m.

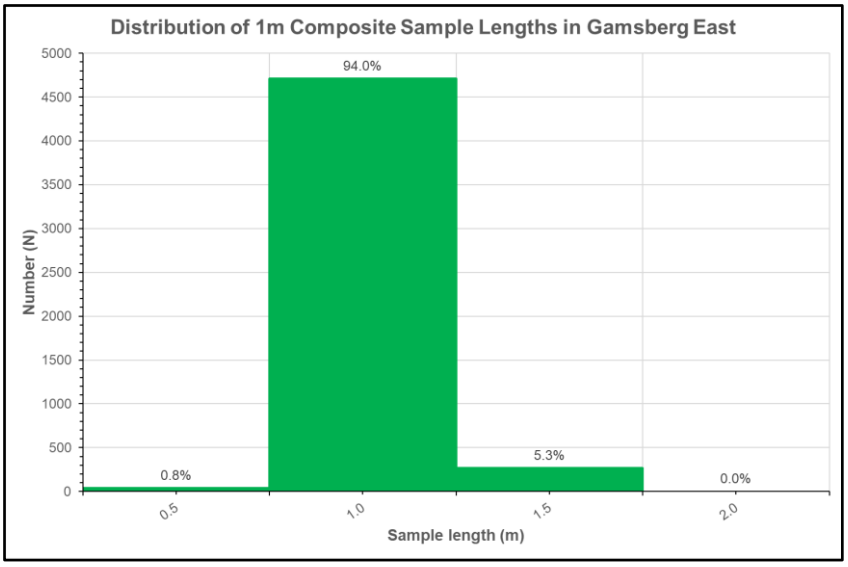


Figure 4.7 Gamsberg East MPO and PEO Sample Length Distribution after compositing to 1 m.

According to Abzalov (2016) composites should not change the mean grade or metal content. Tabulated Zn grades (%) for uncomposited samples vs 1 m composites are shown below in Table 4.3.

Table 4.3: MPO and PEO: Summary of statistics for Zn % for variable length composites and 1m composites.

	MPO		PEO	
	Variable composite	1 m composite	Variable composite	1 m composite
N	459	531	1229	1382
Mean (%)	10.207	10.120	7.177	7.183
Standard Devation (%)	5.212	5.052	3.849	3.714
Variance (%^{2})	27.167	25.525	14.812	13.793
Median (%)	10.250	10.200	6.180	6.170
Mode (%)	11.000	10.200	4.860	4.860
CV	0.511	0.499	0.536	0.517
Kurtosis	2.259	2.320	4.496	4.428
Skewness	-0.036	-0.017	1.186	1.176
Maximum (%)	25.100	24.150	24.500	24.500
Minimum (%)	0.230	0.456	0.049	0.183
IQR (%)	7.980	7.697	4.290	4.149
Range (%)	24.870	23.694	24.451	24.317

For MPO and PEO the difference between the means of the variable length composites and 1 m composites are 0.087 Zn % and - 0.006 Zn % respectively. Indicating that compositing did not significantly affect the mean Zn % grade. A slight decrease in standard deviation, CV, IQR and range confirms the expected decrease in variability. Furthermore, the shape of the grade distribution remains largely unchanged, as can be seen in the similarity of the skewness and kurtosis parameters before and after compositing. In view of the above- analysis, it was considered valid to proceed to the next step of the EDA with the 1 m composited dataset consisting of 1 913 samples.

4.3. Comparison of Drill Type

From metadata captured in the database, as well as historical reports, it is known that, with the exception of three historical holes drilled by OCC (Reid & Harley, 2009), all holes are diamond core. In the First Stage Data Analysis, sample types were populated using this information. In the Gamsberg East dataset, diamond core represents 88.4% of composites (Figure 4.8). In the combined MPO and PEO 96.9 % of samples are diamond core (Figure 4.9).

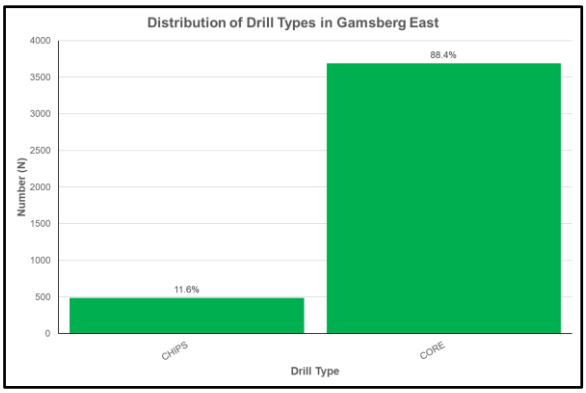


Figure 4.8 Gamsberg East Distribution of drill methods.

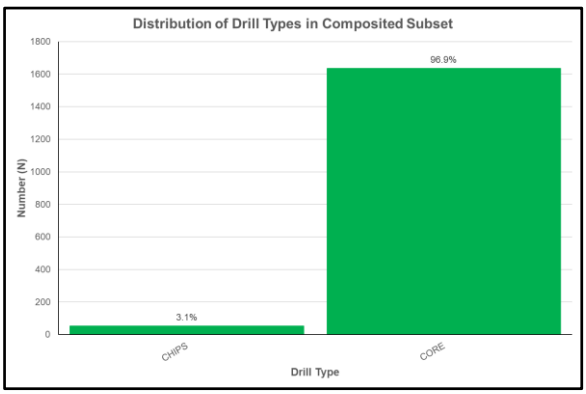


Figure 4.9 Gamsberg East MPO and PEO Distribution of Drill Types 1 m composites.

The summary statistics (Table 4.4) for the combined MPO and PEO shows that the chip samples have a lower mean grade, less variation in grade and a more peaked and skewed distribution compared to the diamond core samples.

Table 4.4 Summary Statistics per drill type.

	MPO		PEO		Combined	
	CHIPS	CORE	CHIPS	CORE	CHIPS	CORE
N	5	454	47	1182	52	1636
Mean (%)	14.362	10.161	7.200	7.176	7.889	8.004
Standard Devation (%)	4.252	5.207	2.312	3.898	3.284	4.503
Variance (%^{2})	18.077	27.115	5.343	15.193	10.782	20.275
Median (%)	15.350	10.250	6.450	6.150	6.590	6.805
Mode (%)	-	11.000	-	4.860	-	10.200
CV	0.296	0.512	0.321	0.543	0.416	0.563
Kurtosis	3.502	2.263	3.067	4.431	5.596	3.118
Skewness	-0.530	-0.028	0.444	1.184	1.372	0.803
Maximum (%)	19.550	25.100	12.700	24.500	19.550	25.100
Minimum (%)	8.160	0.230	1.840	0.049	1.840	0.049
IQR (%)	3.450	7.953	2.785	4.353	3.283	6.050
Range (%)	11.390	24.870	10.860	24.451	17.710	25.051

Since there are only 52 chips samples (3.1% of the combined MPO and PEO) it was not considered practical to treat these as a separate population at this stage.

4.4. Comparison of Assay Method

Various methods are listed in the database under “GenericMethod” in the Assay sheet. However, many of these entries are blank or recorded as a combination of UN – indicating an unknown method, and an additional code – for example, AROG_UN, where the first part of code indicating an Aqua Regia digest (AR) on ore grade material (OG). The “UN” portion of the code indicates that the rest of the method is unknown.

In the First Stage Data Validation process, these data were examined, and it was found that 64 batches had two different assay methods. These were edited as described in section 3.2.

As a result of that, three assay methods remain. The proportion of assay methodology is graphically summarised below in Figure 4.10 for all composites in the Gamsberg East dataset.

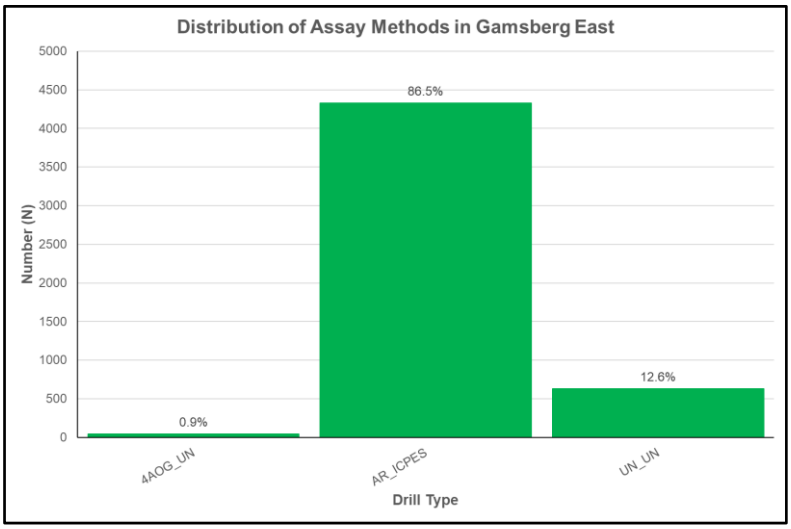


Figure 4.10 Gamsberg East Distribution of assay methods.

A cumulative probability distribution plot of Zn grades (%) was plotted per method across all composites to compare the methods for bias (Figure 4.11). The CPD plots for the AR_ICPES and 4AOG_UN methods display similar shapes, with the plots for the UN_UN method showing a distinctly different shape. The summary statistics (Table 4.5) explain the shape of UN_UN in Figure 4.11.

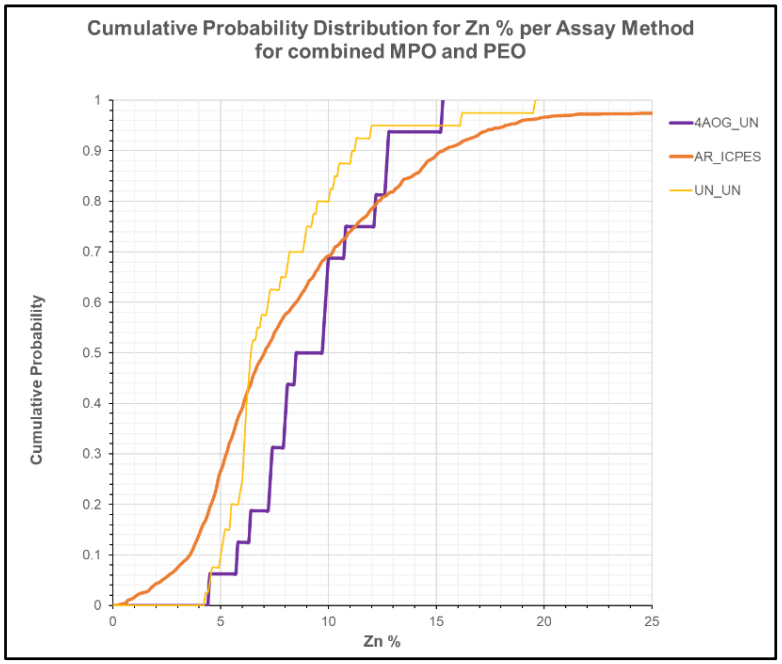


Figure 4.11 Zn % CPD plots comparing different assay methods.

Table 4.5: Summary Statistics per assay method.

		4AOG_UN	AR_ICPES	UN_UN
Zn	N	43	4340	631
	Mean (%)	3.960	3.864	0.807
	Standard Devation (%)	4.581	4.744	2.134
	Variance (% ^{2})	20.986	22.506	4.552
	Median (%)	2.055	1.414	0.070
	Mode (%)	0.027	4.860	0.880
	CV	1.157	1.228	2.645
	Kurtosis	2.500	4.086	22.860
	Skewness	0.909	1.341	4.030
	Maximum (%)	15.270	24.500	19.550
	Minimum (%)	0.024	0.001	0.003
	IQR (%)	7.564	5.995	0.244
	Range (%)	15.246	24.499	19.547

It can be seen that the UN_UN method has the lowest mean grade, is a highly skewed, leptokurtic distribution. This, alongside the IQR indicates that most samples have low grades, which contributes to the shape of the CPDs.

The summary statistics and CPD plots also suggest that higher grade material is more likely to have the assay method recorded. However, the more pronounced stepped nature of the CPD plots for 4AOG_UN and UN_UN indicates that the data is sparse. Conversely, the smoothness of the CPD plot for AR_ICPES indicates high data density. The sparsity of the data for the other methods makes the comparison unreliable.

Historical reports only make mention of assays being done using an Aqua Regia digest with an ICP-OES finish (Potgieter, 2016). For 43 samples the method is listed as 4AOG_UN. This indicates a 4-acid digest on ore grade samples with an unknown finish. Since the digestion on these samples are specifically recorded as a different method, these samples could indicate a high-grade population and should be examined spatially.

These samples all occur in GAMD014-0-0 and GAMD015-0-0. A 3D spatial plot of assay method is shown below in Figure 4.12. Since 4AOG_UN method only occur in two drill holes and these are located apart from one another, these samples appear to be spatially uncorrelated.

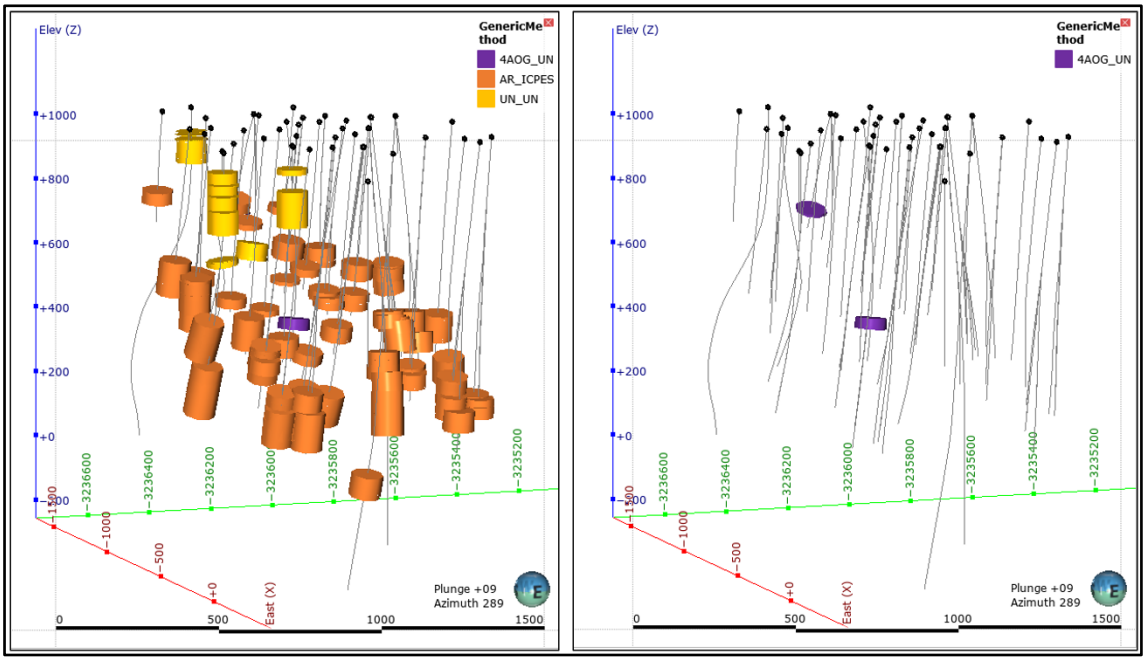


Figure 4.12 Gamsberg East 3D spatial plot of all assay methods (left) and 4AROG_UN method (right).

The conclusion from the 3D spatial plot can be reaffirmed by looking at a histogram for Zn grade of 4AOG_UN samples plotted over the Zn % grade for the entire population. In Figure 4.13, the highlighted portions of the bars represent these samples. Although 4AOG_UN samples only represent 1.18 % of the total population, the relative frequency distribution still shows that the distribution of these samples is roughly the same as that of the population, with the bulk of the 4AOG_UN occurring at low grades. From this, samples assayed using the 4AOG_UN cannot be said to form a distinct population.

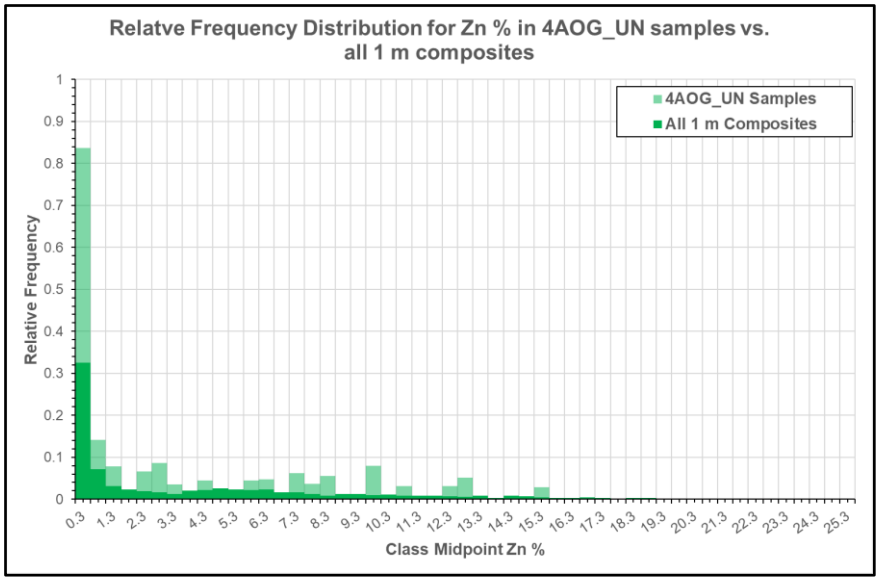


Figure 4.13 Distribution of Zn grade with that of 4AOG_UN samples (50 % transparency).

4.5. Correlations and Bivariate Scatterplots

Scatterplots are a simple and useful way to summarise bivariate data and can provide a quick way of checking the correlation between variables or for outliers in duplicate data. Correlation coefficients can be calculated from these plots and range from -1 to 1, indicating how similar two variables are. (Sinclair, 1998). It was decided to use correlation matrices, which are easily generated in Microsoft Excel, to first identify strong correlations numerically, which would then be investigated visually.

The correlation matrix for all elements of interest for variable composites of all rock types is shown in Table 4.6. From the off-diagonal cells highlighted correlation matrix it can be seen that strong correlation exists between Cd and Zn (0.91), Ag and Pb (0.69), and Fe and SG (0.60), SG and weaker correlation between S and Zn (0.52) as well as S and Cd (0.51).

Table 4.6 Correlation Matrix for all rock types.

	SG (g/cm^3)	Zn (%)	Pb (%)	Cu (%)	Ag (ppm)	Fe (%)	Cd (ppm)	Co (ppm)	S (%)
SG (g/cm^3)	1.000								
Zn (%)	0.470	1.000							
Pb (%)	0.162	0.220	1.000						
Cu (%)	0.017	0.073	0.166	1.000					
Ag (ppm)	0.065	0.114	0.693	0.096	1.000				
Fe (%)	0.663	0.394	0.064	0.084	0.077	1.000			
Cd (ppm)	0.429	0.905	0.225	0.058	0.147	0.380	1.000		
Co (ppm)	0.147	0.115	0.056	0.083	0.090	0.232	0.109	1.000	
S (%)	0.365	0.517	0.120	0.086	0.244	0.603	0.506	0.259	1.000

A correlation matrix for the combined MPO and PEO 1 m composites shows a different picture (Table 4.7). Here, Cd and Zn, and Ag and Pb more strongly correlated but the correlation of Fe with SG and S weakens. Instead, a strong correlation between Cu and Fe is observed.

Table 4.7 Correlation matrix for composite combined MPO and PEO.

	SG (g/cm^3)	Zn (%)	Pb (%)	Cu (%)	Ag (ppm)	Fe (%)	Cd (ppm)	Co (ppm)	S (%)
N	**1209**	**1913**	**1913**	**1913**	**1913**	**1913**	**1913**	**1913**	**1913**
SG (g/cm^3)	1								
Zn (%)	0.29203	1							
Pb (%)	0.06355	0.14754	1						
Cu (%)	0.08012	-0.22968	-0.13818	1					
Ag (ppm)	0.03047	0.09154	0.87473	0.05348	1				
Fe (%)	0.42371	-0.25708	-0.13115	0.71002	-0.00152	1			
Cd (ppm)	0.19974	0.80194	0.19537	-0.18716	0.1234	-0.22612	1		
Co (ppm)	0.14707	-0.08149	0.01914	0.17963	0.08488	0.27408	-0.06415	1	
S (%)	-0.0507	-0.03073	-0.00465	0.41585	0.10559	0.27303	0.01603	0.19103	1

Bi-variate scatterplots for Cd and Zn, Ag and Pb and Cu and Fe were drawn for the MPO and PEO rock types combined as well as for the two rock types individually. The R^2 value calculated for each element pair.

Figure 4.14 displays the bivariate scatter plots for Cd versus Zn. Whilst good correlation between the two variables exists for the combined rock types the Cd/Zn correlation is weaker in MPO, stronger in PEO.

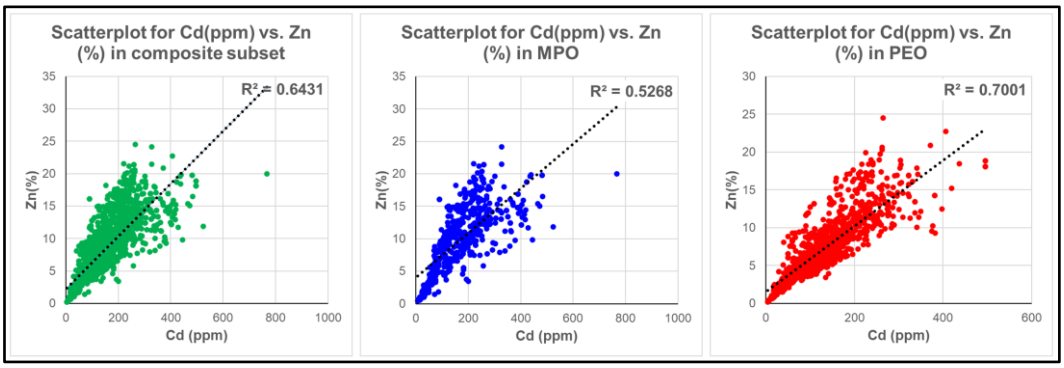


Figure 4.14 Bivariate scatterplots for Zn vs. Cd for the MPO and PEO units combined(left), MPO (centre) and PEO (right).

Cadmium can occur in sphalerite in concentrations up to 1 % and earn refinery credits (Jones, 1997 cited in Emsbo, *et al.*, 2016). Within the dataset, some estimated mineral percentages were logged and are shown in Table 4.8. Although the data is sparse, it does suggest that PEO has a higher occurrence of sphalerite than MPO, which could explain the higher correlation of Cd to Zn seen for the PEO.

Table 4.8 Logged mineral percentages per rock type for MPO and PEO.

Logged Mineral content (%)	**MPO**	**PEO**
Chalcopyrite ($CuFeS_2$)	1.6	3.1
Galena (PbS_2)	0.6	0.6
Sphalerite (ZnS)	15.3	15.4
Pyrrhotite ($Fe_{(1-x)}S$)	9.5	22.4
Pyrite (FeS_2)	3.2	6.2
Magnetite (Fe_3O_4)	10.5	1.1

The Ag/Pb correlation is stronger in both the individual rock units PEO and MPO than for the rock units combined see Figure 4.15 below. Logged mineral percentages indicate roughly similar percentages of galena in both units. Since Ag is known to occur with Pb in the Gamsberg deposit, this could explain the correlation between those elements in both units.

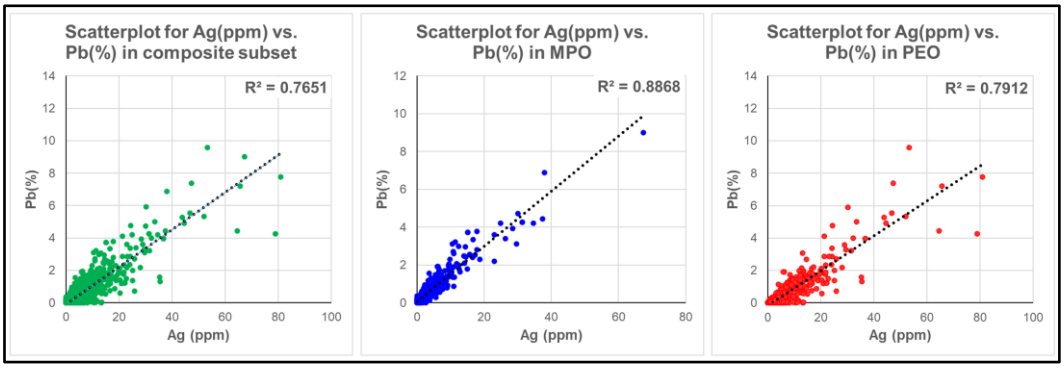


Figure 4.15 Bivariate scatterplots for Pb vs. Ag for the MPO and PEO units combined(left), MPO (centre) and PEO (right).

The Cu/Fe correlation is very weak in MPO and strong in PEO presented in the bivariate scatter plots appearing in Figure 4.16. As with the Cd/Zn and the Ag/Pb correlations, logged mineral percentages suggest that magnetite is 10 % more abundant in MPO than PEO, which is expected since MPO is a magnetite -garnet amphibole rock. In addition, chalcopyrite is twice as abundant in PEO than in MPO. More chalcopyrite, which has Cu and Fe, in PEO and more magnetite, which mainly has Fe, in MPO results in the observed correlations.

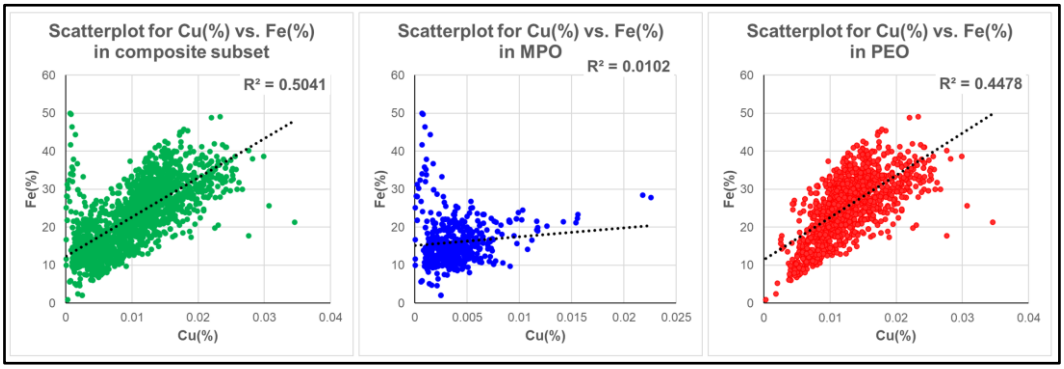


Figure 4.16 Bivariate scatterplots for Cu vs. Fe for the MPO and PEO units combined(left), MPO (centre) and PEO (right).

One use of correlations would be to act as indicator, in the sense that if two variables have a strong correlation (high R^2 value), the regression could be used to estimate a missing value for one of those variables, from the variable that is present. In the composited dataset this application is not applicable since all variables, except for SG have the same number of values (Table 4.7). SG has a correlation of 0.42371 with Fe. Although this correlation is not particularly strong, it could be useful in estimating SG. Historically, SG values were assigned per rock type (Reid & Harley, 2009; Potgieter, 2016). Using a regression equation to calculate SGs or coregionalisation to inform co-kriging could provide a better estimate.

4.6. Analysis of Outliers

An outlier is a value that appears inconsistent with the majority of the other data points (Sinclair, 1998). Outliers can cause large variability in estimates of statistical parameters and can result in unusually high values in block estimation or even negative grade where it coincides with negative kriging weight (Sinclair, 1998). Outliers may be indicative of a geological domain with very different properties and continuity, which might need separate consideration during estimation. An outlier population could be as the result of errors (sampling, assaying or contamination, etc.), or it could be a legitimate sub-population based on geology. One of the purposes of data evaluation is to distinguish the latter type of outliers. (Sinclair, 1998). Outlier analysis should be done on original, uncomposited assays. If composites are used, the outlier values may already have been smoothed (Rossi & Deutsch, 2014).

The assay and outlier analyses were done in Microsoft Excel. Since the two rock types identified in section 4.1 have different geological and mineralogical properties, the outlier analyses were done individually for both. One of the purposes of outlier analyses is to identify different geological domains (Sinclair, 1998), doing the analysis on a combined domain would only highlight that it should be domained.

To calculate outliers, the 10th and 90th percentiles were calculated for each element. An inter quantile range was calculated and a multiplier of 3 used to determine the upper and lower threshold for outliers. All values beyond these thresholds were considered outliers. The choice of the percentiles and the multiplier was informed by default values used in the statistical package *JMP 13* (SAS Institute Inc., 2016). The results are shown below in Table 4.9.

Table 4.9: Outliers for MPO and PEO.

		SG (g/cm^3)	Zn(%)	Pb(%)	Cu (%)	Ag(ppm)	Fe(%)	Cd(ppm)
MPO	1st Quartile	3.470						
	3rd Quartile	3.780						
	10th Percentile		2.644	0.028	0.001	0.300	9.780	46.280
	90th Percentile		16.780	1.652	0.007	9.900	23.220	304.400
	IQR	0.310	14.136	1.624	0.006	9.600	13.440	258.120
	Low Threshold	2.540	-39.764	-4.845	-0.016	-28.500	-30.540	-728.080
	High Treshold	4.710	59.188	6.525	0.024	38.700	63.540	1078.760
	Number of outliers	3	0	14	0	3	0	0
PEO	1st Quartile	3.400						
	3rd Quartile	3.740						
	10th Percentile		3.464	0.020	0.007	1.200	13.980	55.180
	90th Percentile		12.780	0.997	0.019	10.020	35.240	229.200
	IQR	0.340	9.316	0.977	0.012	8.820	21.260	174.020
	Low Threshold	2.380	-24.484	-2.911	-0.030	-25.260	-49.800	-466.880
	High Treshold	4.760	40.728	3.927	0.056	36.480	99.020	751.260
	Number of outliers	10	0	18	0	17	0	0

For SG, using the 10th and 90th percentiles produced unrealistic low threshold values that do not occur in mineralised rocks. Considering that SG is a normally distributed variable, the 1st and 3rd quartiles were used, with a multiplier of 3.

For the MPO and PEO these outliers were plotted spatially and highlighted to visually establish any spatial relationship between variables outliers, if any is present. The spatial plots of MPO outliers appear in Figure 4.17 and for the PEO the spatial plots of outliers appear in Figure 4.18

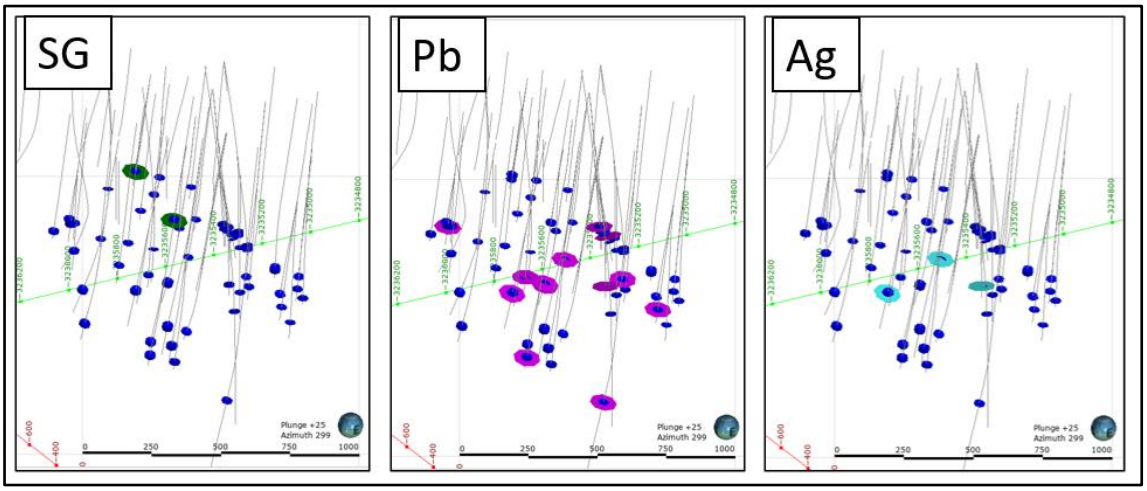


Figure 4.17 Spatial plot of outliers in MPO.

In the MPO, all Ag outliers correspond to Pb outliers. MPO has three SG outliers, three Ag outliers and 14 Pb outliers. All the Ag outliers (three samples) coincide with Pb outliers. Two of these samples show brecciation with galena, pyrrhotite, sphalerite and pyrite.

Outliers of Pb appear to form a cluster around GAMD051-0-0. To the East of this cluster the dip of the MPO unit steepens, indicating the possibility of enrichment in a fold hinge.

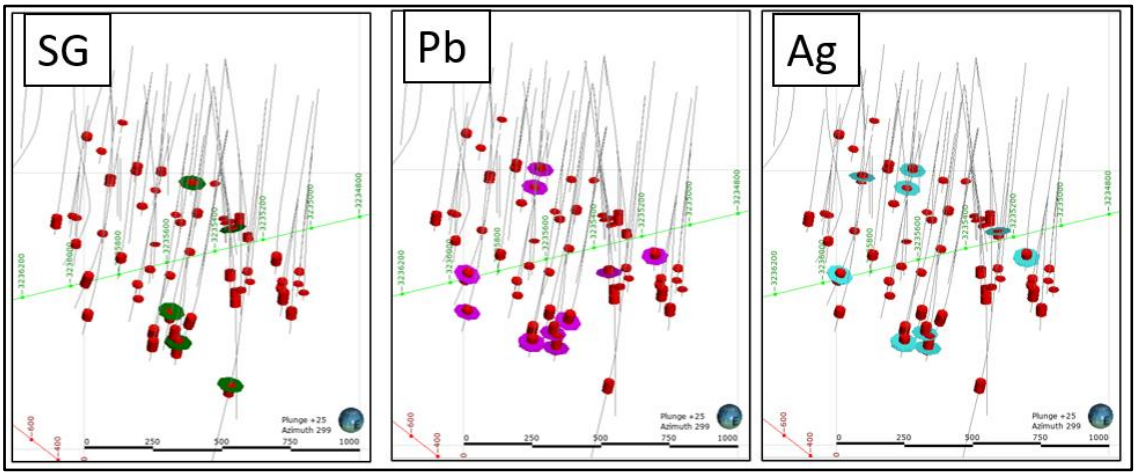


Figure 4.18 Spatial plot of outliers in PEO.

For PEO, most Pb and Ag outliers occur together (14 samples), with a cluster of these (7 samples) occurring down dip to the east. This corresponds to the Ag/Pb correlation in PEO as shown in Figure 4.15 The spatial clustering of these values imply that they represent a distinct population. Further investigation into these samples, does not reveal much. All samples were originally logged as PEO, but additional information regarding mineral percentages and textures are erratically captured and only occur for two of these samples, indicating a medium to coarse grained sample with approximately 10 % Pyrrhotite.

Although some of the outliers in PEO might represent a separate population, the number of data available is too small to create a domain from. Since spatial plots indicate the outlier values to be based on fact and not simply errors, these values will be kept in the dataset for further use.

4.7. Statistics and Histograms for Zn % grade

Since zinc is the economic driver in the deposit in question, it was decided to focus on the distribution of Zn % grades in this research study. Summary statistics were calculated for the 1 m composites in the two lithologies and are presented in Table 4.10 and are discussed below.

Table 4.10: Summary Zn % Statistics of1 m composites in the MPO and PEO.

	Rock Type	1m composite	
		MPO	PEO
Zn	N	531	1382
	Mean (%)	10.120	7.183
	Standard Devation (%)	5.052	3.714
	Variance (% ^{2})	25.525	13.793
	Median (%)	10.200	6.170
	Mode (%)	10.200	4.860
	CV	0.499	0.517
	Kurtosis	2.320	4.428
	Skewness	-0.017	1.176
	Maximum (%)	24.150	24.500
	Minimum (%)	0.456	0.183
	IQR (%)	7.697	4.149
	Range (%)	23.694	24.317

Analysing the statistical parameter values of the 1 m composites in Table 4.10 lead to the following interpretations regarding the shape of the probability distributions of the Zn % in the PEO and MPO units.

Firstly, the order of the measures of central tendency namely the mean, median and mode provide an indication of symmetry of a distribution. In the case of PEO, the Mode (4.86) < Median (6.17) < Mean (7.183) of the Zn % typical of a positive skewed probability distribution. However, for MPO Zn % the Mode = Median (10.20) which is similar to the Mean (10.12), indicating a more symmetrical probability distribution of the grade.

Secondly, in terms of the spread parameters of the Zn % the PEO has the largest range, but a much smaller Inter Quantile Range (IQR) than the MPO. This indicates that PEO has more Zn values in a smaller range around the median and would have a more peaked shape.

Thirdly, the standard deviation values for the PEO and MPO compared to the respective mean values indicate a large spread of data. The coefficient of variation (CV), calculated as the ratio of the mean to the standard deviation, are approximately equal to 0.5 for both PEO and MPO. Since a CV value of 0.3 is indicative of a symmetrical distribution, the calculated CV values correspond to slightly more skewed distributions.

The shape parameters (skewness and kurtosis) indicate that in PEO, the Zn % grade follows a positive skewed (skewness > 0), peaked (kurtosis > 3) distribution. Conversely, in MPO the Zn % grade distribution is slightly negatively skewed (skewness just < 0) and the kurtosis is below 3, indicating an approximate symmetrical, platykurtic distribution shape.

Histograms display information about statistics of variables and can be used to visualise properties such as spread, skewness and range. Histograms are especially useful for data of equal support. Unbiased histograms can be fitted with continuous distribution models, which describe the data probabilistically (Sinclair, 1998).

After compositing to 1 m, the dataset is considered to be of equal support and the Zn % grade histograms were plotted, using bin widths of 0.5 % Zn. These histograms are shown below in Figure 4.19 and Figure 4.20 for the Zn % grade in the MPO and PEO rock units respectively.

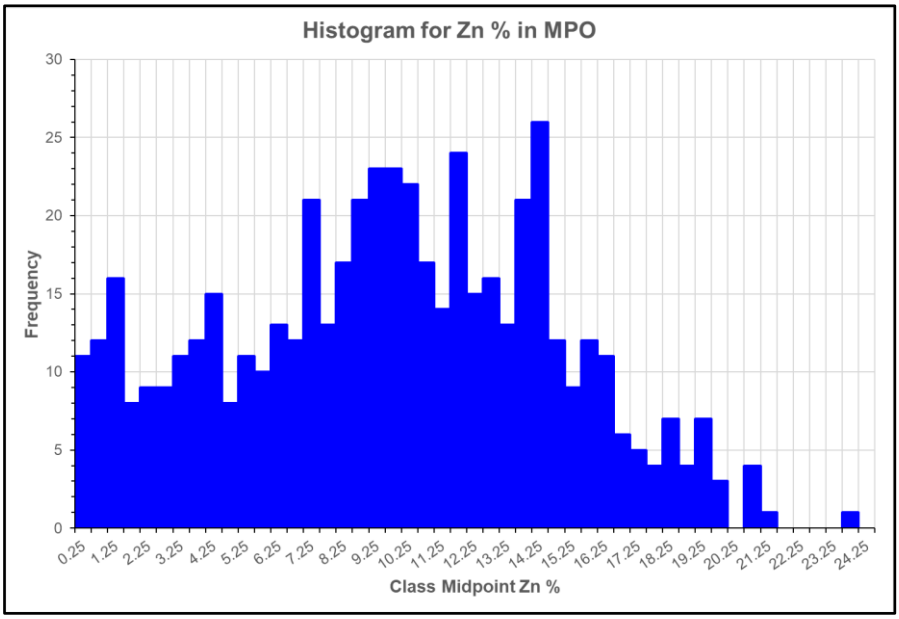


Figure 4.19 MPO Histogram of Zn % grades.

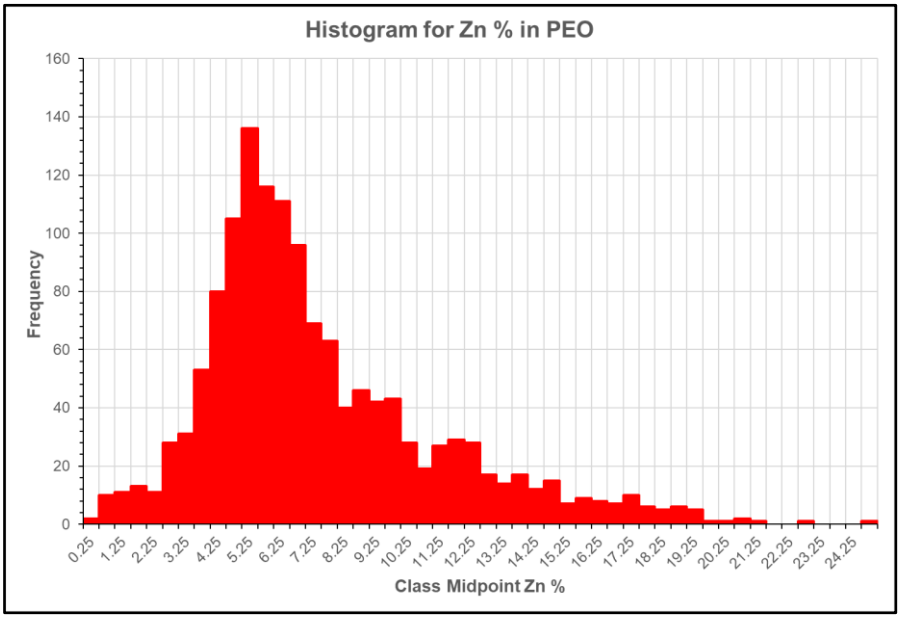


Figure 4.20 PEO Histogram of Zn % grades.

From the plotted histograms, PEO has a distinct positive skewed distribution with large spread, whereas the shape of the MPO distribution closer approximates a normal distribution or even a bimodal distribution. PEO has a more peaked distribution than MPO.

4.8. Models for Distributions

Based on the work done so far; statistics and histogram interpretations of the results, a fifth assumption about the shapes of the Zn % population probability

distribution in the PEO and MPO can now be made. This means that those histograms of the Zn % grades can be represented by probability functions or models.

Considering the measures of middle, spread, variability and skewness, a normal distribution was fitted for MPO and a lognormal distribution was fitted for PEO in JMP13. These probability density functions are displayed below in Figure 4.21 and Figure 4.22 respectively.

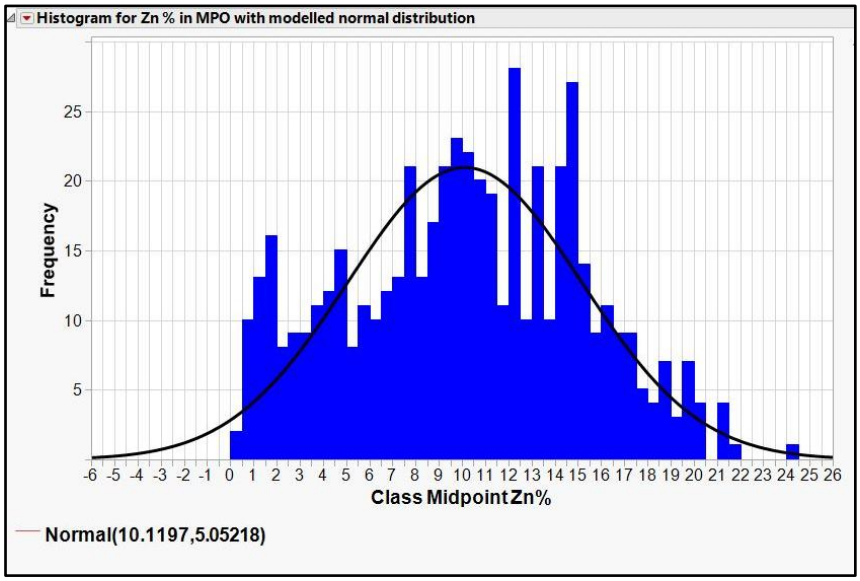


Figure 4.21 MPO Histogram for Zn % grade with modelled normal distribution.

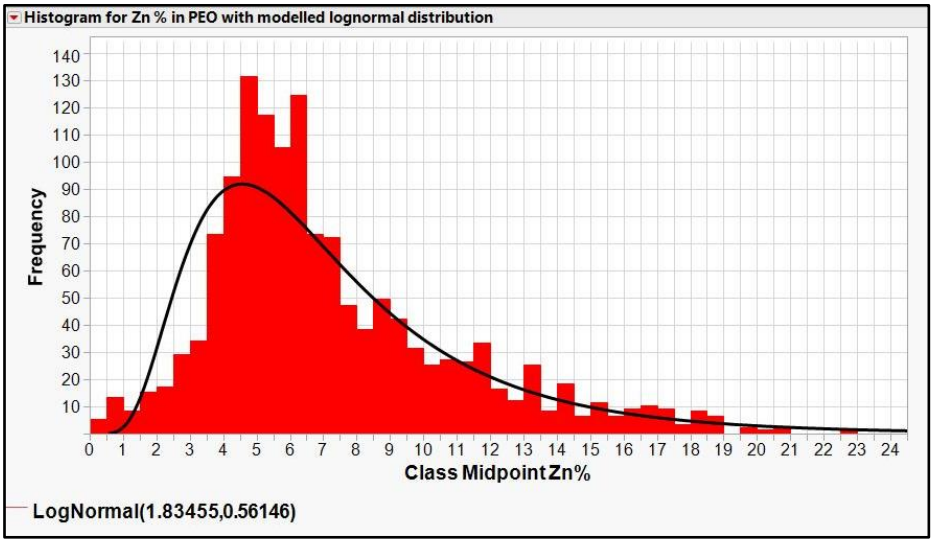


Figure 4.22 PEO Histogram for Zn % grade with modelled lognormal distribution.

Whilst the goodness of fit tests done in JMP13 for both distribution models showed the assumed distributions to be acceptable. Other possible probability distribution models were also considered as part of the investigation.

When assessing all possible fits in JMP13, the best fit for MPO was a mixture of three normal distributions. For PEO, the best fit was a mixture of two normal distributions. These possible distribution models are shown in Figure 4.23 and Figure 4.24, respectively.

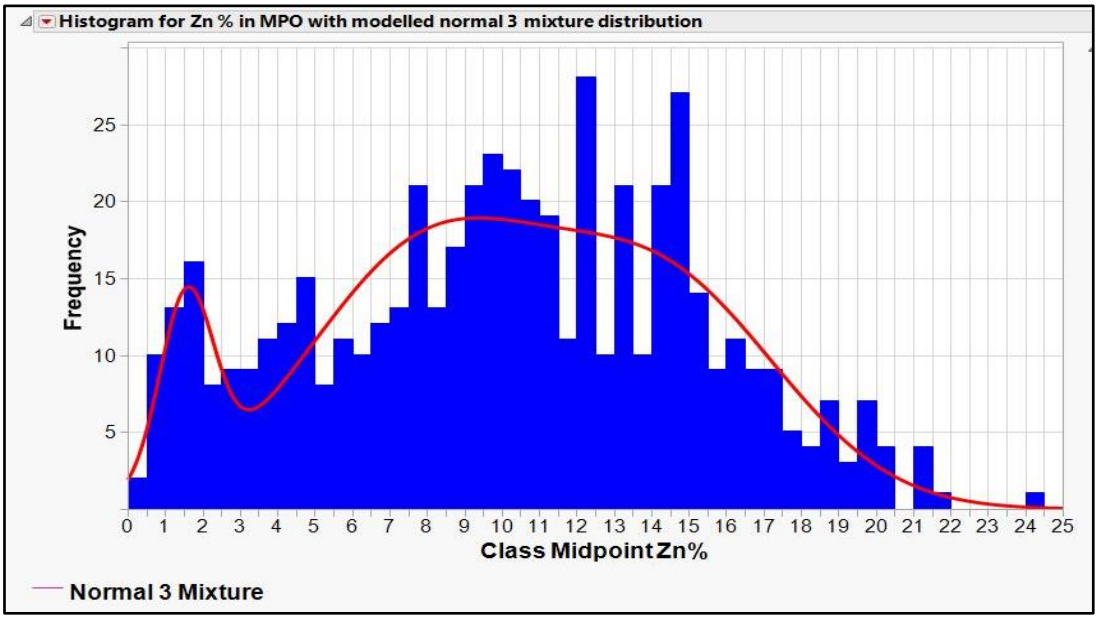


Figure 4.23 MPO Histogram for Zn % grade modelled with a mixture of three normal distributions overlain.

The fitted model confirms what can be observed in the histograms. A low-grade population is identified below approximately 3.6% Zn, with a higher-grade population that could be seen as a single or two separate populations. For PEO, the modelled best fit

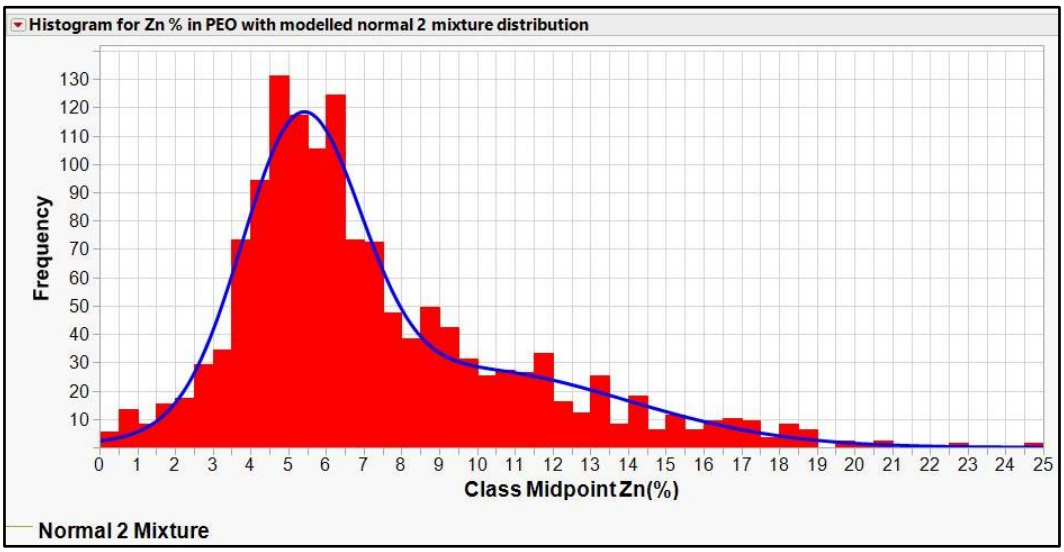


Figure 4.24 PEO Histogram for Zn % grade modelled with a mixture two normal distributions.

In addition to the untransformed histograms, log-transformed histograms were also considered and are plotted for both MPO and PEO and are shown below in Figure 4.25 and Figure 4.26, respectively. After transformation, both distributions show a negative skew behaviour, with the asymmetry highlighted in the tails to the left.

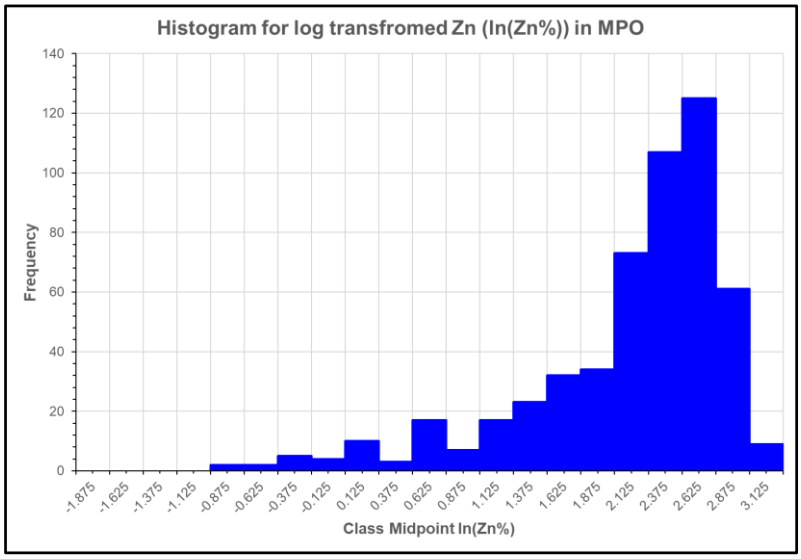


Figure 4.25 MPO Histogram for log transformed Zn (ln (Zn %)).

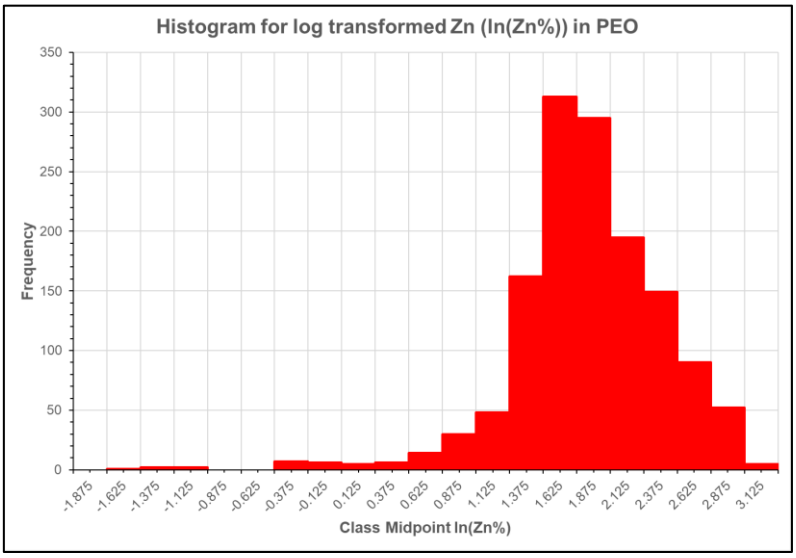


Figure 4.26 PEO Histogram for log transformed Zn (ln (Zn %)).

However, considering that this is a Zn deposit, another model might be more appropriate for describing the underlying distribution of the Zn % values. Dohm (1995) suggest three easy ways of determining the underlying distribution model. The first method involves plotting the percentage cumulative frequency distribution of untransformed ore values against the upper limit of these values on a log-probability on a probit scale. The resulting plot can give an indication of the distribution model. A cumulative normal probability plot, where the natural

logarithm (ln) of the upper limit of grade bins is plotted on the y axis with cumulative probability on the x axis, can be considered an equivalent to the log probability plot (Dohm, 2021).

The cumulative normal probability plot for MPO (Figure 4.27) is linear in the central part, with the lower end diverting downward and the upper end diverting upward. This indicates a hyper-lognormal distribution, to which a compound normal model can be fitted, if the ore values are untransformed. This kind of distribution can form as the result of the mixture of high-grade values.

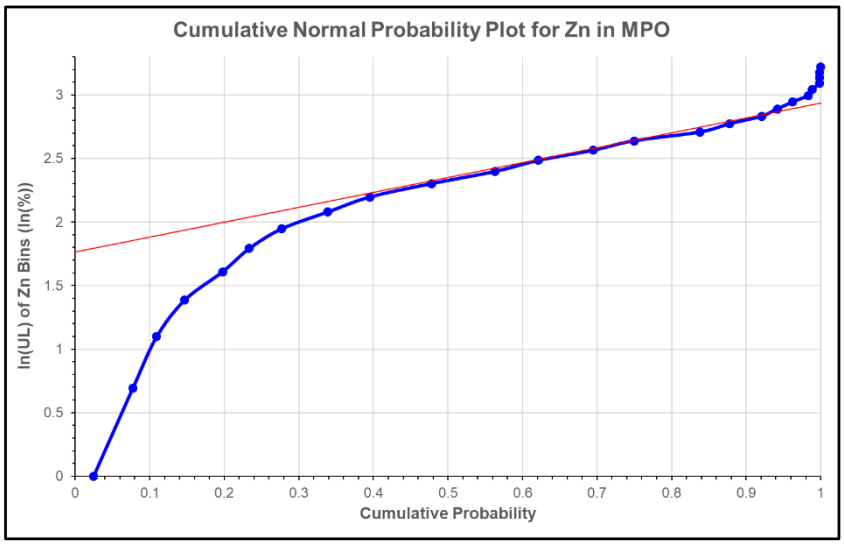


Figure 4.27 MPO Cumulative Normal Probability plot for %Zn grade.

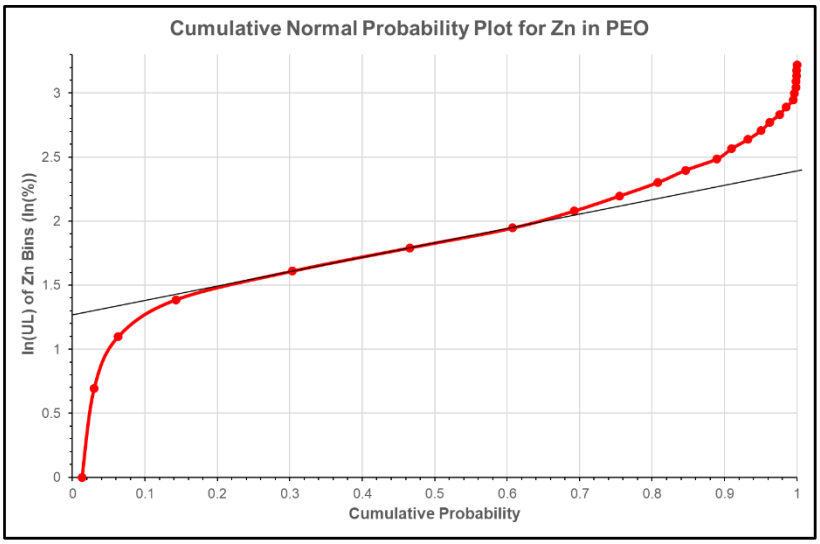


Figure 4.28 PEO Cumulative Normal Probability plot for %Zn grade.

The cumulative normal probability plot for PEO (Figure 4.28) shows the same characteristics, with a linear central part, and the plot diverting downward at the

lower end and concave upward at the upper end. This is similar to the hyper-lognormal distribution identified by Dohm (1995).

Another method suggested by Dohm (1995) involves plotting the logarithms of observed frequencies of transformed data against the class midpoints of the transformed data. The breaks observed in Figure 4.30 are due to bins with no samples occurring within them and the logarithm of zero is undefined or non-existent. For both MPO and PEO, the resulting plots were very irregular, and no clear distribution models could be identified.

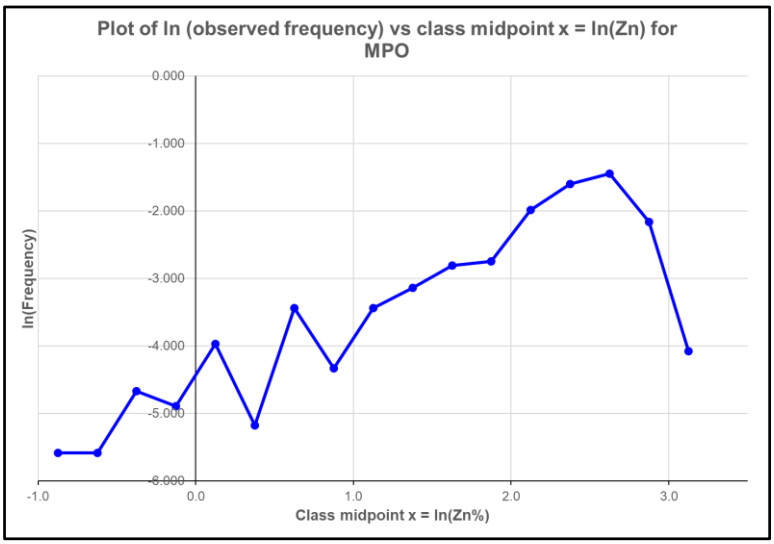


Figure 4.29 MPO ln(observed frequency) vs. class midpoint of x = ln(%Zn).

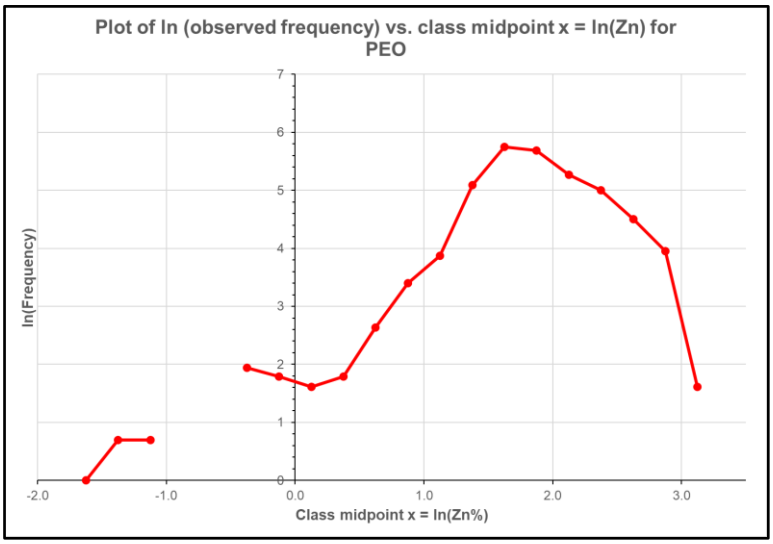


Figure 4.30 PEO ln(observed frequency) vs. class midpoint of x = ln(%Zn).

Although parametric test values as suggested by Dohm (1995) had not been calculated for these log-transformed data, the shape of the distributions for MPO and PEO, both the histogram, as well as the plot of the ln (observed frequency)

vs. class midpoint, suggest that especially MPO, follows a 5-parameter generalised compound lognormal model (GCLN) model (Dohm, 1995; Sichel, *et al.*, 1995). These shapes were also confirmed through personal communication (Dohm, 2021) as well as the comparison of the shapes of the probability density distributions presented by Dohm (1995). This type of probability density distribution model was developed by Sichel and Dohm, for complex ore value distributions, such as those observed for Zn % grades in this research study. In addition to the location, scale and skewness parameters this 5-parameter probability distribution model, has two kurtosis parameters, one describing the peakedness of the distribution and the other describing the shape of the tails.

4.9. Cumulative Probability Graphs

The application of cumulative probability or cumulative relative frequency graphs is a simple graphical technique that can be applied to find and describe multiple populations in applied geochemistry (Sinclair 1974, 1976, 1991 cited in Sinclair, 1998). This method can be used for determining the existence of fundamentally different geological domains for resource estimation (Sinclair, 1998).

Work conducted so far, as well as knowledge of Zn deposits and historical work done, suggests the existence of multiple populations within the MPO and PEO units. The cumulative probability distributions (CPDs) for these two domains confirm that assumption. The CPD for MPO indicates the existence of multiple domains, highlighted by the changes in slopes of the CPD shown in Figure 4.31.

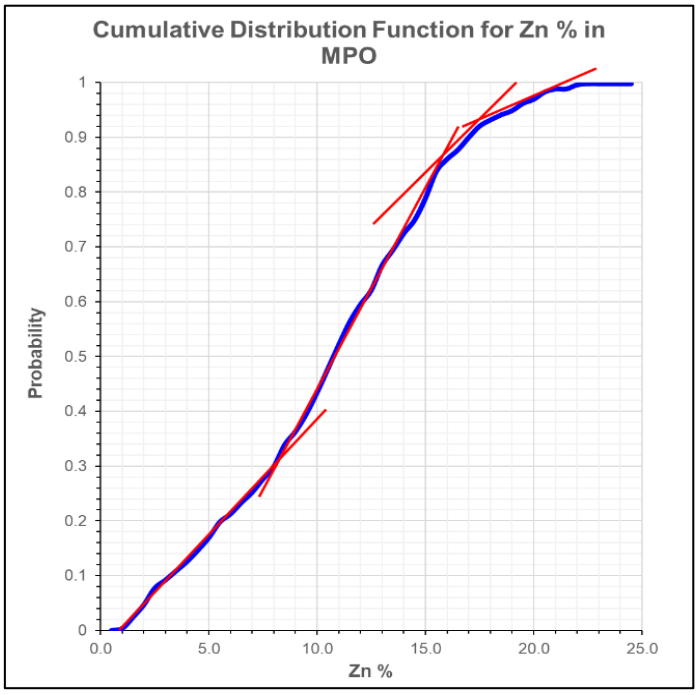


Figure 4.31 MPO CPD plot for Zn %.

Since the Zn % histogram for MPO (Figure 4.19) indicated a bimodal distribution with a low- grade component, the CPD was re-plotted, focusing on the lower end of the distribution where Zn % < 15 %. To get the desired resolution, the dataset was sorted from lowest to highest Zn grade, and the cumulative probability calculated for each individual sample grade as opposed to using grade bins. These were plotted against Zn % grade as points (Figure 4.32), and straight lines were fitted to identify changes of slope of the CPD. The intersection of these lines indicates possible grade populations on the CPD. It can be seen that at approximately 7.4 % Zn there is a change of slope on the CPD, showing the existence of two separate grade populations one consisting of grades below or equal to 7.4 % Zn value and the other with grades above this. It should be noted that break observed at approximately 8.5% Zn is a data artifact, produced by a step in grade from 8.39 % Zn to 8.66% Zn.

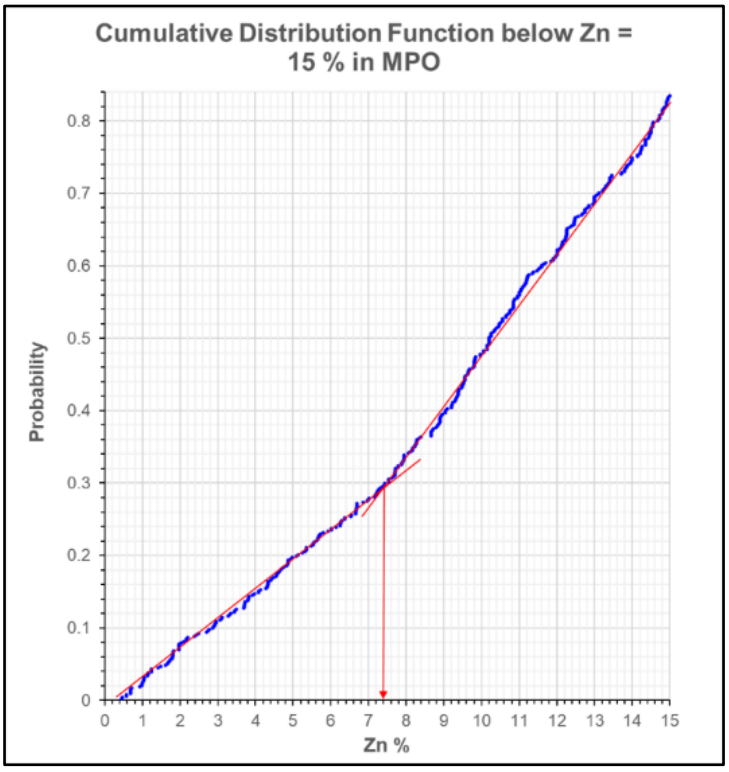


Figure 4.32 MPO CPD plot for Zn % below 15%.

For PEO, the histogram (Figure 4.20) shows a lognormal type distribution, with no clear indication of multiple populations. The CPD (Figure 4.33) however, indicates a bimodal distribution.

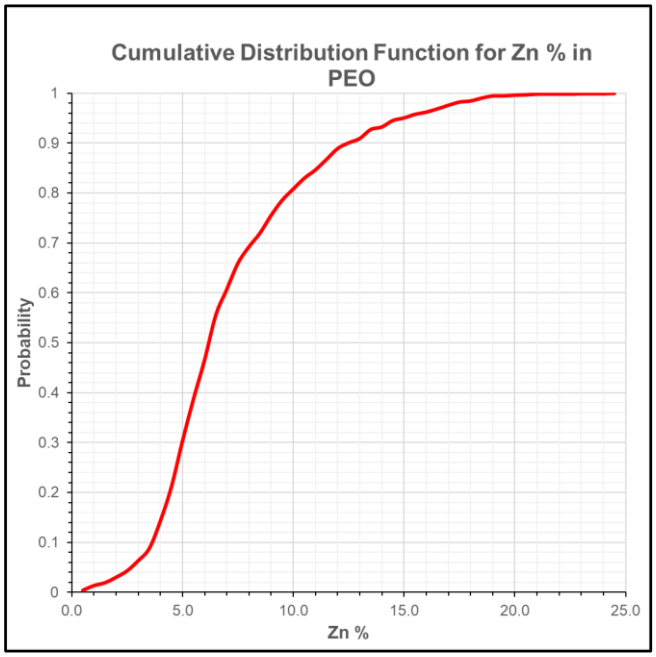


Figure 4.33 PEO CPD plot for Zn %.

The CPD was replotted, as described above for the PEO, focussing on the lower end of the distribution where Zn % < 5 % Zn (Figure 4.34). From it can be seen that at approximately 2.2 % Zn and again at 3.6 % Zn there is a change of slope in the CPD. This indicates the existence of two separate low-grade populations. Since the probability of a sample occurring in the first population is very low (approximately 0.03) these two domains were combined into a low-grade population with Zn % < 3.6 % Zn.

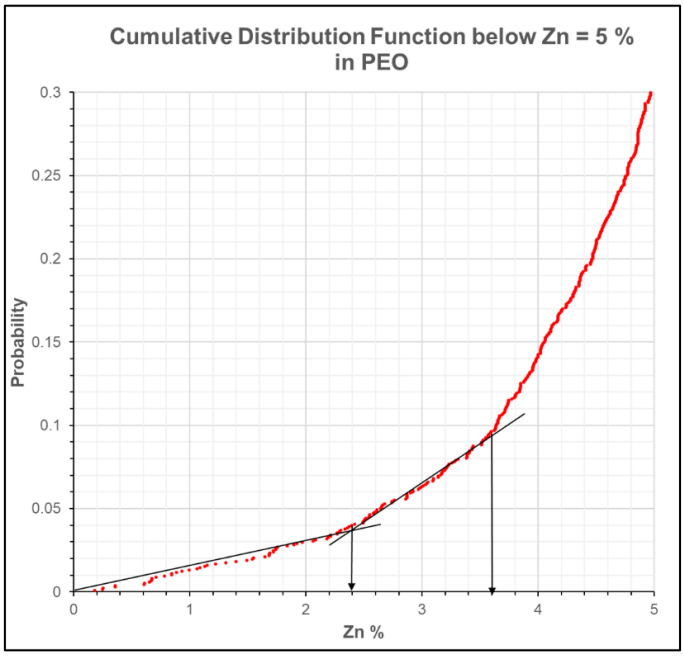


Figure 4.34 PEO CPD plot for Zn % below 5%.

4.10. Summary and Conclusion

By examining the CPD of Zn % grade in the Gamsberg East deposit, indicated a population with Zn % grade greater than 3.5 %. The distribution of sampled rock types within the deposit indicated that MPO and PEO occurred most often. Considering common exploration sampling procedures, these can be assumed to be the ore lithologies. To confirm this assumption, summary statistics were compiled for all rock types, and rock types with mean Zn % grades greater than 3.6 %, indicated by the CPD were identified. These were SBO, MPO, PEO, PEO_Po, CLT and ORE. All these rock types were considered, taking into account the number of samples, spatial distribution and how the unit was handled historically. Based on this, PEO_Po was recoded to PEO and the other units were disregarded.

An examination of sample lengths across the deposit was conducted and it was determined that, based on distribution of sample lengths, a 1 m composite length would be appropriate. Composites were created in Maptek Vulcan. It was also noted that in some instances decompositing did occur.

Mean Zn % grades were compared per drill type, which indicated that chip samples generally have lower grades. However, due to the small number of samples, it was not considered valid to consider these separately. Similarly, mean grades were compared per assay method by examining a CPD and summary statistics. Although 4AG_UN had higher mean grade than the other methods, an examination of these samples in 3D showed them to have no spatial correlation. As such, these samples were not considered a separate population.

Correlation matrices and scatterplots showed correlation between Zn and Cd, Pb and Ag, and Cu and Fe. These correlations can all be attributed to mineralogy, with the difference in correlation between rock types due to the different relative mineral abundance within the rock types. An outlier analysis indicated outlier SG, Pb and Ag values occurring in both rock types. Spatial examination of outlier values showed that within the PEO outlier values do form a discrete population. However, since the sample numbers are low, these were not considered a separate domain. Since outliers were shown to be valid, and not errors, outlier values were retained within the dataset.

Summary statistics for Zn % indicated an approximately symmetrical, platykurtic distribution in MPO and a positive skewed leptokurtic distribution in PEO. The shape of these distributions was confirmed by plotting histograms for Zn % within the MPO and PEO. For MPO a normal distribution was fitted and for PEO a lognormal distribution in JMP13. However, analysis of best-fit models in JMP13 indicated a mixture of 3 normal distributions and 2 normal distributions for MPO

and PEO respectively. Log histograms indicated negative skewed distributions. A cumulative normal probability plot showed hyper lognormal distributions in both MPO and PEO. Personal communication (Dohm, 2021) confirmed that, especially MPO, follows a 5-parameter GCLN distribution.

CPD were plotted for both MPO and PEO, focussing on the low-grade portion of the distribution. This showed that MPO has a population below 7.4 Zn % and PEO has a population below 3.6 Zn %.

The EDA process showed the importance of examining data in a variety of ways. When simply considering summary statistics, it can appear as if certain groups, such for example samples assayed by 4AOG_UN method, represent a separate domain of higher grade mineralisation. However, in this case, examining the data spatially showed that the data could not be said to be spatially correlated. Similarly, if the outliers had not been examined spatially, the values might simply have been removed by applying a grade cap. Spatial examination showed these values as representing a separate population, and therefore valid and not erroneous. By examining all aspects of the data in a variety of ways, a thorough understanding of the dataset and its properties were gained.

5. GEOLOGICAL MODELLING

Geological models are subsurface interpretation based on limited data that simplify the complexity of natural phenomena (Birch, 2014) such as mineral deposits. Some of the key steps involved in creating a geological model, according to Abzalov (2016) is to establish what one wants to represent, and which properties should be modelled, defining domaining criteria, coding data, and creating the domains. Abzalov also stresses the importance of testing the resultant domains to confirm that it fulfils the purpose of the exercise.

Leapfrog Geo was used to model the deposit implicitly. Implicit modelling is a technique that uses radial basis functions (RBF) to generate models rapidly and efficiently from various data sources, such as drill holes, outcrop, and structures (Birch, 2014).

5.1. Properties to be modelled

In section 4.1 it was determined that the zones of interest are the rock types MPO and PEO. These attributes were recorded at time of logging in the Rock_Type column. As stated in section 3.2, some minor recoding was done, with PEO_Po and SBO recoded as PEO in a separate column, to represent a simplified geology.

5.2. Data Validation

Geological data was validated during first stage data analysis. In section 3.3, no overlaps in interval data were found. No additional information exist of how logged data was verified, although the Gamsberg East Competent Persons' Statement refers to the existence of photographs of the diamond core (Potgieter, 2016).

5.3. Geological Modelling Methodology

After the dataset was validated, a new Leapfrog Geo project was created and the drill hole database was imported. After the drill holes had been imported, a new grouped lithology was created, grouping the rock types of interest, as stated above in section 4.3. These groupings are shown in Table 5.1 below and formed the basis for modelling the geology of the deposit.

Table 5.1: Grouped Lithologies in Gamsberg East Leapfrog Geo project.

Grouped Lithology	Rock Type
MPO	MPO
PEO	PEO
	PEO_Po
	SBO
PEO_Other	PEO_Py
	PEO_MR
	ORE
Waste	All other, non-mineralised lithologies

When viewing the drill hole data in 3D, it was observed that the lithologies of interest occurred in a plane, dipping approximately northeast, except for one hole, GAMD061; the easternmost hole in the dataset. With the lithologies of interest dipping as it does, it would be expected that the intersections in GAMD061 occur at depth. However, the intersection on this hole occurs at shallow depths.

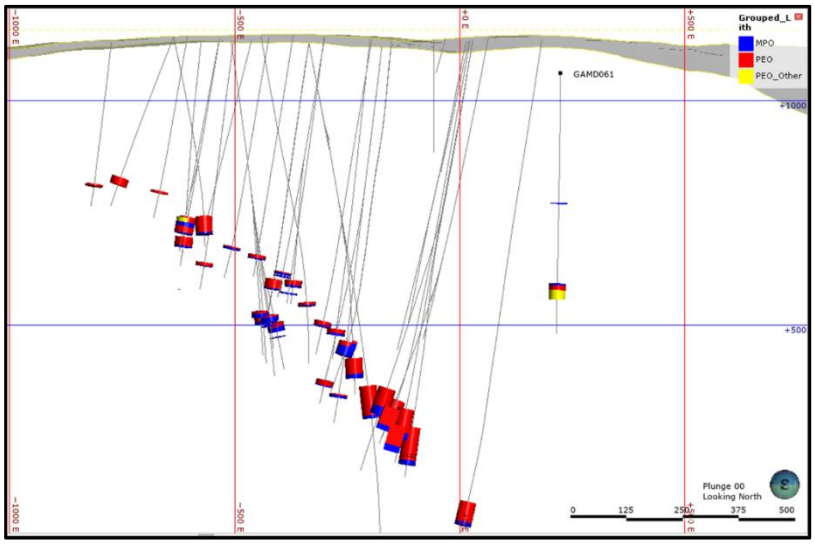


Figure 5.1 Section looking North to view intersection of interest on GAMD061.

When viewing the trace and the collar of this hole in section in Figure 5.1, it also becomes clear that the collar falls below the topography. This raises the possibility that the hole location is recorded incorrectly in the database. GAMD061 has therefore been excluded from the modelling. It was already seen in section 2.6 that GAMD061 does not have assays. Therefore, excluding it will have no impact on the statistics already calculated. To avoid deleting data from the dataset, a new column was created, based on the grouping in Table 5.1, where the intersections on GAMD061 was labelled as "_Incorrect". All other

intervals were transferred to this column as is. Further modelling was based on the MPO and PEO in this column.

In order to create a valid and geologically sound model, a number of options were considered, and the outputs were compared. For the purposes of comparing modelling methods, only one of the zones of interest was considered, except in section 4.4.2 where the nature of the method creates complementary volumes, which necessitates viewing both.

5.3.1. Intrusive model (from Base Lithology)

Although the genetic model for Gamsberg East does not indicate an intrusive origin, the option of using Leapfrog Geo's intrusive models was nevertheless considered. As stated by Stoch et al., (2018), in Leapfrog Geo the contact surfaces that define models are constructed "in accordance with their geometry rather than their genesis." such that "an intrusive contact surface is constrained by either upper or lower contacts of the selected interval."

When creating an intrusive model, various options were trialled. Initially, as a first pass, a model for PEO was created using a global trend. The resultant shape consisted of small, unrealistic blobs, centred around intersections, with little to no continuity. In an effort to remedy this, a non-decaying structural trend was applied, based on the plane formed by the PEO intersections (Figure 5.2).

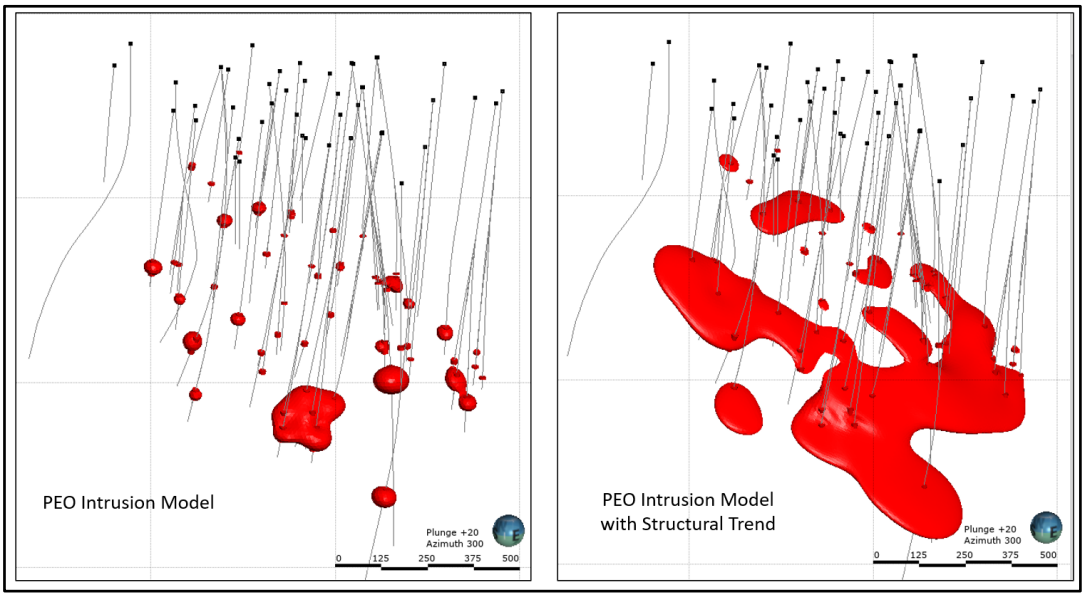


Figure 5.2 PEO Intrusive Leapfrog Geo models from base lithology with no trend (left) and a non-decaying structural trend (right).

Several attempts were made to increase the continuity of the modelled zone, by increasing the strength of the trend, but yielded little to no improvement. Given that this method yielded no realistic outputs, the method was not considered valid.

5.3.2. Deposit model (from Contacts)

According to Stoch et al (2018) “depositional contact surfaces result in volumes above or below the specified surface.” By defining a sequence, known in Leapfrog Geo as the Surface Chronology, older volumes can be truncated by younger ones. The benefit of using this option, would be that it creates complimentary volumes that lie conformably on top of one another, without cutting through one another. Since this method creates volumes above or below a specific surface, some recoding was required, in order to define those surfaces.

In Microsoft Excel, a new column was created where all rock types above the mineralised units were coded as “Hanging Wall”. Similarly, all rock types below the mineralised units were coded as “Foot Wall”. Mineralised units MPO and PEO retained their codes.

A first pass of the model using this coding resulted in non-ore units that occur between the zones of interest, being incorporated into the overlying PEO unit. To resolve this issue, an “Inter Ore” code was created. All waste units, as defined in Table 5.1, occurring between the MPO and PEO units were assigned to this unit. This unit occurs in 10 holes within the area of interest, 59% of the intersections are logged as pelite. The summary statistics of this unit is shown in Table 5.2 below.

Table 5.2: Summary Statistics of Inter Ore units in Leapfrog Geo Deposit model.

	Rock Type	Inter Ore
Zn	N	78
	Mean (%)	3.140
	Standard Devation (%)	5.190
	Variance (% ^{2})	26.932
	Median (%)	0.724
	Mode (%)	5.610
	CV	1.653
	Kurtosis	5.064
	Skewness	1.879
	Maximum (%)	18.150
	Minimum (%)	0.011
	IQR (%)	2.098
	Range (%)	18.139

The high maximum value, large range, large variance, and standard deviation indicate the presence of high-grade Zn % samples in what was assumed to be non-ore lithologies. Of these intersections 19% (15 out of 78) are logged as GPM (Garnet Pyroxene Magnetite). This unit displays very high grades, with an

average of 11.22 % Zn. The high grade of these intersections, as well as the mineralogical similarity to MPO suggest that this unit should be included in MPO. However, for the purposes of comparing the modelling outputs of logged MPO and PEO, this unit will at present remain part of the Inter Ore zone.

The Leapfrog Geo output volumes for both MPO and PEO extended far beyond the extents of the drilling and intersections, although much less so for MPO (Figure 5.3). The extent of these volumes cannot be manually edited.

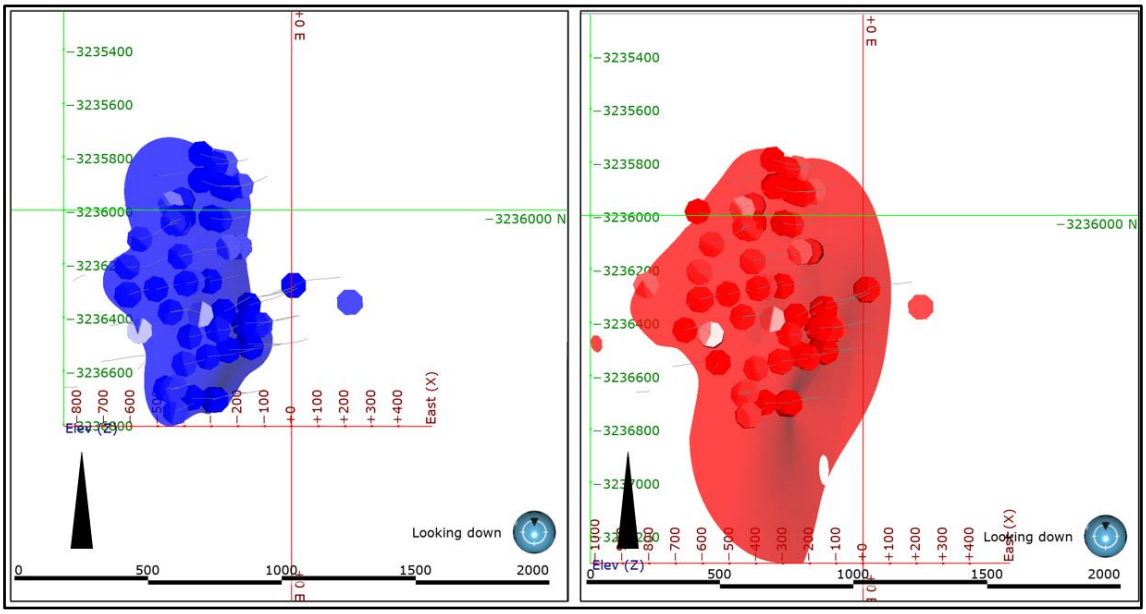


Figure 5.3 Deposit model in Leapfrog Geo for MPO (left) and PEO (right).

Although the resulting outputs were conformable with each other and/or the Inter Ore unit, where it occurred, the PEO volume extends far beyond the available data. Overall, the output volumes could not be considered geologically valid.

5.3.3. Vein Model

The preferred approach for modelling thin, laterally continuous mineralised zones is to use the vein model option in Leapfrog Geo. As input, one requires either a discrete lithology, or if the criteria is more complex, intervals may be individually selected based on specified criteria and assigned to new units.

With vein modelling, a hanging wall surface is generated at the top contact of the specified lithology and a footwall contact at the bottom contact of the specified lithology. Where multiple intersections of the specified unit occur within a single drill hole, multiple sets of hanging wall and footwall points might be generated. This can result in unrealistic zig-zag shapes or intersections of exaggerated thickness. In such cases, a variety of manual editing options exist to generate more realistic shapes. The details of these fall beyond the scope of this study.

Vein models can be set to pinch out where data indicates that the vein no longer occurs. (Seequent Ltd, n.d.) This option was used for Gamsberg East, to limit the extent of the potential orebody. When using this option, it is important to review where the software pinches out veins. In instances where drilling angles are shallow or intersections are thin, the generated models can pinch out where it is not desired. In such cases, individual pinch outs can be excluded. This is also useful where data might not be available due to lack of granularity in drilling, sampling, or logging. In Figure 5.4, the modelled PEO unit is shown in plan-view with and without the pinch out option.

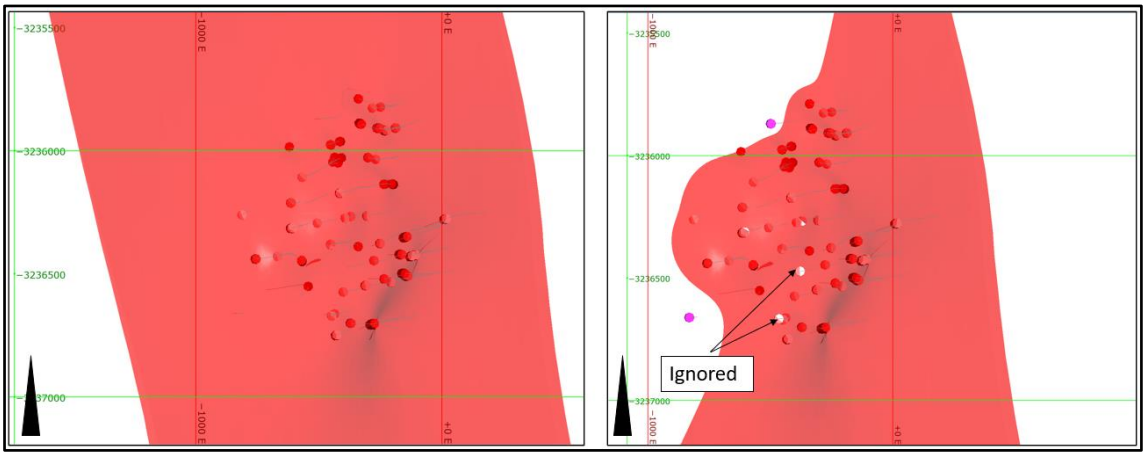


Figure 5.4 PEO in plan-view, without the pinch out option (left) and with the pinch out option (right).
Ignored pinch-outs are indicated.

A failure of this method is that generated outputs tend to over-extrapolate the extent of modelled veins, as can be seen in Figure 5.4. To rectify this, a boundary can be applied around data occurrences. A numeric buffer of 50 m radius was created around drill hole traces and used to guide the boundary.

Since this approach can result in blunt, perpendicular boundaries to the vein, there are other ways of controlling the extent of veins, although these can be a lot more time consuming depending on the size of the dataset and deposit under consideration. Similar to the manual editing options for pinch outs these fall beyond the scope of this study.

To generate final volumes in Leapfrog Geo, the so-called surface chronology has to be defined. This defines the relationship of the various units in age and determines which units cut or overprint which. Once this has been activated, any overlapping areas will result in one unit cutting the other, depending on the relationship. Where units are not to cut one another, but do, due to the way the veins are generated, surfaces can be edited manually to rectify the situation.

For Gamsberg East, the lithological units under consideration were modelled as separate veins, i.e., one for MPO and one for PEO, with pinch outs enabled and a boundary string applied. The model's surface resolution was set to 10m to ensure an appropriate level of granularity.

As a guide, a 50m buffer was created around each drill hole and these were used as guides when drawing the boundary strings for each unit. Since the units occur conformably, they cannot intersect. Some manual editing had to be done to ensure that this is the case.

For PEO a pinch out was created on GAM092. This hole does contain mineralised intersection, but it's logged using the code ORE. As discussed in section 4.2 this unit was excluded from the combined MPO and PEO. However, viewing the data in 3D was decided to include the mineralised intersection in the PEO wireframe. Since no mineralogical data exist, the possibility exist that this intersection could be MPO rather than PEO. However, based on the relative thicknesses of both units in neighbouring holes, it was decided to include the ORE intersection in the PEO and the MPO seems to thin and pinch out in that area.

The final model is shown below in Figure 5.5 in plan plan-view, with the intersections on which these are based.

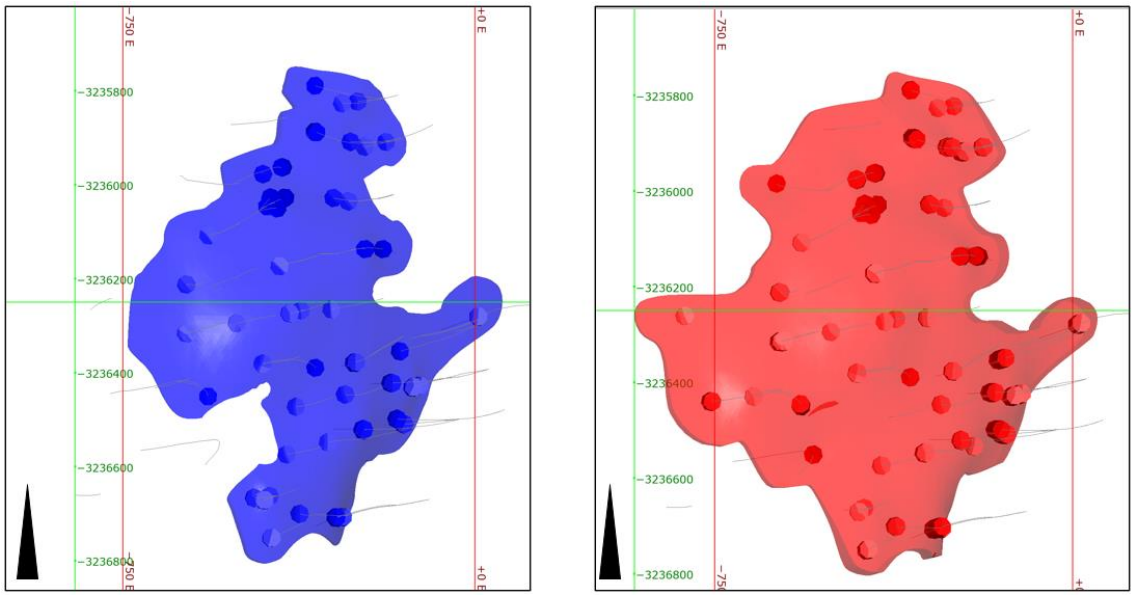


Figure 5.5 Vein model with drill hole intersections and traces for MPO (left) and PEO (right).

5.4. Model Validation

Since the intrusion model, the deposit model did not yield valid outputs, the vein model was chosen as the best method for modelling the units under consideration in Gamsberg East.

In order to validate this decision, the outputs were used to flag the samples that fall within them. These samples were compared to the logged samples. The results are tabulated in Table 5.3

Table 5.3: Summary Statistics for % Zn grade in the modelled domains.

	Rock Type	MPO Simplified Rock Type	MPO Vein Model	PEO Simplified Rock Type	PEO Vein Model
Zn	N	531	527	1382	1478
	Mean (%)	10.120	10.006	7.183	6.875
	Standard Devation (%)	5.052	5.180	3.714	3.952
	Variance (% ^{2})	25.525	26.836	13.793	15.621
	Median (%)	10.200	10.250	6.170	6.071
	Mode (%)	10.200	10.850	4.860	4.860
	CV	0.499	0.518	0.517	0.575
	Kurtosis	2.320	2.191	4.428	4.164
	Skewness	-0.017	-0.050	1.176	0.962
	Maximum (%)	24.150	24.150	24.500	24.500
	Minimum (%)	0.456	0.456	0.183	0.010
	IQR (%)	7.697	8.344	4.149	4.289
	Range (%)	23.694	23.694	24.317	24.490

From Table 5.3 it can be seen that for MPO the overall number of samples remained about the same. The measures of middle (mean, median and mode) remaining approximately the same. The measures of spread (range and IQR) also remain approximately the same, with the range stating the same, but the IQR of the vein model slightly bigger. The measures of variability (variance, standard deviation, and CV) are very similar after modelling with the variance (and consequently the standard deviation) showing a slight increase. This is probably due to the lower sample number. The measures of shape (kurtosis and skewness) show slight changes. The slight decrease in kurtosis, indicates the peak of the distribution flattening with a shift into the tails. An increase in skewness indicates a slight shift in the distribution, as can also be seen though the change to the IQR. However, these changes are small, and it indicates that the shape of the probability distribution for the Zn % grade remains roughly unchanged for the MPO unit.

For PEO, the changes are more noticeable. The vein model incorporates more samples than the combined MPO and PEO. This is to be expected, since as mentioned in section 5.3.3 some ORE intersections were included. In addition to that, it is often the case that some internal waste gets included when modelling, especially where ore/waste boundaries are gradational. As a result, the mean grade is slightly lower and the variance and standard deviation higher. The kurtosis shows a slight sharpening of the peak, and the skewness and CV remain

roughly the same. Similarly, to the MPO, this indicates that the Zn % grade probability distribution is largely unchanged.

Since the modelled domains do not show significant changes to the mean and the shape of the distribution, the model can be assumed to be valid.

5.5. Use of Indicator Kriging (IK) to model subdomains

From sections 3.9 and 3.10 it was shown that the MPO and the PEO have multiple populations. However, these populations could not be resolved spatially through the geological modelling methods as discussed in section 5.4. To resolve these subdomains, it was decided to use Indicator Kriging.

Indicator based methods can be used to relate discrete distributions by assigning indicator values to each geological attribute. Indicator Kriging (IK) furnishes a probability of the attribute being present (Rossi & Deutsch, 2014). IK was conducted in Maptek Vulcan.

From section 3.10, indicator threshold values were identified based on the cumulative distribution probability plots for Zn % in the MPO and PEO. From Figure 4.32 and Figure 4.34, indicator threshold values of Zn = 7.4 % for MPO and of Zn = 3.6 % for PEO were respectively determined. Two additional columns were added to the sample file one for each rock unit and indicators were assigned using a script, where Zn values below the respective threshold grades were assigned an indicator value equal to 0 and Zn values above and or equal to the threshold grades assigned an indicator value equal to 1.

Indicator grade variograms were calculated and modelled in Maptek Vulcan Data Analyser for the MPO and PEO, can be found in Appendix A. These models were applied in an indicator kriging exercise to produce block estimates for the probability that the Zn block grades are above or below the specified thresholds for the MPO and PEO units. The resultant kriged probabilities were then assessed. The object was to identify continuous areas where the kriged indicators are low. This would indicate areas of low probability for the Zn % grade to be above the respective threshold values. Conversely, where the kriged indicator values are high, the probability of the Zn % grade to be above the indicator threshold values, is high.

The MPO heat-scale indicator kriged results for blocks is shown in Figure 5.6, where cold colours represent low probabilities and warm colours high probabilities of grade being above the grade threshold value of 7.4% Zn. Sample indicator values are also plotted as blue (0) and red (1) dots depending on whether the sample grade was below, or it was equal to or greater than the threshold value.

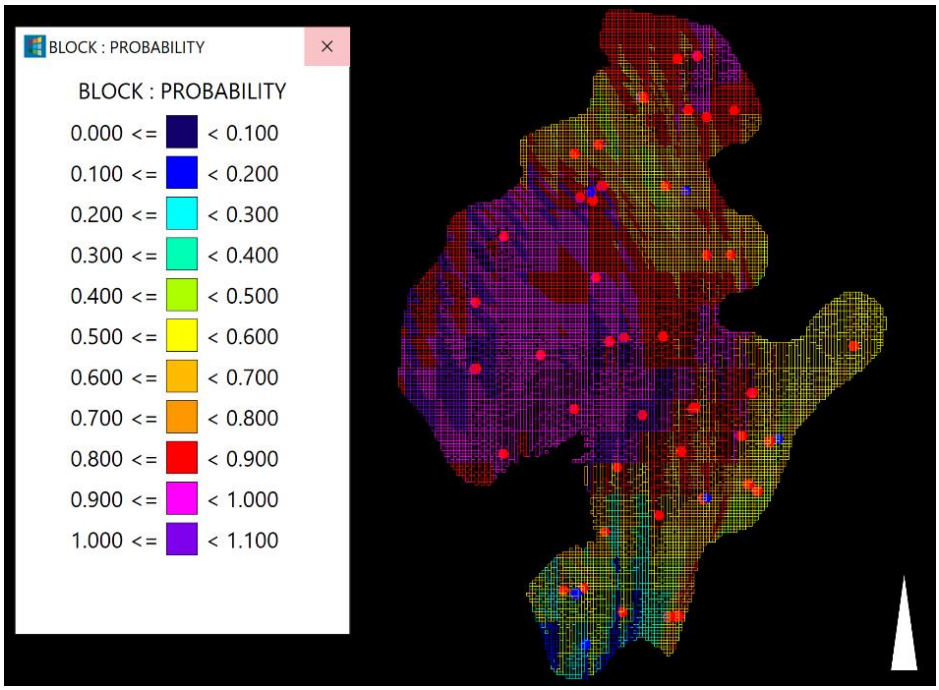


Figure 5.6 MPO heat- scaled indicator kriged block values.
Cold colours represent blocks with a low probability of the Zn % grade being above 7.4 % Zn. Sample Indicator values are plotted as either blue or red dots, depending on whether the Zn % grades were less than the threshold or it being equal to or above it.

The southern limb of the modelled MPO has the lowest probability of being above the threshold, therefore it can be assumed to have low grades. In the south-eastern limb of the MPO, the yellow blocks represent an area of possible low grade, since the probability of grades being above the threshold in this area more 0.5 but less than 0.6. Some samples below the threshold can also be seen in this area. In the northern limb, the occurrence of samples below the threshold are also reflected in blocks where the kriged probability is between 0.5 and 0.6 of the blocks having grades above the threshold value.

The PEO heat-scale indicator kriged results for blocks appear in (Figure 5.7), as before cold colours correspond to low probabilities and warm colours to high probabilities of Zn % being above the grade threshold value of 3.6% Zn. Sample indicator values are also plotted as blue (0) and red (1) dots, depending on whether the sample grade was below, or it was equal to or greater than the threshold value.

For PEO, the kriged indicator block probabilities are generally higher However, the same southern limb as in the MPO, has the lowest probability of being above the 3.6 % Zn cut-off.

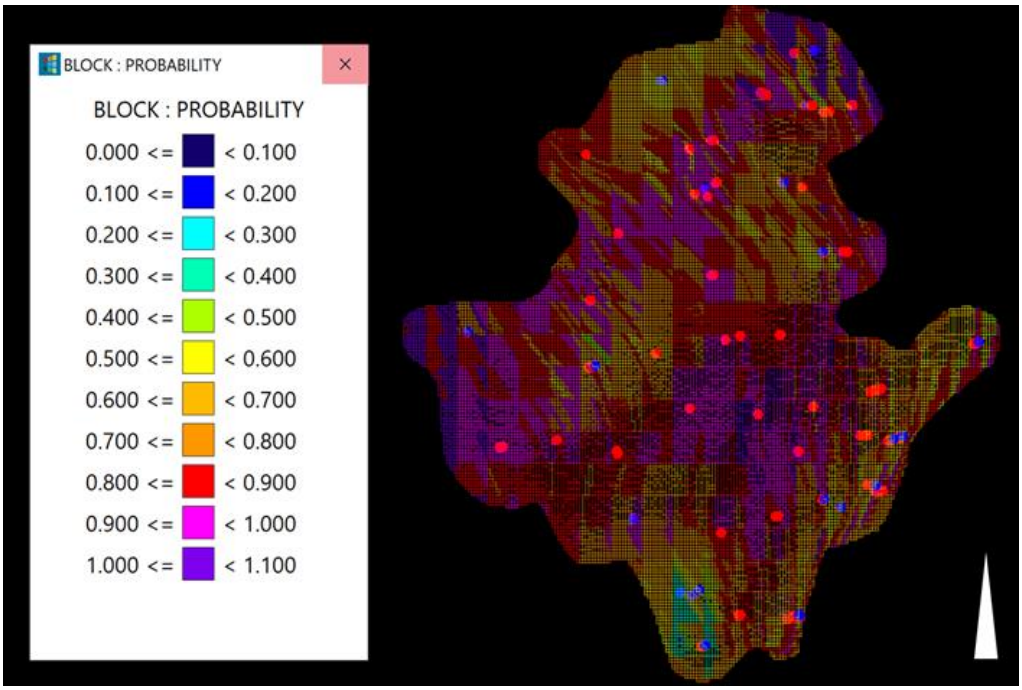


Figure 5.7 PEO heat- scaled indicator kriged block values.
Cold colours represent blocks where the probability of the Zn grade being above the threshold of 3.6 % Zn is low. Sample Indicator values plotted as dots, with blue being an indicator below the threshold and red being an indicator equal or above it.

Considering Figure 5.6 and Figure 5.7, it seems that IK does not sufficiently resolve the MPO or PEO domains into low- and high-grade zones. To confirm this, the domains were split by digitising a string to create a domain where the probability is less than 0.5, based on the IK results (Figure 5.8) and summary statistics and distributions for each subdomain calculated and examined.

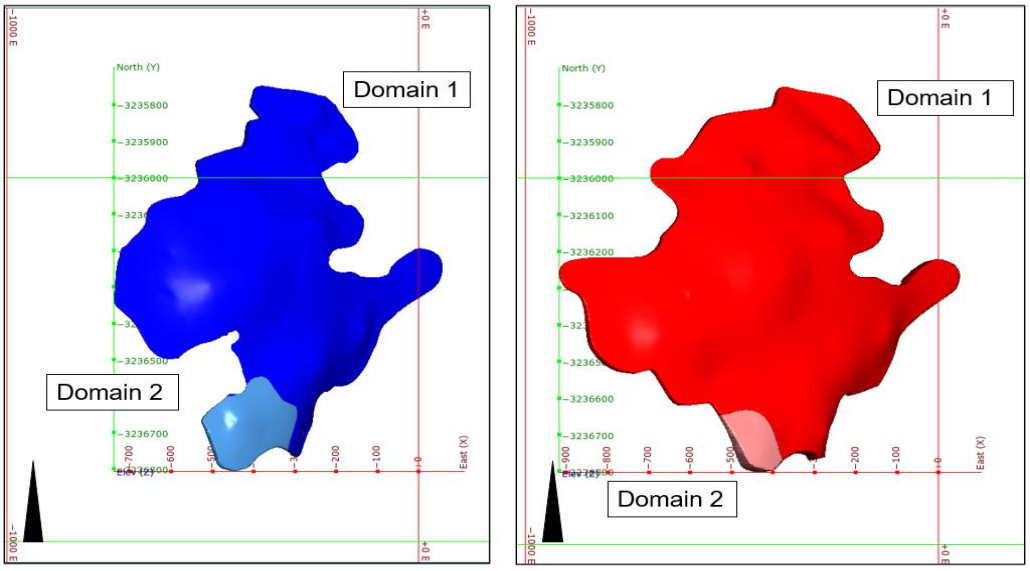


Figure 5.8 MPO (left) and PEO (right) subdomains based on IK probability cut-offs.

The MPO summary statistics in Table 5.4 show that MPO Domain 2 has an average grade that is lower than the threshold value of Zn = 7.4 Zn %.

Table 5.4: Summary Statistics for Zn % in MPO subdomains.

	Rock Type	MPO Vein Model	MPO Domain 1	MPO Domain 2
Zn	N	527	448	79
	Mean (%)	10.006	10.533	7.019
	Standard Devation (%)	5.180	4.976	5.331
	Variance (% ^{2})	26.836	24.764	28.418
	Median (%)	10.250	10.665	6.020
	Mode (%)	10.850	10.850	14.350
	CV	0.518	0.472	0.760
	Kurtosis	2.191	2.339	1.729
	Skewness	-0.050	-0.069	0.395
	Maximum (%)	24.150	24.150	17.000
	Minimum (%)	0.456	0.456	0.570
	IQR (%)	8.344	7.508	10.360
	Range (%)	23.694	23.694	16.430

The distribution in Domain 1 remained very similar to that of the population as a whole, with only variability decreasing, but the shape of the distribution remaining the same. This can be confirmed by viewing the relative frequency distribution for Domain 1 (Figure 5.9). The similarity between the distribution of the MPO as a whole and Domain 1 suggests that the domaining did not split the population, since the shape of the distribution remains unchanged.

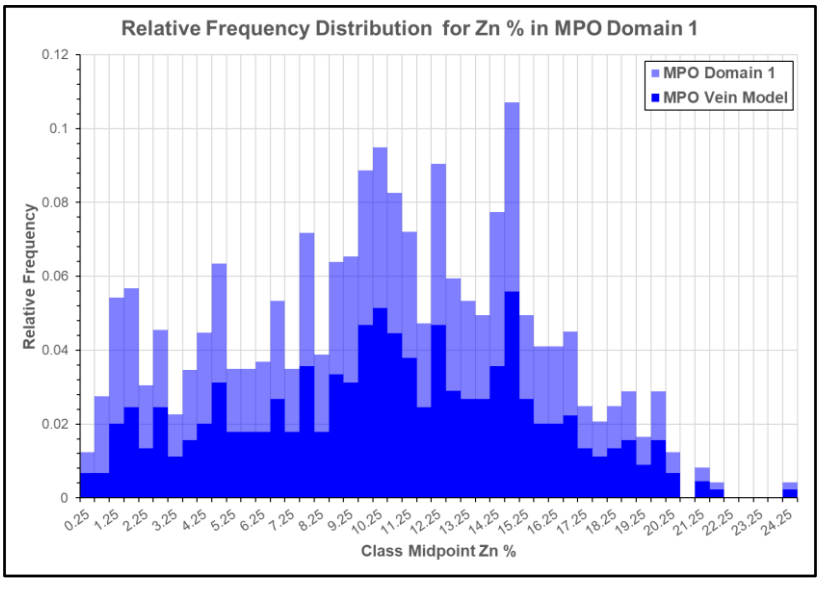


Figure 5.9 MPO Domain 1 Relative Frequency Distribution for Zn %

Only 79 samples occur in MPO Domain 2, which makes use of frequency distributions such as histograms and CPD less informative. For that reason, a

boxplot was used to show the spread of the data within the domain (Figure 5.10). From this, it can be seen that Zn % grades in MPO Domain 2 have a larger spread above the median in the 3rd and 4th quartiles which indicates a positive skewed or lognormal type distribution.

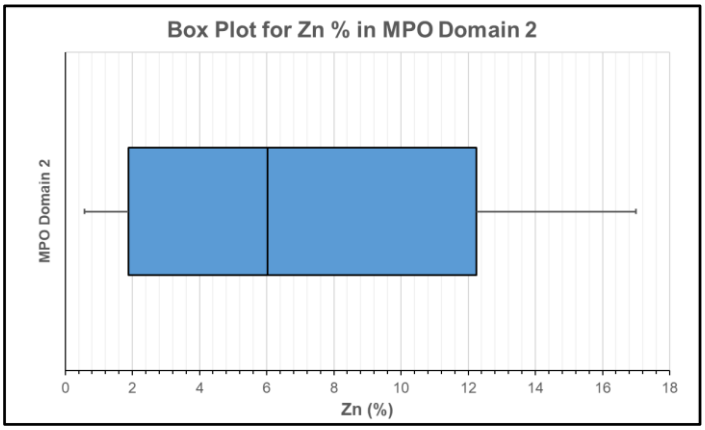


Figure 5.10 Box Plot for Zn % in MPO Domain 2.

The summary statistics for the are shown in Table 5.5 below. Similar to the MPO, Domain 1 in the PEO remains largely unchanged, with measures of middle, shape and variability all indicating a very similar shaped distribution. PEO Domain 2 has a markedly lower grade, but unlike in the MPO, the mean is not below the indicator threshold value. Confirming what was observed in Figure 5.7, where very few blocks showed low probabilities of being below the indicator value. The measures of shape and variability also indicate a highly skewed, leptokurtic distribution, with a much narrower distribution than in the original population.

Table 5.5: Summary Statistics for Zn % in PEO subdomains.

	Rock Type	PEO Vein Model	PEO Domain 1	PEO Domain 2
Zn	N	1478	1419	59
	Mean (%)	6.875	6.948	5.137
	Standard Devation (%)	3.952	3.969	3.087
	Variance (% ^{2})	15.621	15.750	9.529
	Median (%)	6.071	6.126	4.390
	Mode (%)	4.860	4.860	2.870
	CV	0.575	0.571	0.601
	Kurtosis	4.164	4.128	6.792
	Skewness	0.962	0.939	1.706
	Maximum (%)	24.500	24.500	17.065
	Minimum (%)	0.010	0.011	0.010
	IQR (%)	4.289	4.292	2.975
	Range (%)	24.490	24.489	17.055

These are reflected in the relative frequency distribution in Figure 5.11, for PEO domain 1. It can be seen that the grade distribution remains largely unchanged.

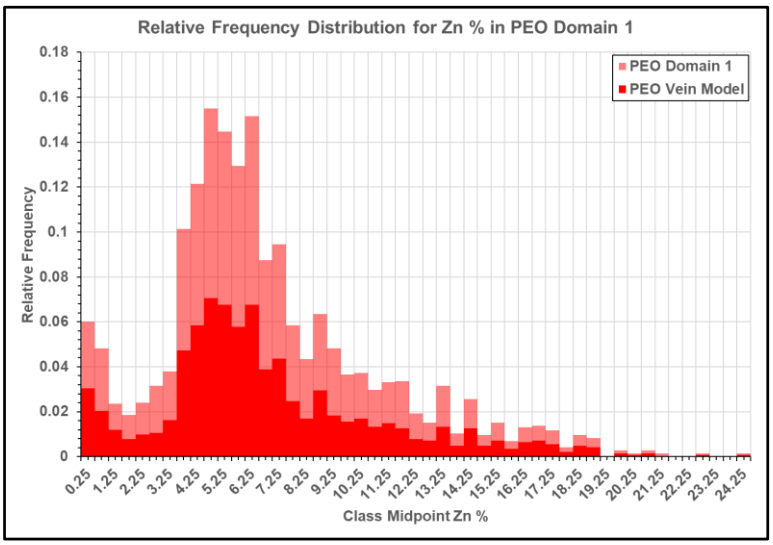


Figure 5.11 Relative Frequency Distribution for Zn % in PEO Domain 1. The distribution for the PEO vein model before domaining is shown at 50% transparency in the background.

Similar to Domain 2 in the MPO, domain 2 in the PEO also have very few samples, making a histogram or frequency distribution less informative and hence the Zn % boxplot for PEO Domain 2 was created and appears in Figure 5.12.

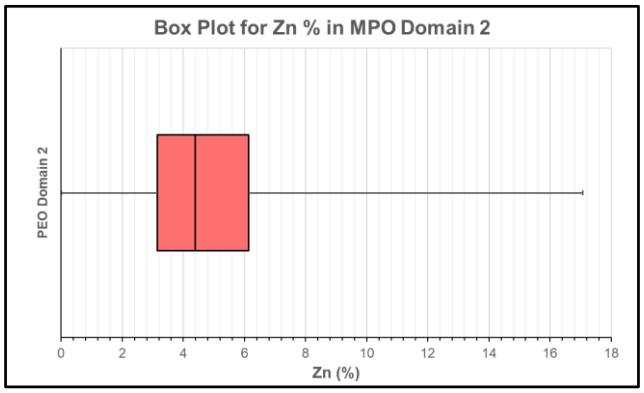


Figure 5.12 Box Plot for Zn % in PEO Domain 2.

The summary statistics and frequency distributions indicate that the Indicator Kriging did not sufficiently separate high and low domains in either the MPO or the PEO rock units. This could be due to a number of reasons.

Firstly, especially in MPO, the CPD plots (Figure 4.32 and Figure 4.34) did not show a clear inflection point, making it difficult to select a threshold value. Although the PEO (Figure 4.34) showed a clearer inflection point, IK still did not resolve the populations.

Secondly, the size of the subpopulation. MPO has 157 samples (29.6 %) below the 7.4 % Zn indicator value whereas PEO has only 133 samples (9.6 %) below the 3.6 % Zn indicator value. In the case of the block these were even less.

Thirdly, the block sizes used might not be appropriate for estimating on the right scale. When examining the indicator values for MPO and PEO in 3D, it can be seen that the downhole distribution of these values is fairly variable, with most areas showing high grade cores (GAMD027-1-0 or GAM055-0-0 in Figure 5.13), or the so-called “bar-code” effect, as in GAMD027-3-0 in Figure 5.13.

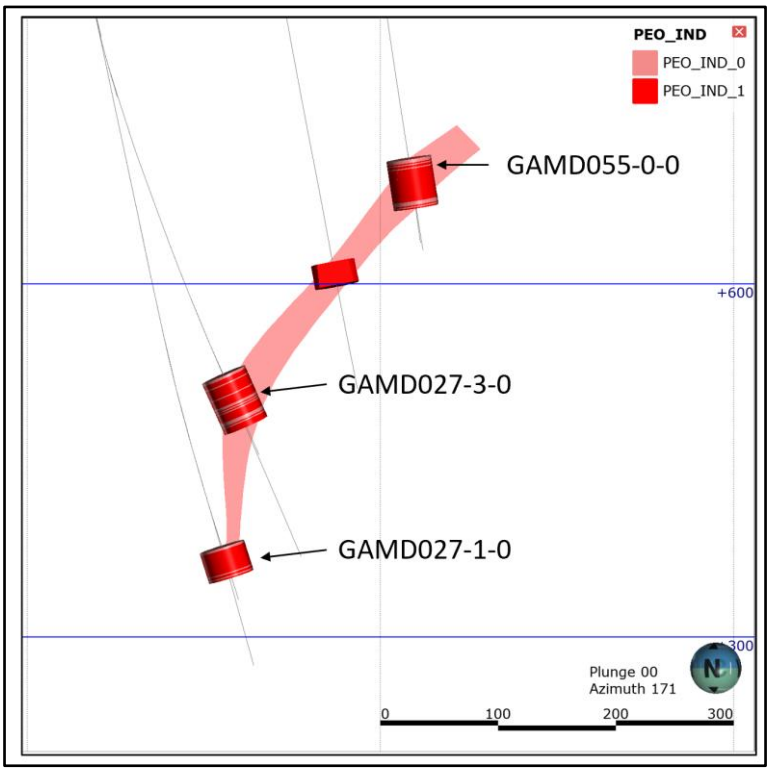


Figure 5.13 Cross section showing core and fringe and barcoding of grades in PEO.

These changes are seen at a sample scale level and is reflected in the nugget effect of 0.3 of the PEO indicator. With sample lengths being 1 m, it implies that to krige an indicator value that accurately reflects a block probability, that block z dimension has to be very small. IK was done on blocks with a z dimension of 2 m. It was considered that reducing the block size to 1 m would not have the desired effect, since the kriging estimate still has to use samples from further afield. Given the small number of samples below the indicator, these are likely to be above the indicator.

From the above it can be said that, given the current size and spatial distribution of the data set, IK could not sufficiently resolve either the MPO or the PEO into grade domains.

5.6. Use of indicators to refine models

Although the use of IK to resolve the modelled volumes was not successful, the assigned indicators proved useful in identifying populations. Another technique that exists in Leapfrog Geo, which could be used to resolve these volumes into high- and low-grade populations based on the indicators. Using the indicator values, the modelled values can be refined in Leapfrog Geo. Refined models allow the user to “subdivide any existing volume from a geological model using any other column of data in your project (e.g., alteration, mineralisation, ungrouped lithologies, etc.)” (Seequent, n.d.).

Within Leapfrog Geo, indicator values were assigned for MPO and PEO using the threshold values discussed in section 5.5. These indicators were then used to refine the modelled volumes into domains where the indicator was = 0 and domains where the indicator was = 1.

The outcomes thereof are shown below in Figure 5.14 with the outline of the unrefined volume as a mesh and the sample indicator values that were used as inputs. In a process similar to that described in section 5.3.3 pinch outs were reviewed on both indicator = 0 volumes.

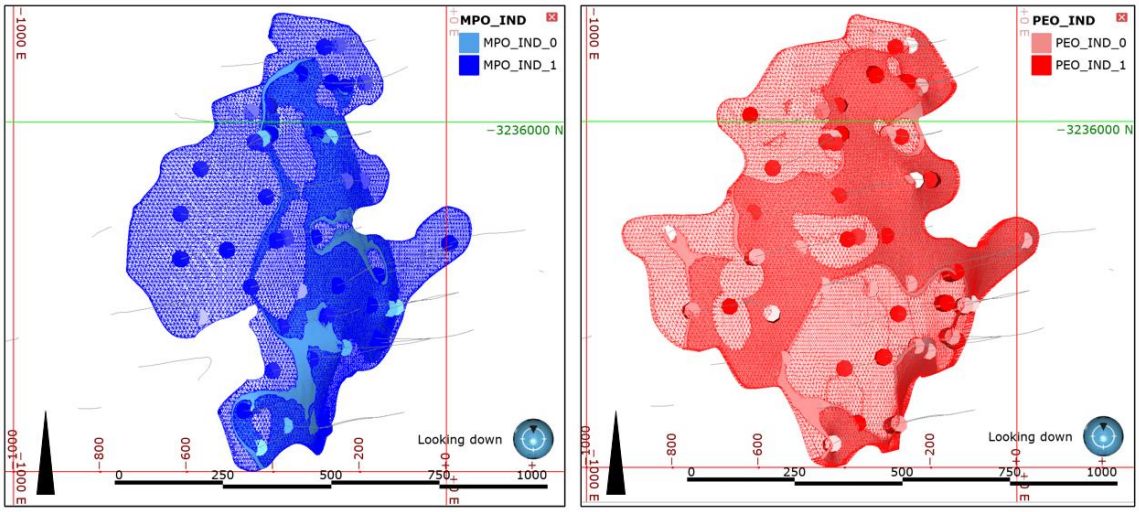


Figure 5.14 MPO (left) and PEO (right) refined volumes based on indicator values.

The summary statistics for these domains are shown in Table 5.6 and Table 5.7.

Table 5.6: Summary Statistics for Zn % in MPO Refined Volumes.

	Rock Type	MPO Vein Model	MPO Refined Volume 0	MPO Refined Volume 1
Zn	N	527	101	426
	Mean (%)	10.006	5.701	11.027
	Standard Devation (%)	5.180	4.747	4.739
	Variance (% ^{2})	26.836	22.538	22.459
	Median (%)	10.250	4.336	11.110
	Mode (%)	10.850	1.810	10.850
	CV	0.518	0.833	0.430
	Kurtosis	2.191	3.204	2.617
	Skewness	-0.050	1.117	-0.175
	Maximum (%)	24.150	17.950	24.150
	Minimum (%)	0.456	0.456	0.676
	IQR (%)	8.344	5.255	6.558
	Range (%)	23.694	17.494	23.474

For MPO, the refined volume based on the values below the indicator threshold (Refined Volume 0) has a small number of samples, but at 5.7 % Zn the mean is well below the indicator threshold value of 7.4 % Zn. However, the higher value of the CV compared to the original population indicates an increase in variability in the grade within this volume. Both the skewness and kurtosis parameters are much higher than in Refined Volume 1 or the original population, which indicates a leptokurtic, highly skewed distribution.

Since the sample number is low, frequency distributions such as histograms and CPD were not considered, but a boxplot was drawn which is shown in Figure 5.15. From this can be seen that the distribution is highly right skewed, with a large range and a IQR smaller than in the unrefined volume.

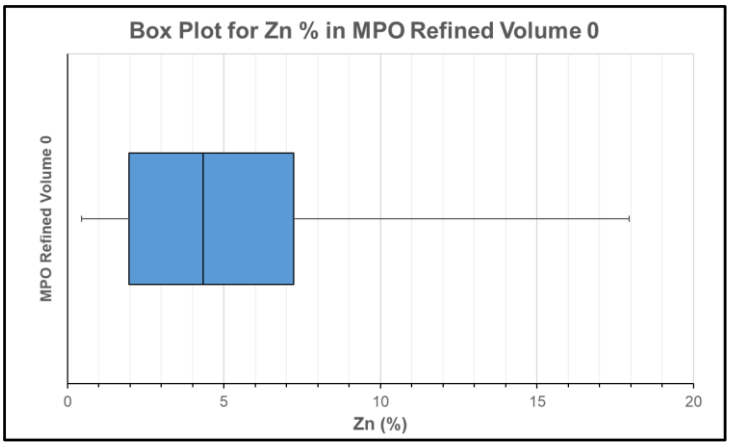


Figure 5.15 Boxplot for Zn % in MPO Refined Volume 0.

For the refined volume based on the values above the indicator threshold (Refined Volume 1) the mean is higher than in the unrefined volume. But from the summary statistics in Table 5.6 can be seen that the shape of the distribution remains largely unchanged. This is confirmed by the frequency distribution (Figure 5.16).

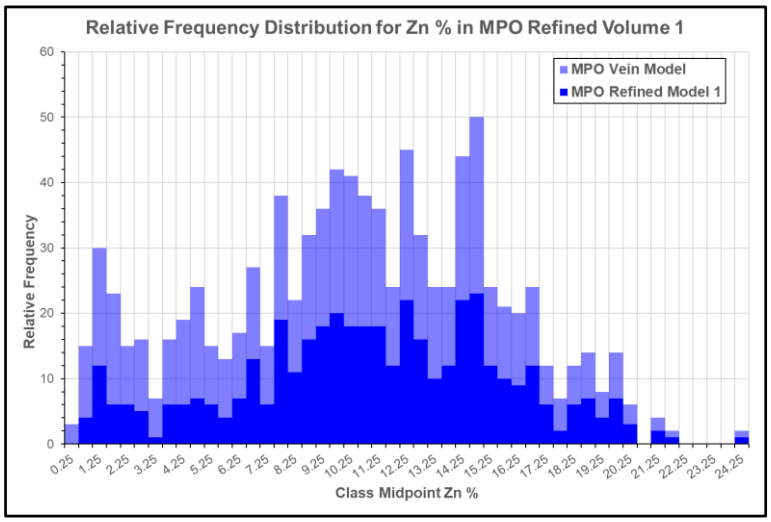


Figure 5.16 Relative Frequency Distribution for Zn % in MPO Refined Volume 1. The distribution for the MPO vein model before refining is shown at 50 % transparency in the background.

For PEO, the summary statistics (Table 5.7) show similarly to MPO, the number of samples in Refined Volume 0 (below the indicator threshold) are small, but the mean grade is above that of the indicator threshold. In the Refined Volume 0 the Zn % grade has a highly skewed, leptokurtic lognormal distribution, indicated by the summary statistics and confirmed by the histogram in Figure 5.17.

Table 5.7 Summary Statistics for Zn % in PEO Refined Volumes.

	Rock Type	PEO Vein Model	PEO Refined Volume 0	PEO Refined Volume 1
Zn	N	1478	158	1320
	Mean (%)	6.875	4.097	7.208
	Standard Devation (%)	3.952	3.141	3.909
	Variance (% ^{2})	15.621	9.866	15.282
	Median (%)	6.071	3.390	6.266
	Mode (%)	4.860	2.870	4.860
	CV	0.575	0.767	0.542
	Kurtosis	4.164	5.601	4.233
	Skewness	0.962	1.546	0.970
	Maximum (%)	24.500	16.300	24.500
	Minimum (%)	0.010	0.105	0.010
	IQR (%)	4.289	2.784	4.252
	Range (%)	24.490	16.195	24.490

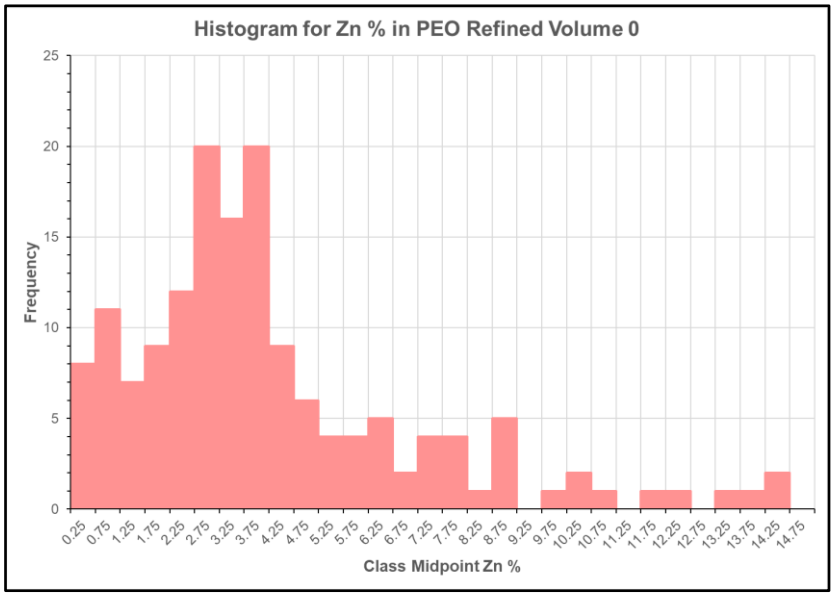


Figure 5.17 Histogram for Zn % in PEO Refined Volume 0.

The refined volume 1 has a largely unchanged distribution as shown in Table 5.7 and Figure 5.18.

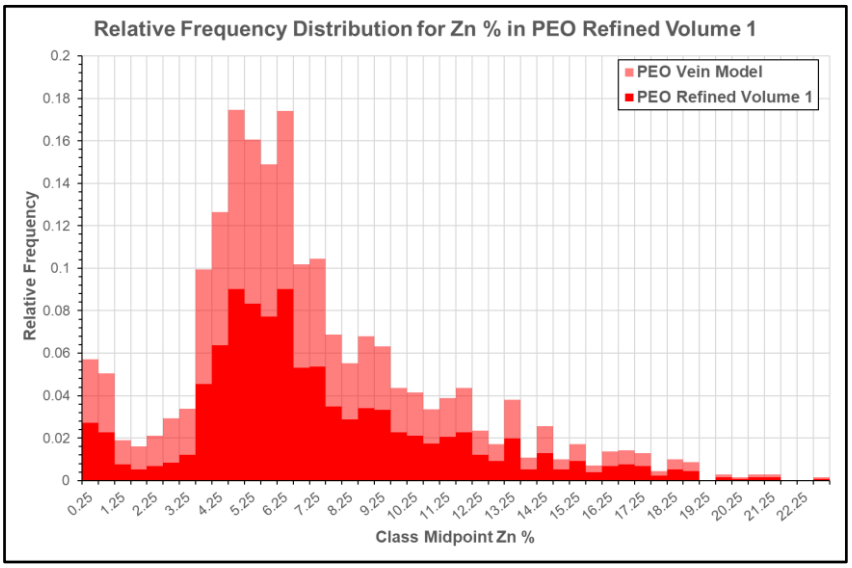


Figure 5.18 Relative Frequency Distribution for Zn % in PEO Refined Volume 1. The distribution for the PEO vein model before refining is shown at 50 % transparency in the background.

From the above distributions and statistics, it can be seen that using the indicators to refine the MPO and PEO volumes did not lead to the creation of satisfactory domains.

Furthermore, a review of historical reports showed that Reid & Harley (2009) identified the same zoning shown in Figure 4.34 in the PEO but did not further examine it due to lack of data.

5.7. Use of grade to define domains.

The existence of a low-grade fringe and a high-grade core zone is well documented in the Gamsberg deposit (Reid & Harley, 2009) and personal experience of the author on other areas of the deposit where its existence has also been observed. Since none of the work conducted thus far indisputably showed this characteristic, it was decided to consider the deposit in its entirety, instead of splitting the deposit by rock type.

From the CDF in Figure 4.2 an indicator threshold value of 3.6 Zn % was identified. Displaying grades above and below this value and examining in 3D shows very clearly that the deposit exhibits a low-grade fringe and a high-grade core, as shown in Figure 5.19 below. Since the distinction is so clear in 3D, it was not considered necessary to again use IK to separate the zones, and the threshold value of 3.6 Zn % was used as criteria to model a core and a fringe zone.

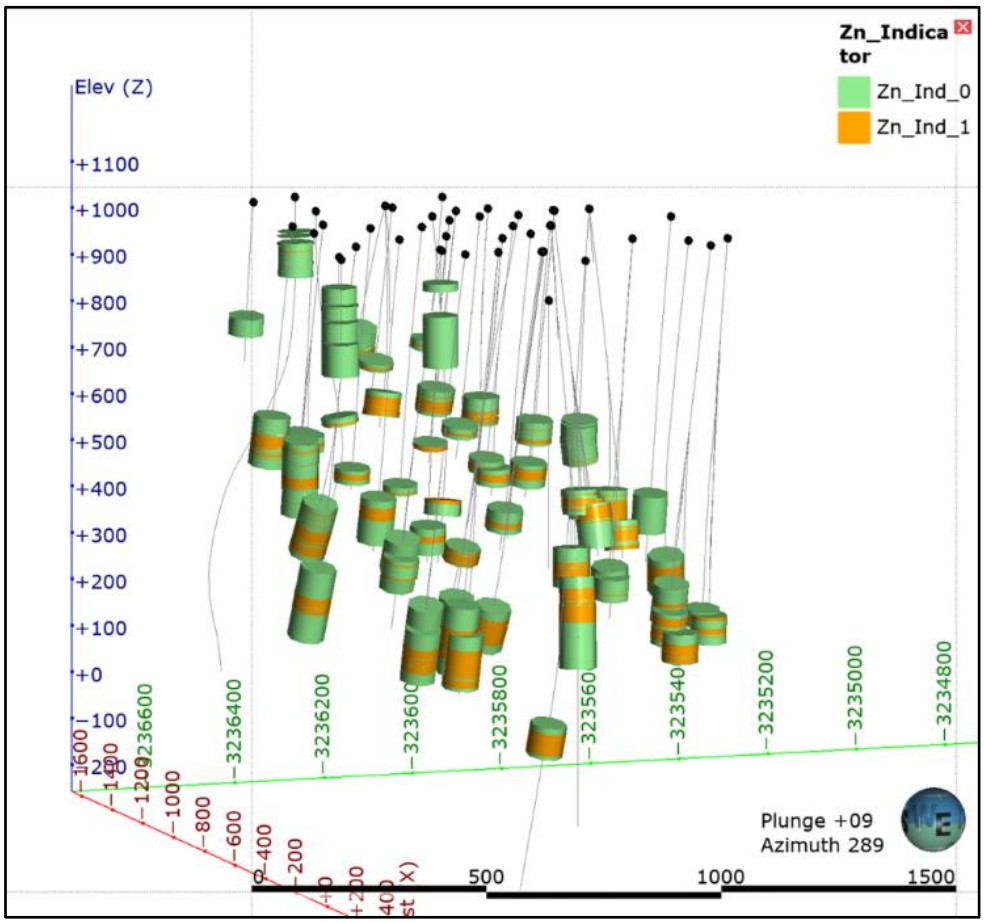


Figure 5.19 Drill holes showing Zn % values above (orange) and below (green) the 3.6 % Zn indicator threshold.

In Leapfrog Geo, the core was modeled by individually selecting intersections above the indicator and modelling those as a vein. The fringe zone was modelled

through a hybrid method of creating offset surfaces and generating a volume between them. Low grade intersections in the hanging wall were selected and used to create a hanging wall that incorporates the selection but is also offset from the hanging wall of the core. The same approach was used for the footwall. A final fringe volume was then generated by applying a boundary to create a volume between these two offset surfaces. The benefit of using this approach is that it generates a volume that fully encompasses the core zone. A cross section through the model is shown below in Figure 5.20.

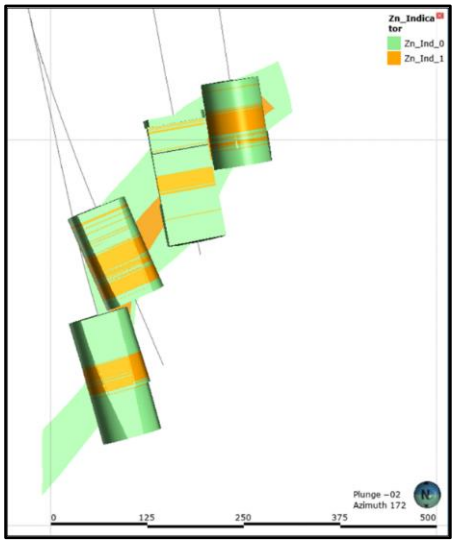


Figure 5.20 Cross section of Core and Fringe Zone.

The summary statistics for the fringe and core zones are shown in Table 5.8.

Table 5.8: Summary statistics for Zn % in Core and Fringe Zones.

		Fringe	Core
Zn	N	2440	1776
	Mean (%)	1.302	7.910
	Standard Devation (%)	2.615	4.434
	Variance (% ^{2})	6.839	19.656
	Median (%)	0.336	6.788
	Mode (%)	0.059	4.860
	CV	2.008	0.560
	Kurtosis	18.763	3.127
	Skewness	3.704	0.717
	Maximum (%)	19.550	24.500
	Minimum (%)	0.001	0.043
	IQR (%)	1.084	5.885
	Range (%)	19.549	24.457

The measures of middle, indicate a positive skewed distribution with Mode < Median < Mean. The high skewness and kurtosis parameter indicate a highly skewed leptokurtic distribution. Furthermore, the large range and the small IQR indicated that although the spread of the values is large, the values mostly occur in a narrow band.

As expected, the core zone has a mean grade well above the indicator threshold value and the Mode < Median < Mean relationship indicate a positively skewed distribution. The skewness parameter indicates that the distribution is more moderately skewed, and the kurtosis indicates a mesokurtic shape.

The histogram for Zn % in the fringe zone (Figure 5.21) confirms the statistics and show highly skewed lognormal type distribution. The histogram for the core zone (Figure 5.22) has an almost bimodal distribution – with the small, low grade peak indicating a population of 194 samples (10.8%) below the indicator value.

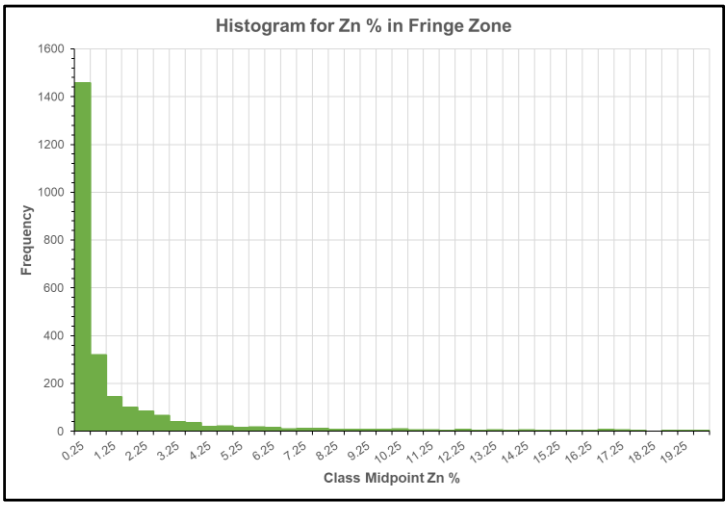


Figure 5.21 Histogram for Zn % in Fringe Zone.

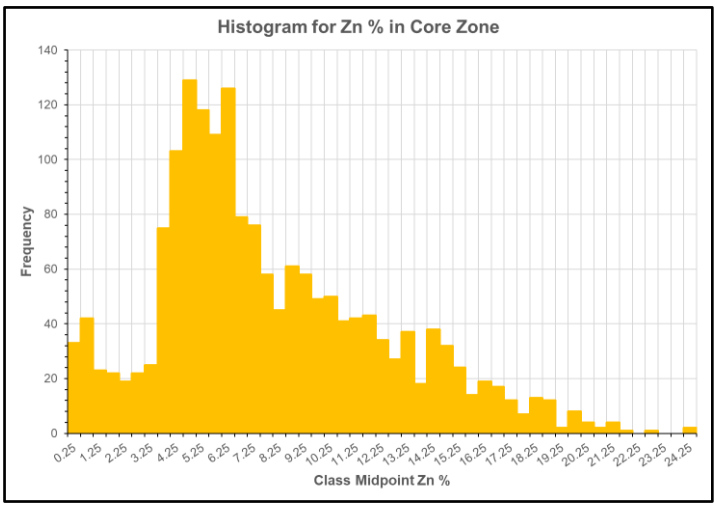


Figure 5.22 Histogram for Zn % in Core Zone.

Further investigation into the origin of the low-grade peak in the histogram for the core zone, show that some holes, such as GAMD33-0-1, GAMD033-2-4 and GAMD033-3-2, lower grade samples occur within the high grade (Figure 5.23).

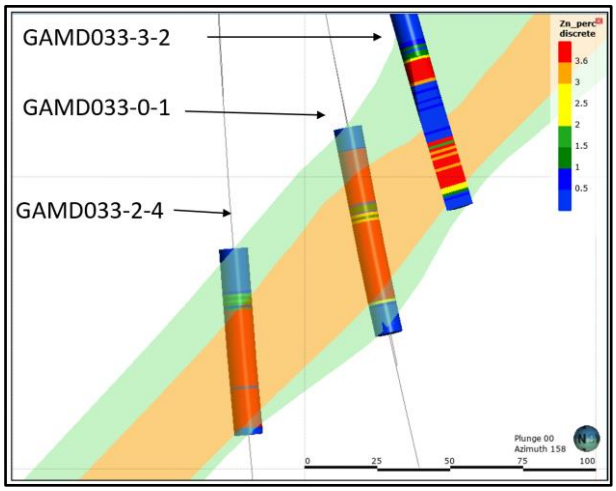


Figure 5.23 Cross section showing mixing of grades in Core Zone.

In some cases (GAMD033-3-2) the low-grade samples were logged as ore lithologies (MPO and PEO). In the case of GAMD033-0-1 the low grade lithologies are logged as GQZ – a garnet quartz rock which is considered part of the lode rock (Anglo American Exploration, 2010). On GAMD033-2-4, the low-grade intersection at 899.45 – 900.45 m is logged as PEO. However, examining the logs indicate a quartz vein occurring at 897.12 – 898.45 m. This intersection has ore grade assays, which would suggest that the PEO and the quartz veins assay had been swapped.

In other cases, such as GAMD029-2-2 (Figure 5.24) the geometry of the vein model is such that although only high grade is selected, the vein still intersects low grades.

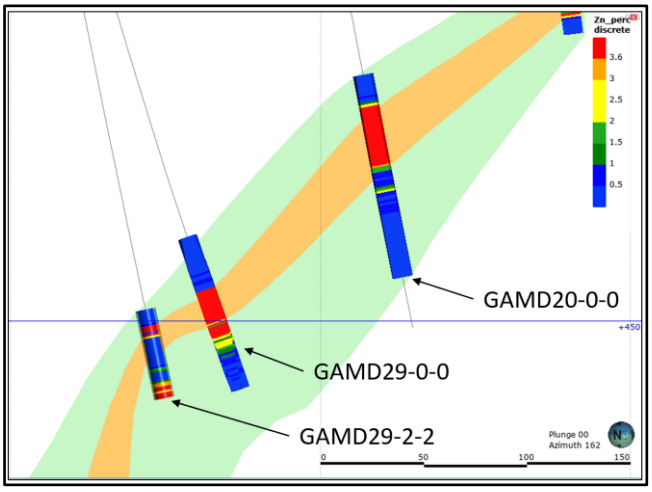


Figure 5.24 Cross section showing geometry including low grades into Core Zone.

This is largely due to the geometry of the orebody, but could also represent issues with data, such as swapped samples or incorrect surveys. With the drilled pattern of wedges, minor errors with surveys or sample depths could compound to make data that is difficult to model accurately. A possible resolution of such issues of geometry is to increase the resolution on the model to produce a finer surface, which better honour contacts. On close spaced drilling, this can help with resolving issues such as shown in Figure 5.24 where there is a significant change in elevation of the intersection in two neighbouring holes.

Often this does not present a practical solution, as changing the resolution can dramatically increases the size of the model and associated processing times, especially in large datasets that is typical of mining projects. A higher resolution model was considered but showed no improvement in the geometry around GAMD029-2-2. When considering Figure 5.24, it is possible that the intersection modelled does not join stratigraphically with the up– or down-dip intersections. On GAMD029-2-2 it is likely that the hole was stopped short and the half-drilled intersection at the end of hole represents the modelled core zone.

After creating the grade shells based on the 3.6 % Zn value from the CDF, it can be said that 2 domains were identified. The distributions within these two domains are better understood than those presented in section 4.8 and represent a well-known characteristic of Zn deposits such as Gamsberg. Compared to the complex GCLN distributions presented in section 4.9, the lognormal and bimodal distributions that the core and fringe model produces can be said to better understood and therefore have a higher confidence. Furthermore, when defining wireframes based on grade, the grade within is considered to be homogenous. That means that the grade shells are realisations of a stationary random function (Emery & Ortiz, 2005).

Based on this, it was decided to continue to the next step of the Mineral Resource Estimation process, using the core and fringe models identified.

5.8. Summary and Conclusion

From the EDA it was concluded that rock type, specifically MPO and PEO, should form the basis for the geological modelling. A new project was created in Leapfrog Geo and the data displayed in 3D. This showed that GAMD061 should not be used in geological modelling, since in this hole, the rock types of interest do not occur where it is expected. The collar of this hole also lies below the topography.

A number of options were considered for the geological modelling and the outputs compared. The intrusive model did not generate valid outputs, even when a structural trend was applied. The deposit model was considered. This entailed

some manual recoding of the input data, with waste above and below the mineralised units recoded as “Hanging Wall” and “Foot Wall” respectively. The first pass deposit model resulted in the waste between the MPO and PEO being included into the overlying PEO. As a second pass, this unit was recoded into an “Inter Ore” unit and modelled separately. The summary statistics of this unit showed it to be mineralised. 19 % of the intersections within this unit were logged as GPM– a unit with similar mineralogy to MPO. Although the output volumes of the deposit model were conformable, the MPO and especially the PEO output volume that extended far beyond the extent of the data. The extent of volumes cannot be edited manually. This model was not considered geologically valid. The vain modelling methodology in Leapfrog Geo is the preferred method for modelling thin, laterally continuous zones. For Gamsberg East, the pinch out option was enabled, which pinches out output volumes where data indicated that the vein no longer occurs. This method also allows for the application of a manually generated boundary. This was applied using a 50 m buffer around drill hole traces. Since this method also allows for manually editing of the output volumes, both the MPO and PEO were reviewed and edited manually to ensure that the volumes do not crosscut. The output of this model was validated by comparing the summary statistics within the modelled domain with the summary statistics of the sampled rock unit.

Since the EDA indicated that both MPO and PEO have mixed populations, an IK method was applied to assist with separating the modelled units into low- and high-grade domains. Threshold values were chosen by examining CPDs for MPO and PEO and indicators assigned accordingly. After IK, domains were identified where the probability of Zn % grades being above the threshold is low. These were domained by cutting the modelled volume with a polyline drawn around the area of low probability. Summary statistics and distributions for Zn % grade was examined per domain and compared to the summary statistics and distributions in the volumes before domaining. From this it was shown that IK did not properly split the volumes into low- and high-grade domains. As an alternative method, the indicator values for MPO and PEO were used to create refined domains within Leapfrog Geo. Summary statistics and distributions showed that this method also did not sufficiently resolve the MPO and PEO into low- and high-grade domains.

Since the existence of a low-grade fringe and a high-grade core is known from literature and experience, it was decided to consider the deposit in its entirety using a threshold value of 3.6 % Zn. When examined in 3D the existence of the fringe and the core was clearly seen. The core zone was modelled by manually selecting intersections above the threshold and creating a vein model. The fringe zone was modelled by creating surfaces offset from the hanging wall and the foot wall of the core zone. se were modelled using the vein methodology and a. The

summary statistics and distribution of the Zn % grade within the fringe and the core zones showed a lognormal and a bimodal distribution, respectively. These distributions are much better understood than the complex GCLN distributions identified in the EDA and can therefore be said to have higher confidence. It was decided to proceed with the modelled fringe and core zones as domains for the resource estimate.

Implicit modelling in a software package such as Leapfrog Geo, allows for the generation of alternative models, using different methodologies. However, it was seen that output should always be validated, to ensure that the resulting model represents a valid geological scenario as well as the input data. It was also seen that indicator methods may prove useful for domaining volumes, either by using IK to krige probabilities, or by modelling assigned indicators through implicit modelling techniques.

6. MINERAL RESOURCE ESTIMATION

According to the Rossi and Deutsch (2014) the primary goal of Mineral Resource Estimation is to forecast the grade and tonnage of material that is to be mined. They refer to two different scenarios – an interim estimate, where the goal is to accurately estimate global recoverable resources, and a final estimation, where the focus is on local accuracy for ore/waste delineations. The two scenarios each require a different approach.

OK is commonly used for interim estimates. Conditional bias is almost always present because of the smoothing effect of kriging where data is widely spaced. Conditional bias usually results in the true grade being less than an estimated grade where the estimates are high and vice versa.

Critical to geostatistical studies is the variogram. It is a measure of variability that increases as the dissimilarity between samples increase. A variogram is also a measure of geological variability of distance and this variability needs to be understood to interpret and model the variogram. (Gringarten & Deutsch, 2001).

When kriging, the definition of the kriging neighbourhood or search volume may have a very notable impact on the results of the kriged estimate. Quantitative Kriging Neighbourhood Analysis (QKNA) uses simple and well-established test to test the appropriateness of the Kriging neighbourhood. The results of QKNA can also be used to inform block sizes, discretisation, and classification of resources (Vann, et al., 2003)

For the purposes of the research study an interim estimate would be appropriate. The first step would be to calculate experimental variograms for Zn and SG in the core and fringe zones and model the spatial continuity. Then the estimation will be set up and executed, after which it will be validated. A classification scheme will be applied, taking into account various factors to classify the resource in terms of confidence. As a final output, a grade tonnage curve will be generated to assess quantity and grade of the estimated Mineral Resource.

6.1. Selection of variable to be estimated

Considering that the purpose of Mineral Resource Estimation is to predict the grade and tonnage of recoverable material, it was decided to focus on the estimation of Zn and SG in the Gamsberg East deposit. Whilst Pb also occur, Zn is the primary value driver at the Gamsberg operation and it was used to define the wireframes in section 5.7.

6.2. Variography

Experimental variograms for Zn and SG were constructed in Maptek Vulcan Data Analyser. Before the process was started, the data was examined for outliers. Since the analysis of outliers in section 4.6 used the uncomposited assays, this outlier analysis was done on composites for the core and fringe zones for Zn and SG. Although it is not strictly correct to do outlier analysis on composites, in this case it was accepted, to ensure that all statistical and geostatistical work is done on the same support. The results are shown in Table 6.1.

Table 6.1 Outlier values for SG and Zn in core and fringe zones.

	Fringe		Core	
	SG (g/cm^3)	Zn(%)	SG (g/cm^3)	Zn(%)
Mean	**3.241**	**1.302**	**3.558**	**7.910**
10th Percentile		**0.033**		**3.632**
90th Percentile		**3.403**		**14.460**
1st Quartile	**2.920**		**3.397**	
3rd Quartile	**3.530**		**3.744**	
IQR	**0.610**	**3.370**	**0.347**	**10.829**
Low Threshold	**1.090**	**-10.077**	**2.355**	**-28.854**
High Treshold	**5.360**	**13.513**	**4.786**	**46.946**
Number of outliers	**5**	**30**	**9**	**0**

The same methodology was used as in section 4.6. Samples with values outside the respective threshold values were excluded from variography only and not from the estimation. This is necessary, since variance is sensitive to outlier values because it is a squared statistic (Gringarten & Deutsch, 2001; Rossi & Deutsch, 2014). The construction and modelling of variograms followed the guidelines as set out by Gringarten and Deutsch (2001) and Rossi and Deutsch (2014).

When modelling the downhole variograms to find the nugget effect, it is important to keep in mind that the data used also included drill core samples of lengths greater than 1 m, that were decomposited to 1 m. This reduces the small-scale variance, since longer samples were replaced by several 1m composites of the same grade.

After nugget effects had been estimated using downhole variograms, variogram maps were used to check for anisotropy. Abzalov, (2016) explains that variogram maps are 2D diagrams which display calculated variogram values along all directions on a reference plan. These variogram maps and variogram models for Zn & SG in the Core and Fringe zones are presented in Appendix B,

The maximum extent of the orebody is approximately 800 m - based on that, a range of 400 m was chosen for the experimental variograms. Beyond half the domain size, the variogram starts to leave data out of calculations (Rossi & Deutsch, 2014). Based on the drill spacing in the major direction, a lag of 50 m was chosen with a default tolerance of 50%.

According to Rossi & Deutsch (2014) angle and lag tolerances should be kept as small as possible. Tolerances that are too small will result in noisy variograms, but tolerances that are too large will average out the spatial continuity. For the variograms maps and subsequently, the experimental variograms, angle tolerances were adjusted visually. From previous work conducted in *MINN7043* it is known that fairly large bandwidths are necessary to be able to encompass sufficient data in an environment of sparse information.

The standardised experimental variograms were calculated for Zn % and SG (g/m^3) in the fringe and the core zones. Models were fitted to the experimental variograms, using the nuggets effects estimated from the respective downhole variograms.

Each experimental variogram was fitted with a spherical model with two structures in addition to the nugget effect. Variograms were not strictly modelled to a sill of 1. The same model was used in all orthogonal directions, but the ranges modelled separately. Fitting models were challenging, due to low number of pairs in the experimental points. The objective of the fitting was to get the best possible fit in the major direction, by focusing on experimental points representing the highest number of samples.

All experimental variograms show geometric anisotropy, where the sill is reached at different distances in different directions (Rossi & Deutsch, 2014), which is typical of base metal deposits. The clustering of data due to wedged holes could be the source of high variability on short scale.

Figure 6.1 shows the orthogonal semi-variogram for Zn in core zone as example of the observed geometric anisotropy. All the Zn and SG experimental variograms and models for Core and Fringe are shown in App**endix B.**

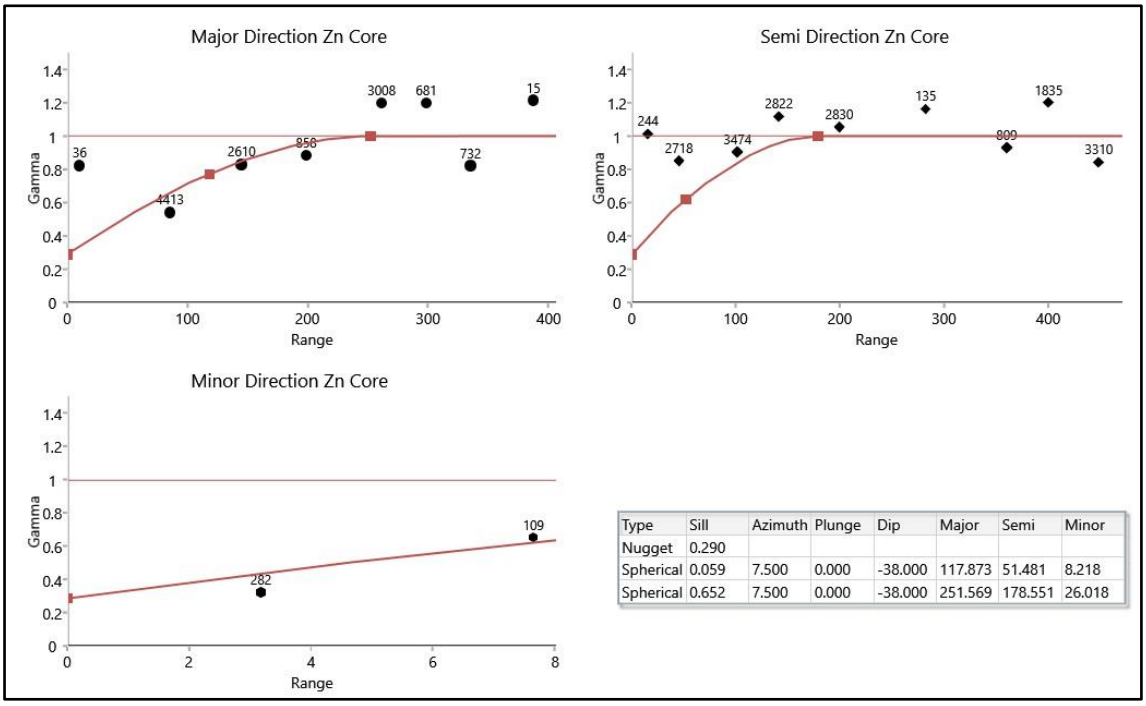


Figure 6.1 Experimental Semi-variogram for Zn with fitted model in core zone.

6.3. Kriging Plan

Rossi and Deutsch (2014) states that kriging plan "*mostly determines the quality of the grade estimate*." Some aspects of the kriging plan are discussed below.

6.3.1. Quantitative Kriging Neighbourhood Analysis (QKNA)

QKNA is a simple and well-established methodology to test the appropriateness of the Kriging neighbourhood parameters (Vann, et al., 2003). It is a resource intensive process and requires multiple runs to optimise various parameters such as block size, sample numbers and discretisation to minimise conditional bias.

QKNA was conducted in Maptek Vulcan for Zn % in the core and fringe zones. The results of the QKNA showed that no configuration of block size, search radius and discretisation yielded good results for KE and SLOR, and that different configurations of neighbourhood parameter yielded similar results. When optimising the number of samples, it was observed for both the core and the fringe that increasing the number of samples had a positive impact on both the SLOR and the KE.

Given the inconclusive results of the QKNA, the focus of this research study, and supported by the fact that no additional data had been added since that study, it was decided to use adapted Kriging neighbourhood parameters of the QKNA conducted by Reid & Harley (2009); this adaption is presented in Table 6.2.

Table 6.2: Adapted QKNA after Reid & Harley (2009).

	Direction	MPO (Reid & Harley, 2009)	PEO (Reid & Harley, 2009)	Adapted Fringe	Adapted Core
Search Radius					
	X	180	200	200	250
	Y	180	200	180	180
	Z	5	15	30	30
Parent Block Size					
	X	100	100	100	100
	Y	100	100	100	100
	Z	4	4	4	4
Subblock Size					
	X	5	5	5	5
	Y	5	5	5	5
	Z	2	2	2	2
Discretisation (X/Y/Z)		5 x 4 x 1	5 x 5 x 1	5 x 5 x 1	5 x 5 x 1
Minimum no. of samples		10	10	10	10
Maximum no. of samples		40	40	40	40

Block size. Block sizes were left unchanged from the optimised block size. Since no additional data had been added and the core and fringe zones are thicker than the MPO and PEO, Reid & Harley's (2009) block sizes, which allows "reasonable approximation of the geometry of the MPO and PEO wireframes" was considered appropriate.

Search Ranges. Search ranges were adapted based on the core and fringe zone variograms for Zn. Rossi and Deutsch (2014) states that maximum search ranges should be based on the "reliability and the effectiveness" of the variogram and not simply its range. As a first pass, search range similar to the variogram range was used. As second and third passes the range was extended until upward of 99 % of blocks were estimates.

Declustering. Due to wedged holes, samples are spatially clustered and would require declustering. A cell declustering method was applied in Maptek Vulcan with samples declustered to a 40m cell, based on a plot of declustered mean for Zn % vs. cell size plot (Figure 6.2).

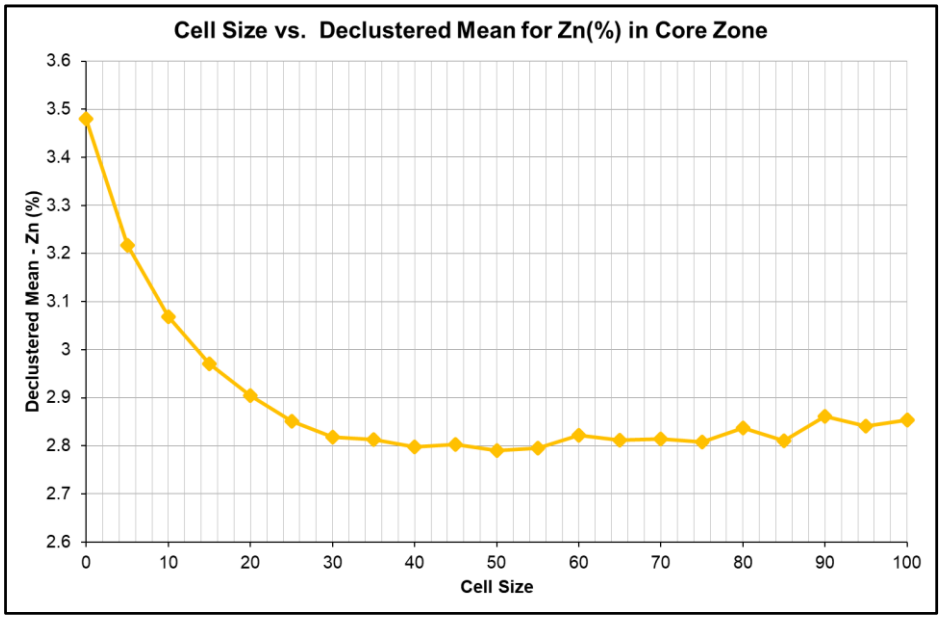


Figure 6.2 Plot of declustered mean vs cell size for Zn in core zone.

Number of octants, drill holes and samples. As a first pass, the number of samples were kept the same as what Reid & Harley used in 2009. For the second pass a minimum of 8 samples was used.

In Gamsberg East sample are clustered due to the drilling of wedged holes, Since the data was already declustered using a cell declustering method, it was not deemed necessary to decluster samples by using an octant-based search or adding additional limitations.

6.3.2. Boundaries

Another consideration is how to treat boundaries between wireframes/estimation domains. When using grade shells, there is a dependency between the domains, which occurs due to spatial continuity in the deposit. Gradational boundaries are very common in geological settings due to the nature of mineralisation systems and are characterised by departure from stationarity for the variable of interest (Larrondo & Deutsch, 2005). Emery and Ortiz states that estimating grade domains separately will result in creating a boundary that is not present in the geology (Emery & Ortiz, 2005). Since the final wireframes were based on grade, a soft boundary approach should be used. Larrondo and Deutsch (2005) suggest OK with soft boundaries as the best conventional approach. Contact Analysis was done in Maptek Vulcan for Zn at the Core/Fringe boundary to confirm the use of a soft boundary (Figure 6.3).

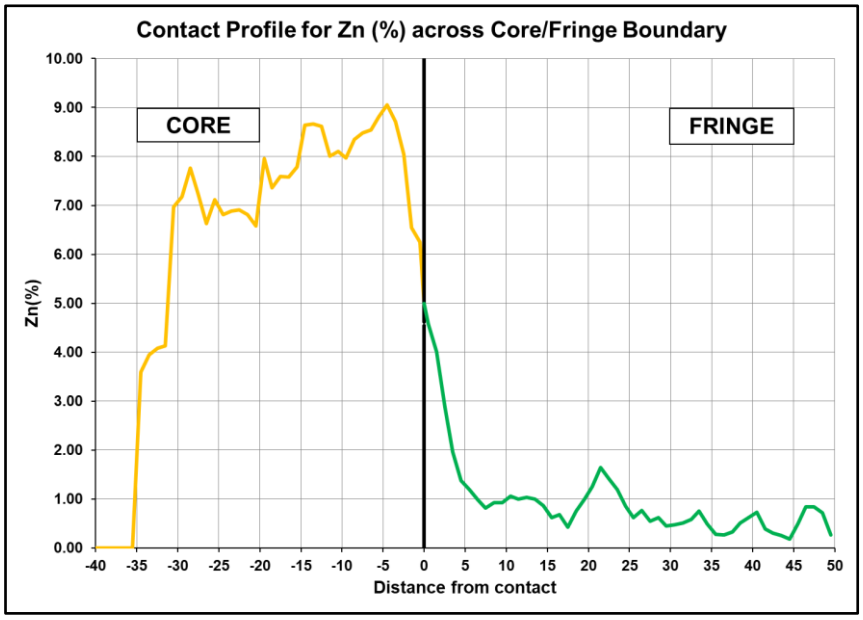


Figure 6.3 Contact Profile for Zn across Core/Fringe Boundary.

6.3.3. Grade Capping

In Table 6.1 outliers for Zn and SG in the core and fringe zones are shown. Outlier values were excluded in variography, as stated in section 6.2. Zn showed no outliers in the core zone, but 30 values fall above the high threshold in the fringe zone. These values represent separate high-grade intersections within the fringe zone that could not be modelled separately, due to lack of continuity. Since these values represents real samples and not errors *per se*, it was not capped. Instead, a distance restriction was placed on the influence of the isolated high-grade samples within the low-grade fringe during the estimation process.

For SG, five outliers occur in the fringe zone and nine in the core zone. Three of the values in the core zone are above the threshold value, whereas the rest are below. Looking at Table 6.1, it can be seen the low threshold value for both the core and the fringe zone represent an unrealistically low value for the SG of mineralised rock. In addition to that, some values not identified as outliers has unrealistically low SG values. In the fringe zone, 23 values (of which five were identified as outliers) below 2.65 g/cm^3 occur and in the core zone seven values (of which six were identified as outliers) below 2.65 g/cm^3 occur. Since 2.65 g/cm^3 is the average density of lithospheric rocks, these values were set to that. This was considered a conservative approach given that the average density for both the core and the fringe zone are above that.

The process of setting up a kriging plans should be iterative – outputs are compared to production data to calibrate the parameters. Where no production data exists, such as with Gamsberg East, the output has to be validated by other

means (Rossi & Deutsch, 2014). During the estimation process for Gamsberg East, every iteration of the block model was validated though a histogram of Zn in the core zone and a swath plot. Where the estimate failed to satisfactorily reproduce the distribution of Zn, kriging neighbourhood parameters were adjusted, and a new run completed. The final estimation parameters for SG and Zn in the fringe and the core zone are presented in Appendix C.

6.4. Validation

After estimation, blocks were exported to Microsoft Excel. Summary statistics and histograms were plotted for SG and Zn in the core and fringe zones. Summary statistics for Zn in the in the database and the block model are shown below in Table 6.3.

Table 6.3 Summary Statistics for the Zn % block estimates in the core and fringe zones and corresponding samples.

	Rock Type	Core Blockmodel	Core Database	Fringe Blockmodel	Fringe Database
Zn	N	29915	1776	78381	2440
	Mean (%)	7.670	7.910	1.097	1.302
	Standard Devation (%)	2.309	4.434	0.955	2.615
	Variance (% ^{2})	5.332	19.656	0.912	6.839
	Median (%)	7.482	6.788	0.858	0.336
	Mode (%)	7.283	4.860	0.270	0.059
	CV	0.301	0.560	0.871	2.008
	Kurtosis	3.946	3.127	10.309	18.763
	Skewness	0.545	0.717	1.857	3.704
	Maximum (%)	17.468	24.500	10.960	19.550
	Minimum (%)	1.206	0.043	0.000	0.001
	IQR (%)	2.784	5.885	1.465	1.084
	Range (%)	16.262	24.457	10.960	19.549

Observations from Table 6.3 show that although the overall mean grades are fairly well estimated, the shape of the distribution in the core zone is changed. This is confirmed by the frequency distribution for the core zone (Figure 6.4) where the distribution for the block model is plotted as shaded bars in the background. The variance and spread of the dataset are reduced in the estimated blocks, as would be expected. This also corresponds to an increase in the kurtosis as data shifts into the peak.

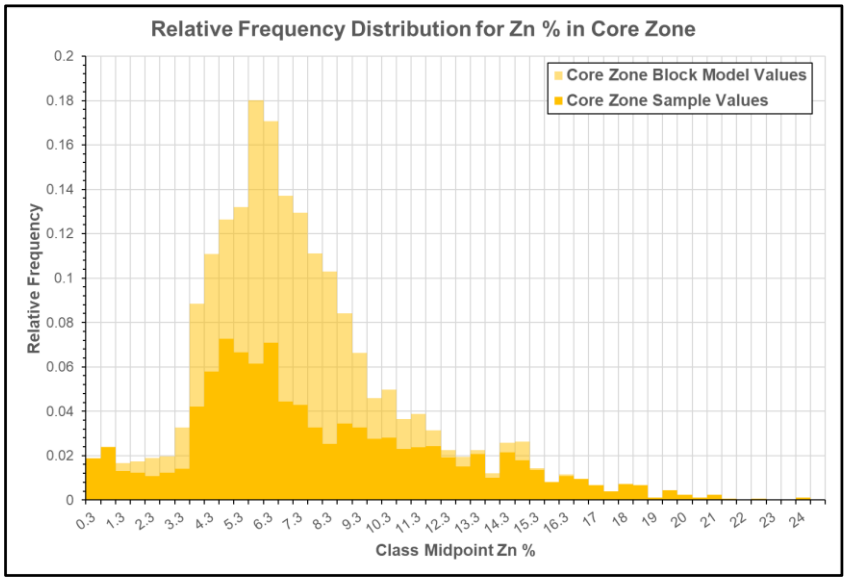


Figure 6.4 Relative frequency distribution for Zn in the core zone of the block model (50% transparency) and the database.

Table 6.3 highlights that the changes to the distribution in the fringe zone is more pronounced. The mean is lower, but the spread and variability decreases. Although the general shape remains positively skewed, the skewness and kurtosis decrease, indicating an overestimation of the lowest grades. The lower spread of values is also due to the use of distance restriction, which limits the influence of high grades.

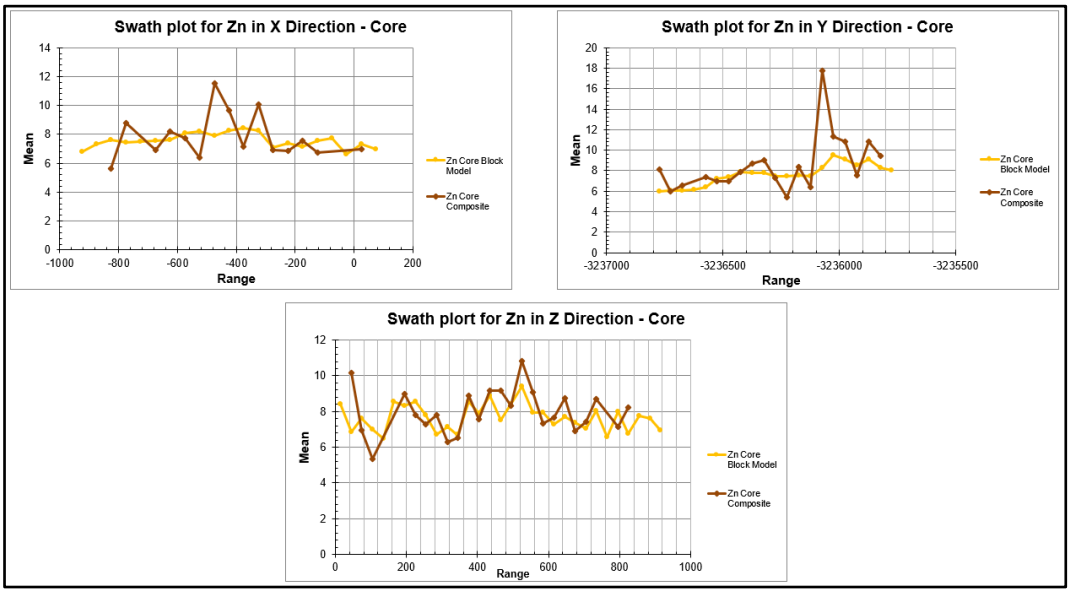


Figure 6.5: Swath Plot for Zn in core zone.

The swath plot for Zn in the core zone is shown in Figure 6.5. A complete set of swath plots for the Core and Fringe estimation validation appear in Appendix D.

Figure 6.5 shows that a high degree of smoothing is still present in the estimate of Zn in the core zone. It also indicates that few samples are used to estimate many blocks – which inherently leads to smoothing. For this estimate, to reduce smoothing, the first and second passes had short search distances. in an attempt to avoid over smoothing. However, in order to estimate the remaining blocks, the third pass had to have large search distance.

Although various iterations of estimate were done, the SLOR and KE did not perform well for any of the configurations. Below in Figure 6.6 the SLOR for the Zn % estimate in the core zone is plotted. From this can be seen that for the majority of the deposit, especially at the edges of the orebody and where data is sparse, the SLOR is low, indicating conditional bias.

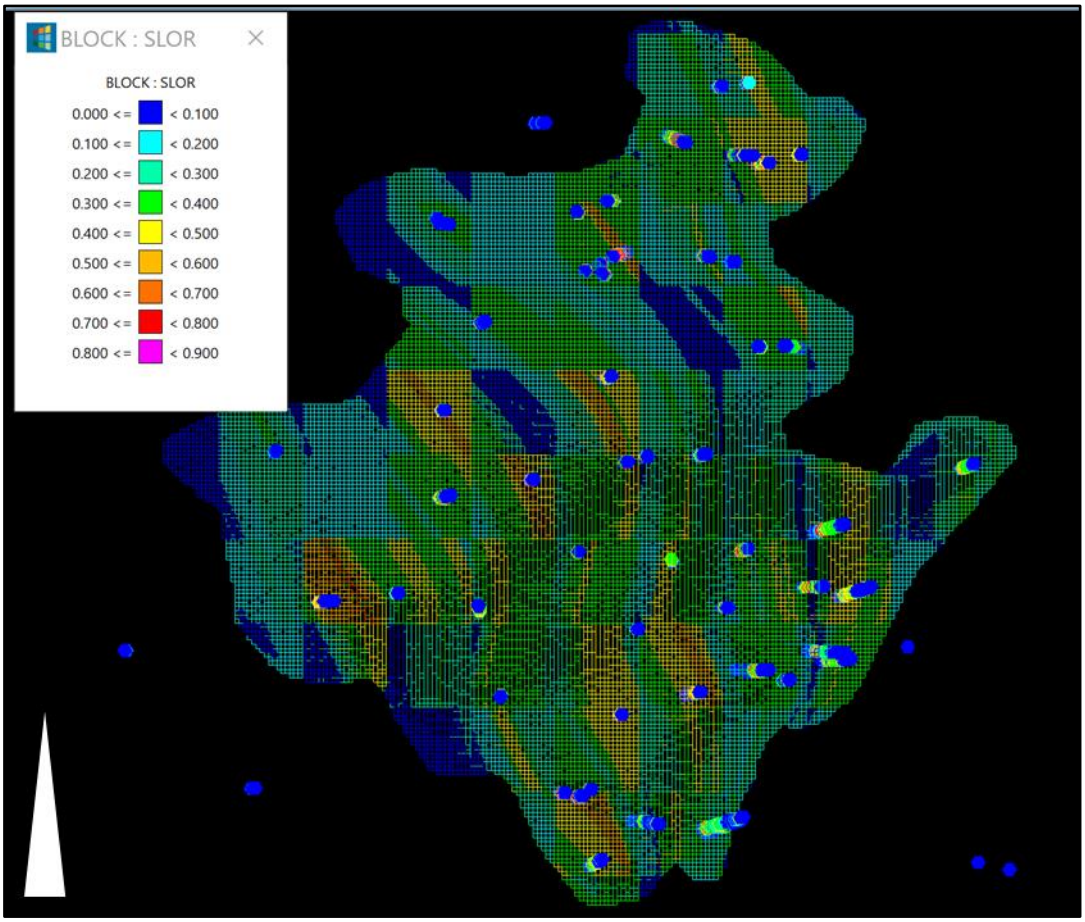


Figure 6.6 SLOR for Zn estimate in core zone.

Although validations for the block models did not perform well, the swath plot and histogram do indicate that the general distribution is roughly reproduced by the estimate. With data that is so sparse, it becomes a challenge to estimate in a fashion to meets all the validity requirements.

6.5. Resource Classification

For the purpose of classifying the mineral resource, reference was made to the SAMREC code of 2016. The code defines an Inferred Mineral Resource as “that part of the Mineral Resource for which quantity and grade or quality is estimated on the basis of limited geological evidence and sampling” (SAMREC, 2016).

Looking simply at the data distribution on Gamsberg East, as well as the inferences about ore extent and continuity made during geological modelling (section 5.3) and grade estimation (section 6.2), it is clear that the entire deposits should be classified as an Inferred Mineral Resource.

When considering metrics such as drill spacing, KV and KE (Figure 6.7) some areas are better informed and can therefore be said to have higher confidence. However, the area shown in Figure 6.7 possibly represents a separate domain, as seen from outlier analysis (section 4.6) and scatterplots (section 4.5). It was not defined as such and this could justify not upgrading this area without additional drilling information, since it could be argued that the area is not well-understood or accurately handled in domaining and estimation.

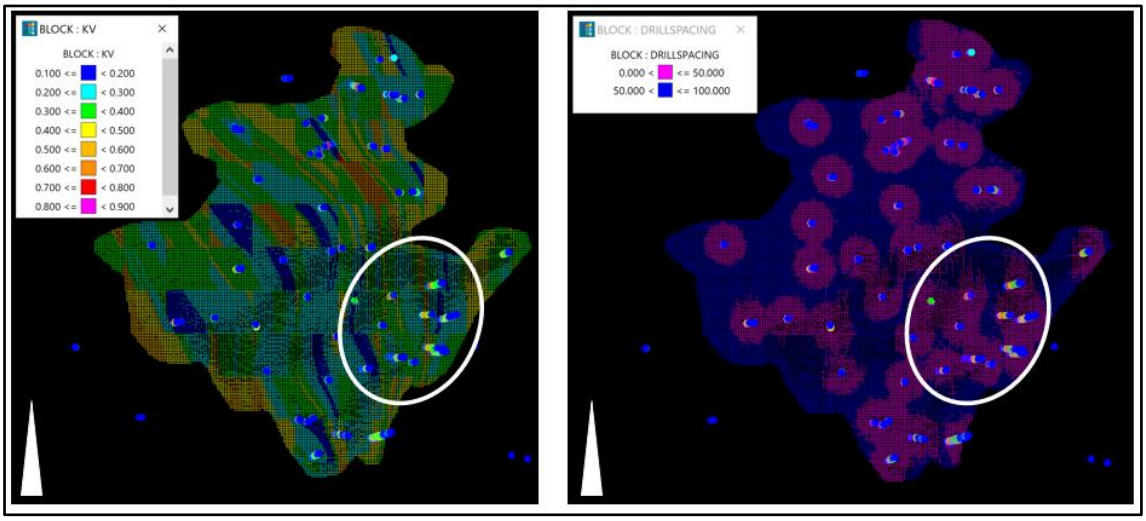
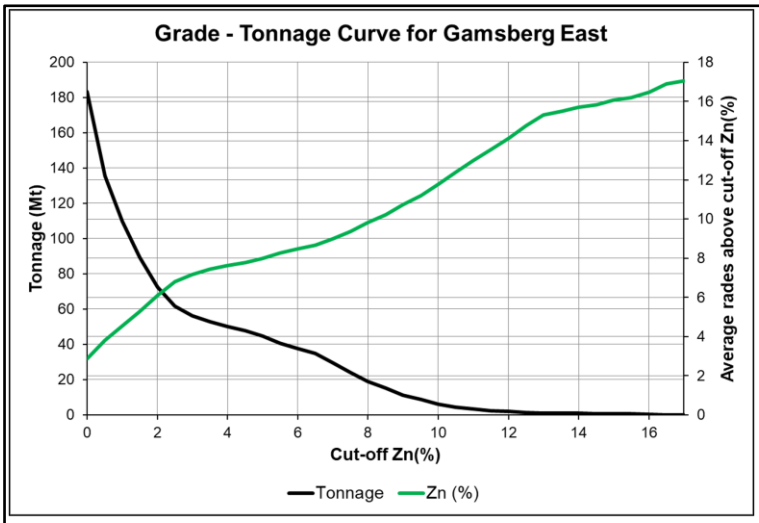


Figure 6.7 KV (left) and drill hole spacing (right) in Gamsberg East. Circle indicates area of higher confidence.

6.6. Grade Tonnage Curves

To assess the total size (volume or tonnage) and metal content of the deposit, a grade-tonnage curve was generated in Maptek Vulcan. The grade tonnage curve, shown in Figure 6.8 estimate above a cut-off grade of 4 % Zn is 50.17 Mt with an average grade of 7.62 % Zn.



Cutoff Zn(%)	Average Grade above cut-off Zn(%)	Tonnage (Mt)
4	7.62	50.17
4.5	7.78	47.84
5	7.99	44.76
5.5	8.27	40.56
6	8.47	37.70
6.5	8.65	34.79
7	9	29.39
7.5	9.37	24.20
8	9.83	19.03
8.5	10.21	15.37
9	10.74	11.30
9.5	11.19	8.66
10	11.78	6.22
10.5	12.39	4.43
11	12.98	3.25
11.5	13.54	2.48
12	14.11	1.89
12.5	14.76	1.39
13	15.3	1.10
13.5	15.51	1.01
14	15.71	0.91
14.5	15.83	0.83
15	16.06	0.68
15.5	16.19	0.60
16	16.46	0.36
16.5	16.89	0.12
17	17.04	0.08

Figure 6.8 Grade Tonnage curve for Gamsberg East, with tabulated grade and tonnage at incremental cut-off values.

Reid & Harley (2009) declared 58.6 Mt at 7.96% average grade Zn above a 4 % Zn cut-off. The Mineral Resource estimate from this research study, consistently indicate lower tonnages with grades comparable to the 2009 block model. One possible reason for this is the impact of estimated SG. This study estimated a SG based on recorded values, whereas assigned average SG values based on rock type were used in the 2009 block model. Since rock type is not recorded in the 2009 block model of Reid & Harley, a comparison is difficult to do and would not be accurate.

The grade shell approach used in this study includes waste lithologies, which could result in global density being lower than the SG values for mineralised rock used in the 2009 study.

Another possibility is the change in methodology. Reid & Harley modelled the Gamsberg East orebody based on rock type, whereas this research study used a grade approach, as discussed in section 5.7.

Thirdly, the inclusion of eight drill holes that had previously been excluded, as discussed in section 3.2.5, could have an effect on the estimated grade and tonnage, although this effect is more likely to have a localised effect, unlike the global effect observed.

Lastly, Reid & Harley (2009) conducted work in unfolded or flattened space. This research study was not conducted in unfolded space.

6.7. Summary and Conclusion

For the purposes of the research study an interim estimate, which estimate global recoverable resources was considered appropriate. Zn is the main economic driver; therefore it was decided to estimate Zn % grade through OK. In addition to that, SG values were also estimated to calculate tonnages. Since the fringe and core zone were chosen as domains, variograms were calculated for Zn and SG within these zones. First, downhole variograms were constructed to determine the nugget effect. Here it had to be kept in mind that some decompositing had occurred which could result in lowered short scale variability. The directions of variography were chosen through the use of 2D variogram maps. Experimental variograms were constructed, taking care to exclude outlier values. Spherical models with 2 structures each were fitted for each variable in each domain. Due to the sparsity of experimental data, experimental variograms were badly structured and therefore difficult to fit models to. The focus of the variogram modelling was on achieving the best fit through points representing the highest number of samples, along the major directions.

Next, a kriging plan was developed. QKNA was conducted to optimise block size, search radius, discretisation, and sample numbers. QKNA in Maptek Vulcan had inconclusive results. Considering that no additional data had been added since the previous resource estimate, it was decided to adapt the Kriging neighbourhood parameters from that study.

A boundary analysis for Zn % grades between the fringe and the core zone showed a gradational boundary, which indicated that the use of a soft boundary between these zones would be appropriate. This approach is also considered appropriate where domains are based on grade, as is the case with the core and the fringe zone. From outlier analysis, no Zn values were considered to be outliers, but there were 30 samples above the high threshold within the fringe zone. Since these represent real high grade values, which could not be modelled separately, it was decided not to cap these values but rather limit their influence during the estimation process. SG showed 14 low outlier values, as well as 16 values below 2.65 g/cm^3 which is considered the average density of lithospheric rock. These values were set to 2.65g/cm^3.

The estimation was executed and the estimated Zn % grade in blocks compared to the distribution in the samples. Where the estimation failed to reproduce the distribution, estimation parameters were adjusted and the blocks re-estimated. To validate the estimate, block models were exported to Microsoft Excel and summary statistics and histograms produced for Zn % grade in the fringe and core zones. The final estimate reproduced mean grades in the core zone, but

showed a lower variance and spread, and an increase in kurtosis. In the fringe zone the estimated mean, as well as the spread of the values was lower than that of the samples, but the overall shape of the distribution was unchanged. The lower spread of values could also be attributed to the use of a distance restriction. In addition to comparing distributions for Zn % grades in the fringe and core zones, swath plots were also plotted for all elements across all domains.

The Mineral Resource estimate was classified as Inferred based on data density and inferences made about ore extent and grade continuity. Metrics such as drill spacing, KV and KE indicated an area of higher confidence. This area was identified as potentially being a separate domain in the EDA. Since it was not treated as such, upgrading that area to Indicated could not be justified. Finally, a grade tonnage curve was constructed to assess the total tonnage of the deposit. The estimated grade tonnage curve showed a lower tonnage at a comparable grade to what was estimated in the previous study. Possible causes for this could be the change in modelling methodology, the estimation of SG, the inclusion of previously excluded holes and not estimating in unfolded space.

Although care was taken in setting up the Mineral Resource estimate, the metrics still yielded poor results and the resulting estimate has an Inferred classification. Swath plots and distributions indicated that the estimate replicated the samples fairly, although the estimate is smoothed when compared to sample data. With wide drill spacing necessitating long search ranges a smoothed estimate with low KV and KE is to be expected.

7. OVERVIEW AND SUMMARY

A historical dataset, such as the one forming the basis of this research study poses many challenges. These include questions on data integrity, lost or missing metadata, incomplete reporting, a lack of supporting documents and even a lack of context regarding company policies over time.

In stage 1 of this research study, manual data validation on the drill hole database was done to assess the size, condition, and completeness of the dataset and to prepare it for the next steps in the resource estimation process. During this stage a number of cases were encountered where crucial additional information was not available. For the most part, careful and methodical examination of the data and the existing metadata helped to resolve these questions. It must also be said that experience and an understanding as well as familiarity with industry protocol also proved useful during this stage of the study. As frustrating as the process of EDA can be, it is very useful and informative in helping the practitioner familiarise themselves with the dataset and understanding its limitations.

Next, the dataset was examined and interrogated statistically to gain a better understanding of the grade distributions and characteristics of the deposit. Grade probability distributions were examined for bias, by comparing different data collection techniques – such as drill types and assay methods. Although none was noted in this particular dataset, it could also be due to the fact that some of this information had to be inferred during Stage 1. Outlier analysis and correlations pointed to the possibility of high Pb/Ag domains with textural and structural characteristics. Grade domaining typical of Zn deposits were observed using CDF plots.

Based on sampling statistics, as well historical reporting, two main domains of interest were identified during this stage and the grade probability distributions examined, described, and modelled for each domain. Although these domains were recorded as distinct geological units, it showed complex multimodal grade probability distributions, beyond the statistical prowess of an ordinary mine geologist.

Stage 2 of the study was concerned with creating a valid geological model for the deposit. By using implicit geometry modelling techniques in Leapfrog Geo, several alternative models could be considered. Models were assessed based on the geological soundness of their outputs, as well the appropriateness of the methods and assumptions associated with any of the specific technique.

Since the grade distributions seen in stage 2 indicated mixed grade domains, a number of techniques were explored during the geological modelling stage in an attempt to resolve the modelled domains into low- and high-grade domains.

Indicator Kriging was used to predict the probability of blocks below the chosen indicator value. Blocks with a high probability of being below the indicator were few and fairly discontinuous. Where they showed continuity, a domain boundary was applied. Summary statistics of the low- and high-grade domains indicated that the indicator kriging subdomains had distributions very similar to those in the original domain.

The same indicator threshold values were used to implicitly refine the geological models in Leapfrog Geo. Just as with the indicator kriging, the resulting domains were small, discontinuous and statistically similar to the original domain. Examining the indicator kriging results in 3D, a core and fringe zone within the deposit were revealed. This distinction had not been readily visible when viewing normal grade values. The core and fringe were modelled in Leapfrog Geo using a combination of techniques to create a high-grade vein-shaped domain and a low-grade fringe that fully encompasses it. Grade distributions within these domains have clearer and simpler distributions than in the models based on rock types. In addition to that, using grade shells allows for the assumption of stationarity.

During this process a number of interesting observations were made regarding the dataset, including the identification of swapped samples, mineralised units occurring between the main mineralised lithologies and the identification of the fringe and core zones. These were not noted earlier due to their spatial nature. Instances such as these show the importance of, and impact of data visualisation.

Stage 3 involved the estimation of mineral resources using domains as identified and modelled in the previous stages. Since Zn % is the main element of interest, it was estimated alongside SG (g/cm^3) in order to calculate global grades and tonnages. Although it had previously been assumed that there is not enough SG data to estimate, the detailed EDA examination showed that there were.

Experimental variograms were calculated and modelled for each variable in each zone, including finding the nugget effect with the use of downhole variograms. The directions for the variograms were chosen by using variogram maps to orientate the major direction of the orthogonal variogram. Experimental variograms were poorly defined prior to stabilising at the sill due to large drill spacing. In an attempt to find data points, large tolerances and bandwidths were used, which may not accurately reflect directional continuity. Variograms did show geometric anisotropy. Fitting variogram models were challenging, due to sparse experimental points. The focus of the fitting was to get the best possible fit in the major direction, focusing on experimental points representing the highest number of samples.

Given that the deposit is still in exploration stage, with widely spaced data (> 100 m), an interim estimate was done. A kriging plan was devised to fulfil the requirements of an interim estimate. This process was iterative, with estimated distributions being checked against sample distributions and adjustments to parameters made. A final iteration that roughly reproduced the distribution of Zn in the core zone was selected.

This model was then validated by examining summary statistics, grade distributions and swath plots. KE and SLOR were also examined but did not perform well. Swath plots indicated smoothing, and also highlighted that few samples are being used to estimate many blocks, which makes smoothing inevitable.

Within the context of the SAMREC code, the Gamsberg East deposit would be classified as Inferred. A number of inferences was made regarding the continuity of grade, which was based on scant data. However, when considering additional metrics such as drill spacing and Kriging Variance, one area in particular has a higher confidence level. This area, as indicated in Figure 6.7 coincides with Pb/Ag outliers correlation and outlier as identified in section 4.5 and section 4.6. Considering its outlier values, this area could represent a discrete domain which should be treated as such in the future if more drilling information is collected.

Since the aim of the interim estimate was to determine grade and tonnage of the deposit, a grade-tonnage curve was constructed. This resulted in an Inferred Mineral Resource estimate of 50.17 Mt with an average grade of 7.62 % Zn above a 4 % Zn cut-off compared to the 2009 Reid & Harley estimate of 58.6 Mt at 7.96 % Zn average grade above a 4 % Zn cut-off. Overall, for all cut-offs considered, this research study estimate produced fewer tonnes at comparable grades in comparison to the 2009 preliminary assessment estimate. Possible reasons for the discrepancy are the use of default SG values by Reid & Harley the difference in modelling and estimation methodology and the addition of data.

8. CONCLUSIONS AND RECOMMENDATIONS

The objective of this study was to use a variety of statistical and graphical techniques to describe, interrogate and visualise the Gamsberg East dataset with the aim of gaining confidence and understanding in the characteristics and limitations of the data. Through multiple stages of data compilation, analysis and processing, various characteristics of Gamsberg East and its associated dataset became clear. The importance of a multi-stage, multi-disciplinary approach also became evident in that relevant and important qualities of the dataset, such as the core and fringe definition, only became apparent when looked at with indicator kriged values; intended for a different purpose.

Another important learning for this practitioner is to be cautious of relying too heavily on historical documents The Reid & Harley report of 2009, supported by the distribution of sampled rock types, lead to the idea that the zones of interest must be based on the MPO and PEO lithologies only. Although that approach might not be incorrect *per se*, the grade distribution within those lithologies were too complex for this practitioner to resolve and that avenue of research is beyond the scope of this research study. The aim of the study is to utilise simple techniques to add value and confidence.

Another example of this is the use of default SG values by Reid & Harley, as is often applied in practice. Although it might be the case that within the MPO and PEO domains not enough data occur for an estimate, it is not the case when using grade domains.

Even though validations on the estimates did not perform particularly well, the fact that the input data had exhaustively been investigated does lend confidence to the final estimate. A thorough understanding of the data and its limitations also contributes to the understanding of why the final estimates are what they are.

From this research study, the following recommendations can be made for future estimations of this deposit:

- In order to reduce conditional bias, the use of simulation techniques should be considered.
- Additional elements should be added to the EDA and the estimation to maximise the understating and value of the Gamsberg East orebody. Pb, specifically, is an element of interest in Gamsberg East and should form a part of the estimate. So too should Mn, which is an important deleterious element in Zn concentrates.
- All iterations of the geological model presented, showed the orebody to be undulating. Unfolding or flattening the orebody prior to variography and

estimation would produce better variograms and estimates. Dynamic Anisotropy could also produce satisfactory results, since this method considers undulations during estimation.

- Further investigation into the Gamsberg East database is required. During the course of this research study, it become clear that there are instances where data that was reported to have been present, such as QA-QC samples, are not present in the database used for this research study. Similarly, the re-assays that were outstanding were for the most part never included. This should be investigated and if possible, resolved.
- The experimental variograms constructed for this research study was poorly structured and resulted in difficulties when fitting variogram models. Focus on constructing better variograms, by taking more care and time to adjust parameters such as lag, and angle tolerances would result in better variograms and ultimately better kriging metrics and estimates.
- The classification should be revisited. Drill spacing indicated areas of higher confidence. If estimates are made with better variograms, resulting in better kriging metrics, these areas can be upgraded from Inferred to Indicated.
- It is recommended that as a best practice guideline, the research methodology and findings of this research study be incorporated alongside the EDA reference work of (Sinclair, 1998; Abzalov, 2016), and variography (Gringarten & Deutsch, 2001) be considered for future use on similar deposits. This will ensure that the learnings of this research study are retained.

REFERENCES

Abzalov, M. Z., 2014. Design Principles of Relational Databases and Management of Dataflow for Resource Estimation. In: N. Hanson, ed. *Mineral Resource and Ore Reserve Estimation: The AusIMM Best Practice Guide.* Carlton(Victoria): The Australasian Institute of Mining and Metallurgy, pp. 47-51.

Abzalov, M. Z., 2016. In: *Applied Mining Geology.* 1 ed. Basel: Springer International Publishing, pp. 178, 189, 187, 189-190, 193, 202, 207-208, 235-236, 239, 245, 265, 275, 291.

Anglo American Exploration, 2010. *Gamsberg Project Manual v.3,* s.l.: Unpublished Internal Report.

Anglo Base Metals, 2009. *Gamsberg East Conceptual Study Report,* s.l.: Unpublished Internal Report.

Birch, C., 2014. New systems for geological modelling–black box or best practice?. *The Journal of The Southern African Institute of Mining and Metallurgy,* Volume 114, December 2014, pp. 993-1000.

Chanderman, L., Dohm, C. E. & Minnitt, R. C. A., 2017. 3D geological modelling and resource. *The Journal of the Southern African Institute of Mining and Metallurgy,* Volume 117, February 2017, pp. 189-197.

Chilès, J.-P. & Delfiner, P., 2012a. Random Functions. In: *Geostatistics: Modelling Spatial Uncertainty.* Hoboken: John Wiley & Sons, Inc, pp. 16 -17.

Chilès, J.-P. & Delfiner, P., 2012b. Multivariate Methods. In: *Geostatistics: Modelling Spatial Uncertainty.* Hoboken: John Wiley & Sons, Inc, p. 299.

Cloete, E. M., 2018. *The Geostatistical Investigation of the Gamsberg East Deposit – Northern Cape, South Africa,* s.l.: Unpublished.

Davis, J. C., 2002. In: *Statistics and Data Analysis in Geology.* 3 ed. New York: John Wiley & Sons, pp. 461, 462.

Deutsch, J. L., Szymanski, J. & Deutsch, C. V., 2014. Checks and measures of performance for kriging estimates. *The Journal of The Southern African Institute of Mining and Metallurgy,* Volume 114, March 2014, pp. 223 - 230.

Dohm, C. E., 1995. *Improvement of Ore Evaluation Through Identification of Homogeneous Areas Using Geological, Statistical and Geostatistical Analyses.* Johannesburg: Ph.D Thesis, University of Witwatersrand.

Dohm, C. E., 2021. *Personal Communication.* s.l.:s.n.

du Toit, M. C., 1998a. Zinc. In: M. Wilson & C. Anhaeusser, eds. *The Mineral Resources of South Africa: Handbook.* Pretoria: Council for Geoscience, pp. 676-681.

du Toit, M. C., 1998b. Lead. In: M. Wilson & C. Anhaeusser, eds. *The Mineral Resources of South Africa: Handbook.* Pretoria: Council for Geosciences, pp. 424 - 432.

Emery, X. & Ortiz, J. M., 2005. Estimation of mineral resources using grade domains: critical analysis and suggested methodology. *The Journal of the South African Institute of Mining and Metallurgy,* 105(April), pp. 247 - 255.

Glacken, I. & Blackney, P., 1998. *A practitioners implementation of indicator kriging.* Perth, The Geostatistical Association of Australasia.

Google, 2018. *Aggeneys, 29° 13' 20'' S, 18° 54' 39'' E, 932m.* [Online] Available at: https://www.google.com/earth/index.html [Accessed 25 October 2018].

Gringarten, E. & Deutsch, C., 2001. Teacher's Aide Variogram Interpretation and Modeling. *Mathematical Geology,* 33(4), pp. 507 - 534.

Hodkiewicz, P., 2013. *Leapfrog 3D.* [Online] Available at: https://www.leapfrog3d.com/__data/assets/pdf_file/0017/539/new-software-for-faster-and-better-3d-geological-modelling.pdf [Accessed 20 January 2019].

Isaaks, E. H. & Srivastava, R. M., 1989. In: *An Introduction to Applied Geostatistics.* Oxford: Oxford University Press, pp. 107, 238, 401, 405, 525.

Larrondo, P. & Deutsch, C. V., 2005. An Update on Kriging Near Boundaries. *Centre for Computational Geostatistics Report 7*, pp. 304-1 - 304-3.

Leuangthong, O., McLennan, J. A. & Deutsch, C. V., 2004. Minimum Acceptance Criteria for Geostatistical Realizations. *Natural Resources Research,* Volume 13, no. 3, pp. 131-141.

Minnitt, R. C. A. & Deutsch, C. V., 2014. Cokriging for optimal mineral resource estimates in mining operations. *The Journal of The Southern African Institute of Mining and Metallurgy,* Volume 114, March 2014, pp. 189-203.

Nowak, M. & Leuangthong, O., 2016. *SRK Consulting.* [Online] Available at: https://www.srk.com/en/publications/conditional-bias-in-kriging-lets-keep-it [Accessed 05 December 2021].

Potgieter, J. E., 2016. *Gamsberg East Competent Person's Statement Mineral Resources,* Aggeneys: Internal Report, Black Mountain Mining.

Reid, S. & Harley, M., 2009. *Gamsberg East Preliminary Mineral Resource Assessment, Aggeneys, Northern Cape, South Africa,* Johannesburg: Internal Report, Anglo American MinRED.

Rivoirard, J., 1987. Two key parameters when choosing the kriging neighborhood. *Mathematical Geology,* Volume 19, no. 8, p. 851–856.

Rossi, M. E. & Deutsch, C. V., 2014. In: *Mineral Resource Estimation.* Dordrecht: Springer Science and Business Media, pp. 31, 38, 41, 52, 97-108, 133, 134, 135, 139, 143, 145, 147 - 148, 195 - 198.

SAMREC, 2016. *The South African Code for the Reporting of Exploration results, Mineral Resources and Mineral Reserves. 2016 Edition.* [Online] Available at: https:/www.samcode.co.za
[Accessed 1 February 2022].

SAS Institute Inc., 2016. *JMP® 13 Predictive and Specialized Modeling..* Cary: SAS Institute Inc.

Seequent Ltd, n.d. *Leapfrog Geo 4.0 Help, Contact surfaces. Seequent Ltd..* [Online] Available at: https://help.seequent.com/Geo/4.0/en-GB/Content/geo-models/veins.htm#pinch-out
[Accessed 18 July 2021].

Seequent, n.d. *Leafrog Geo Wolf Pass Geological Modelling - Creating a Refined GM.*[Online] Available at: https://my.seequent.com/learning/3507/3526/3539
[Accessed 30 October 2021].

Sichel, H., Dohm, C. & Kleingeld, W., 1995. New generalized model of observed ore value distributions. *Transactions of the Institution of Mining and Metallurgy,* 104(2), pp. 116-123.

Sinclair, A. J., 1998. Exploratory Data Analysis : A Precursor to Resource/Reserve Estimation. *Exploration and Mining Geology,* Volume 7, nos. 1 and 2, pp. 77-90.

Stoch, B. et al., 2018. 3D implicit modeling of the Sishen Mine: new resolution of the geometry. *Mineralium Deposita,* pp. 835-853.

Vann, J., Jackson, S. & Bertoli, O., 2003. *Quantitative Kriging Neighbourhood Analysis for the Mining Geologist - A Description of the Method With Worked Case Examples..* Bendigo, Victoria, s.n., pp. 215-223.

Vedanta Zinc International, 2018. *Vedanta Zinc International : Operations and Projects.*[Online] Available at: https://www.vedanta-zincinternational.com/our-operations/gamsberg
[Accessed 28 October 2018].

Wackernagel, H., 2003. Ordinary Kriging. In: *Multivariate Geostatistics : An Introduction with Applications.* Berlin, Heidelberg: Springer, pp. 79-88.

APPENDIX A: INDICATOR VARIOGRAMS FOR MPO AND PEO

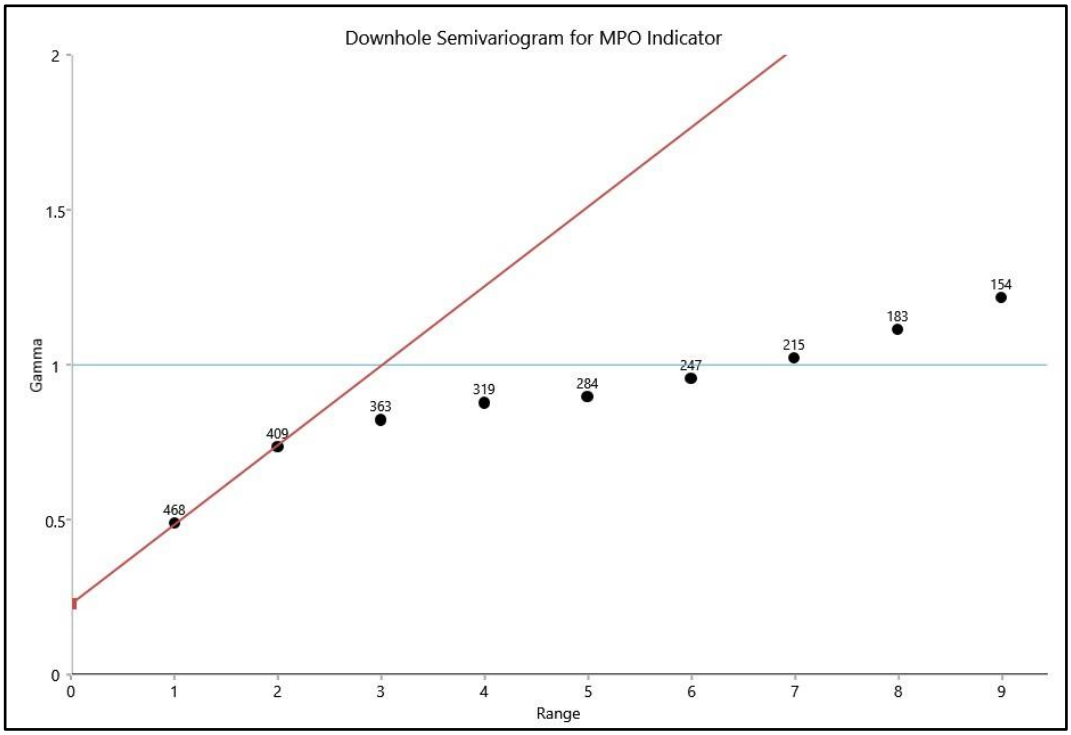


Figure A.1 Downhole semivariogram for MPO Indicator.

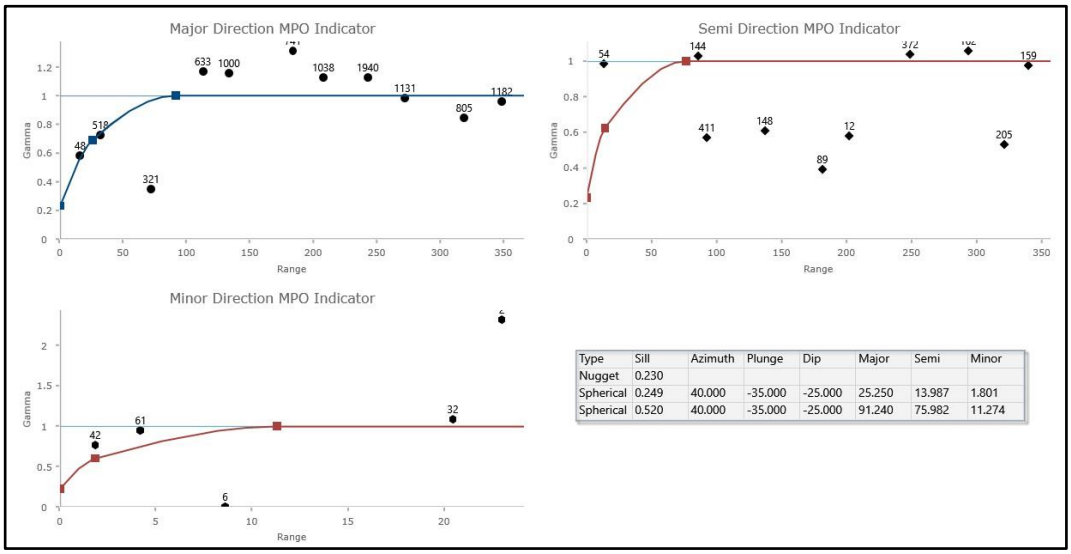


Figure A.2 Orthogonal variogram for MPO Indicator.

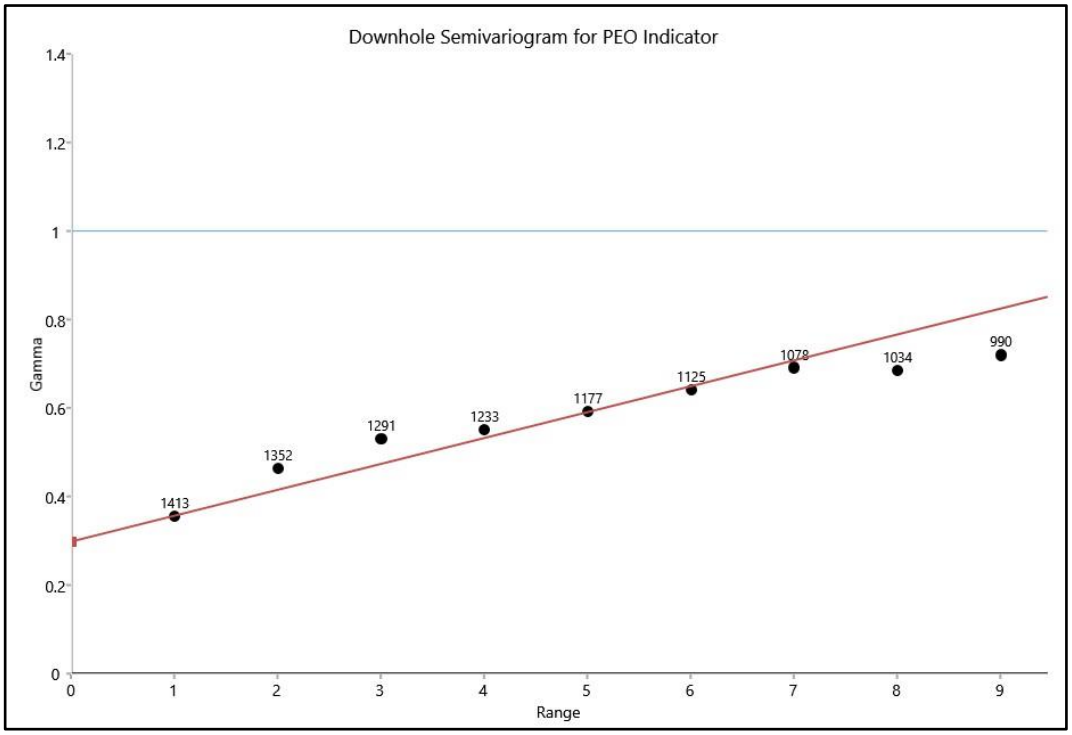


Figure A.3 Downhole semivariogram for PEO Indicator.

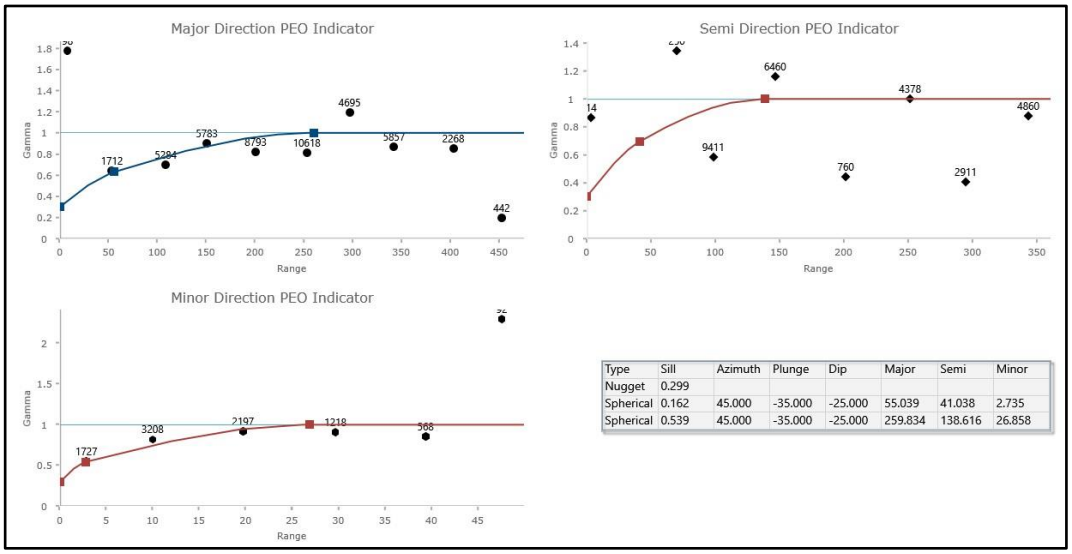


Figure A.4 Orthogonal variogram for PEO Indicator.

APPENDIX B: VARIOGRAMS FOR CORE AND FRINGE ZONE

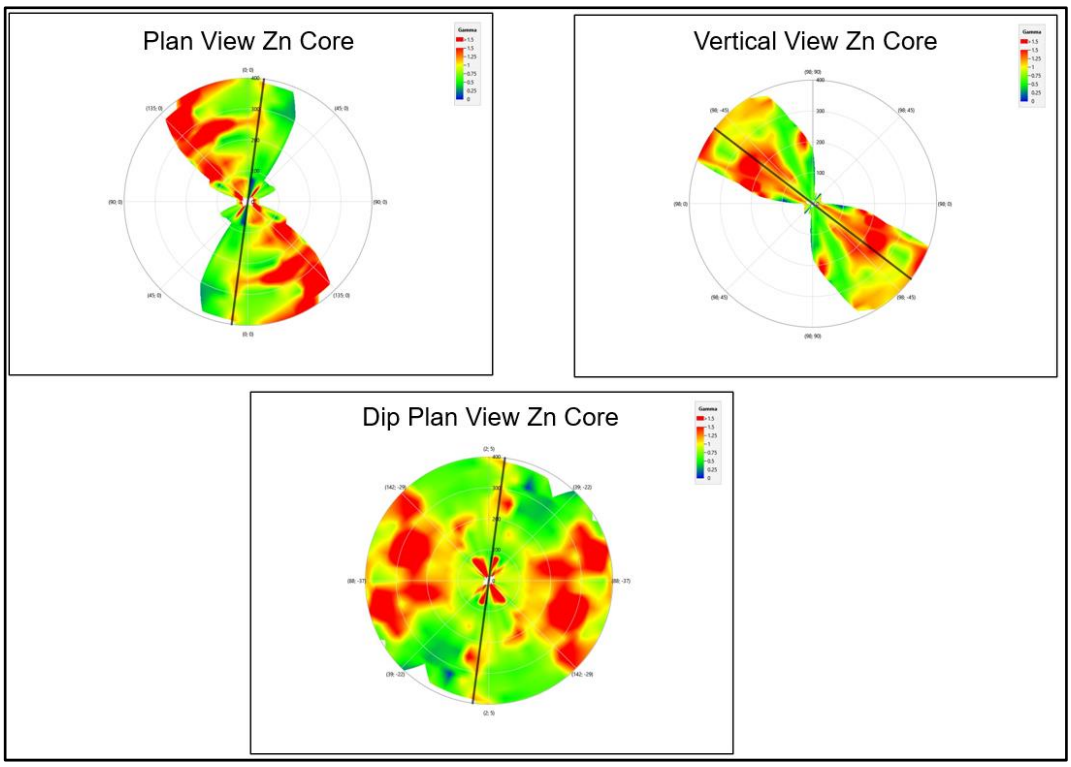


Figure B.1 Variogram maps for Zn in core zone.

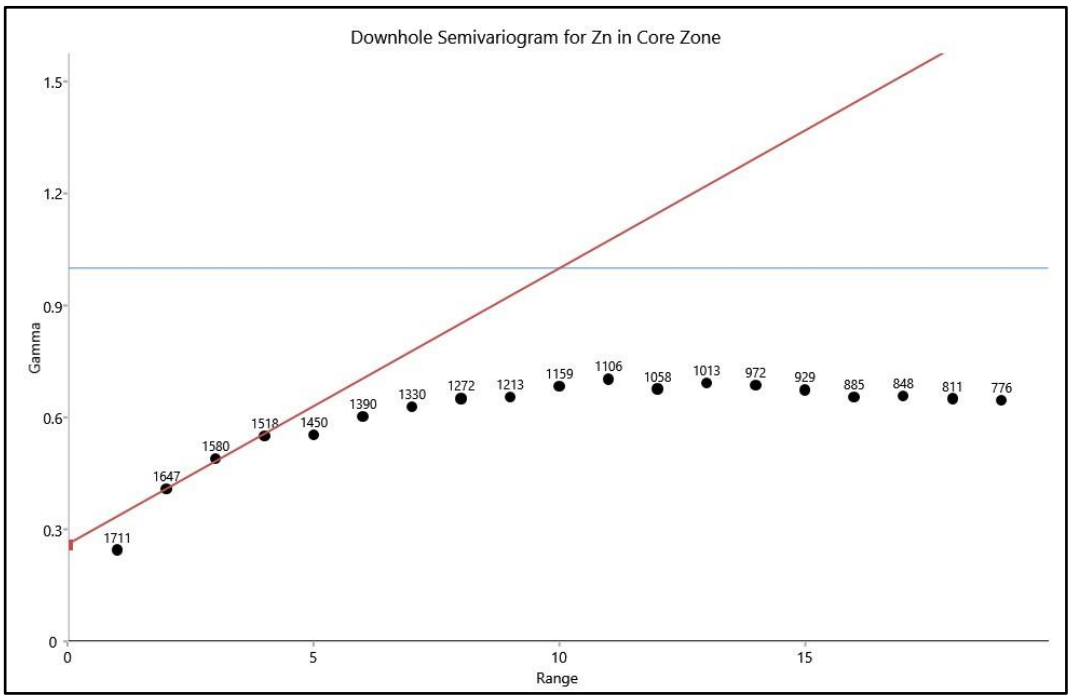
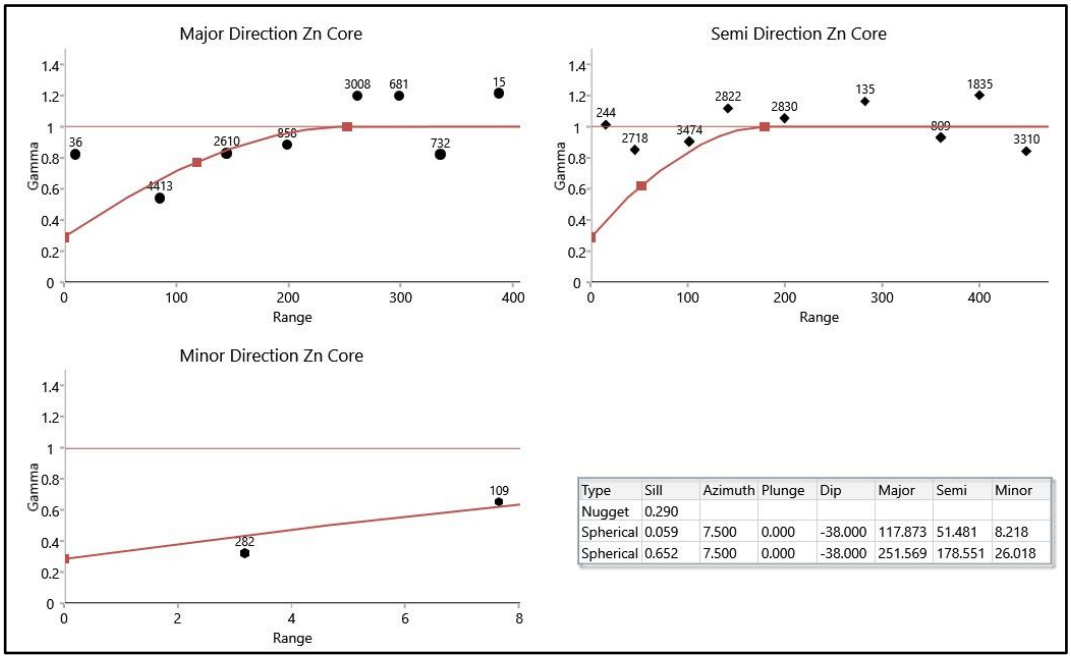


Figure B.2 Downhole semivariogram for Zn in core zone.



Type	Sill	Azimuth	Plunge	Dip	Major	Semi	Minor
Nugget	0.290						
Spherical	0.059	7.500	0.000	-38.000	117.873	51.481	8.218
Spherical	0.652	7.500	0.000	-38.000	251.569	178.551	26.018

Figure B.3 Orthogonal semivariogram for Zn in core zone.

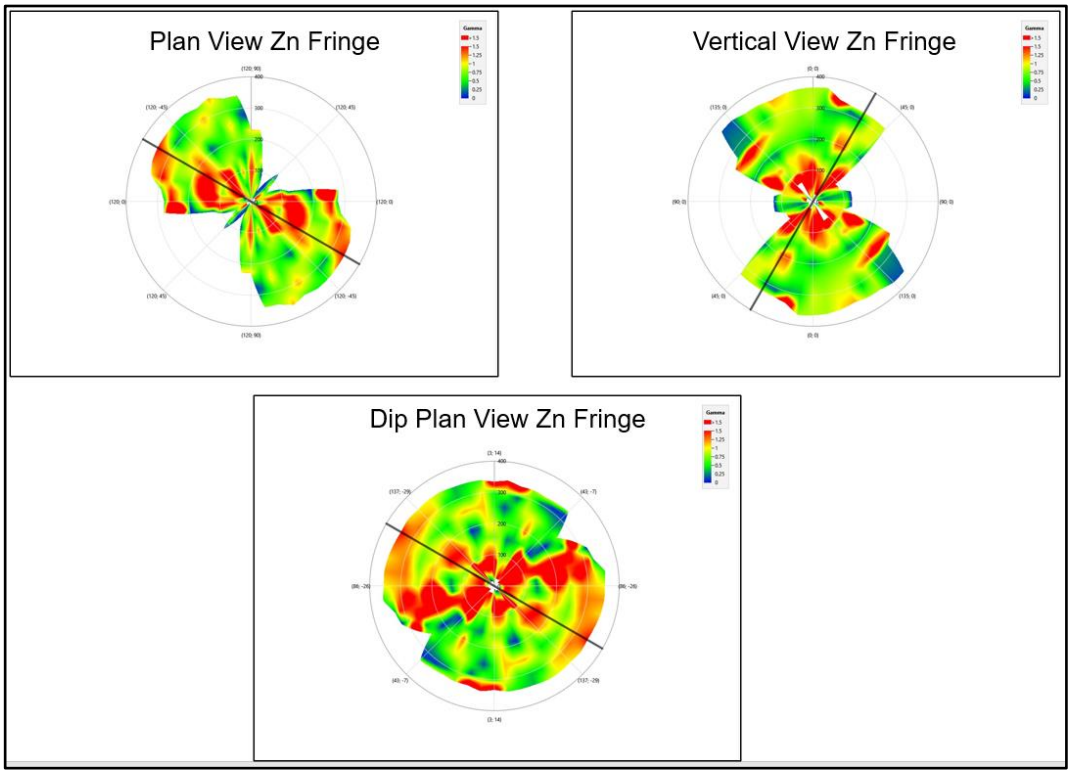


Figure B.4 Variogram map for Zn in fringe zone.

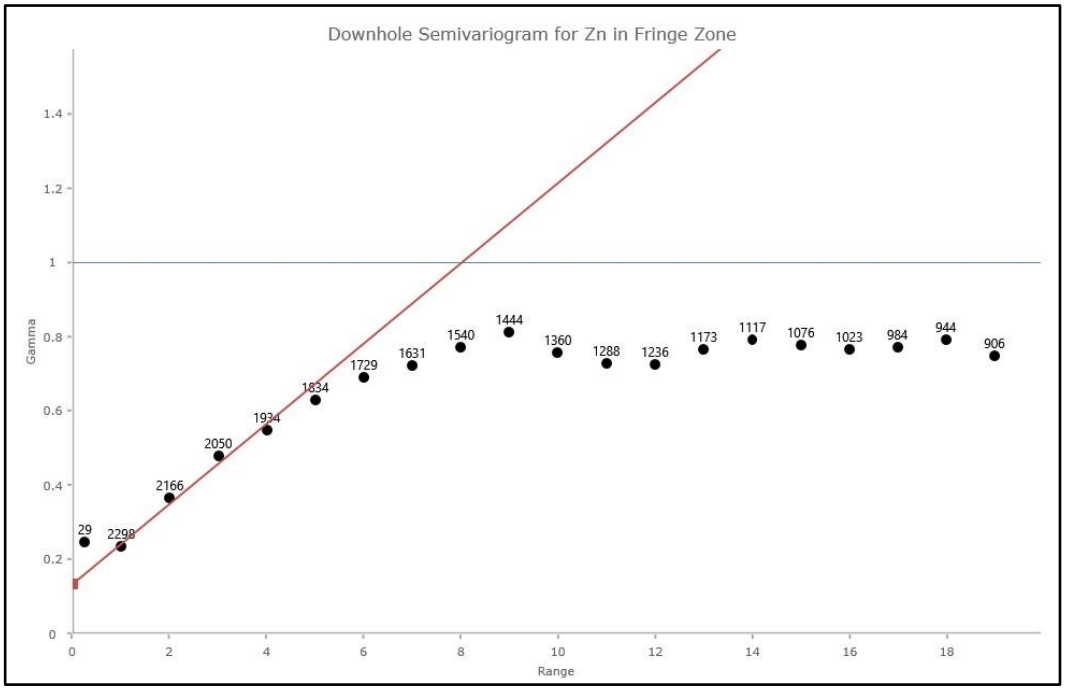


Figure B.5 Downhole semivariogram for Zn in fringe zone.

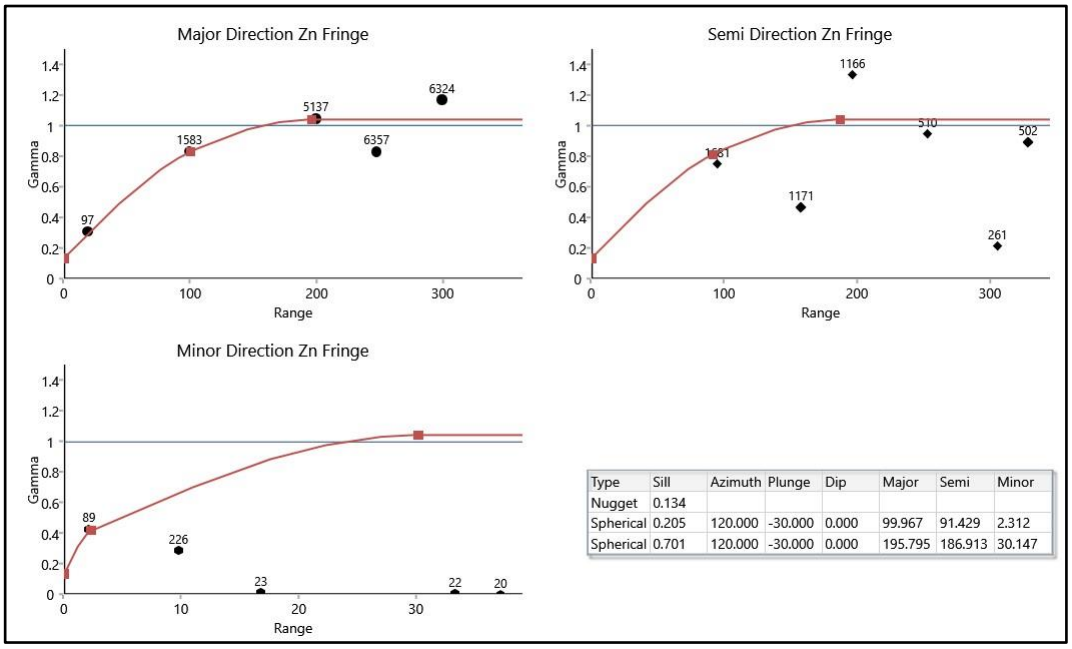


Figure B.6 Orthogonal semivariogram for Zn in fringe zone.

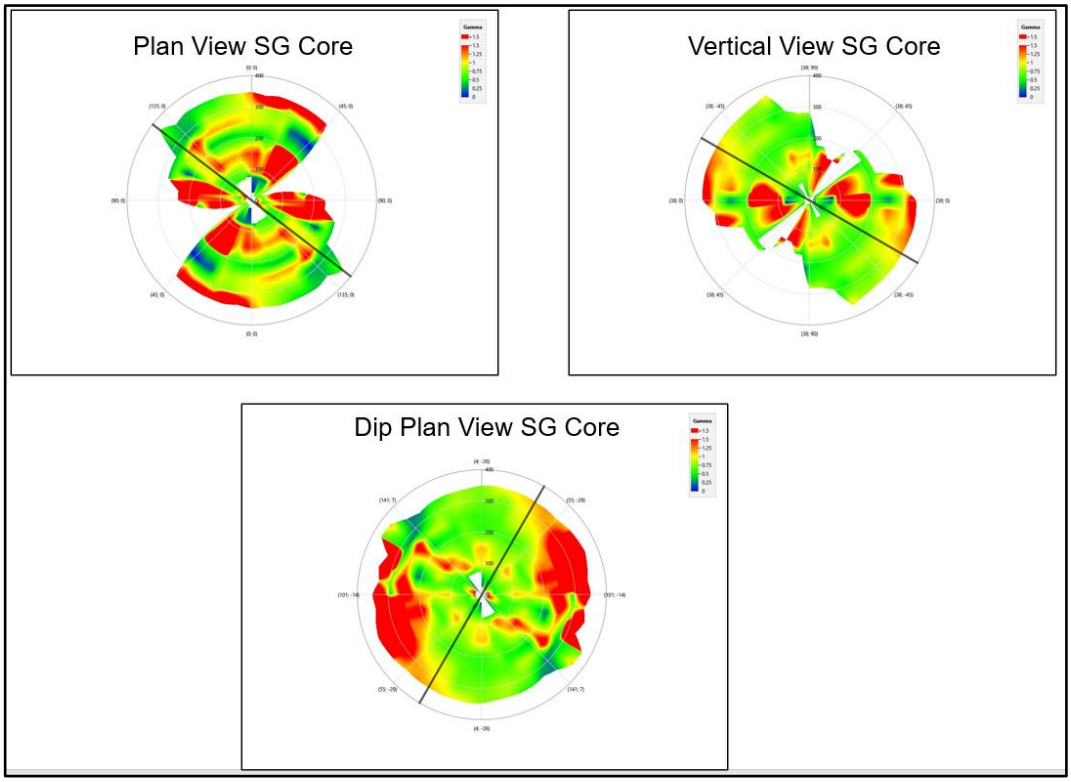


Figure B.7 Variogram maps for SG in core zone.

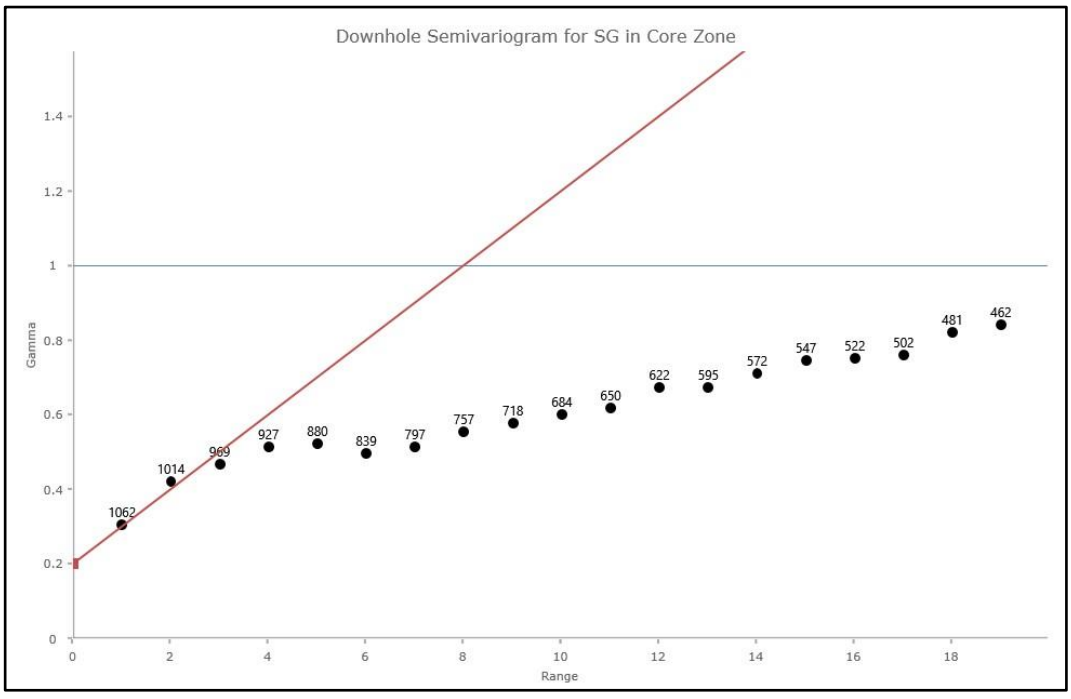


Figure B.8 Downhole semivariogram for SG in core zone.

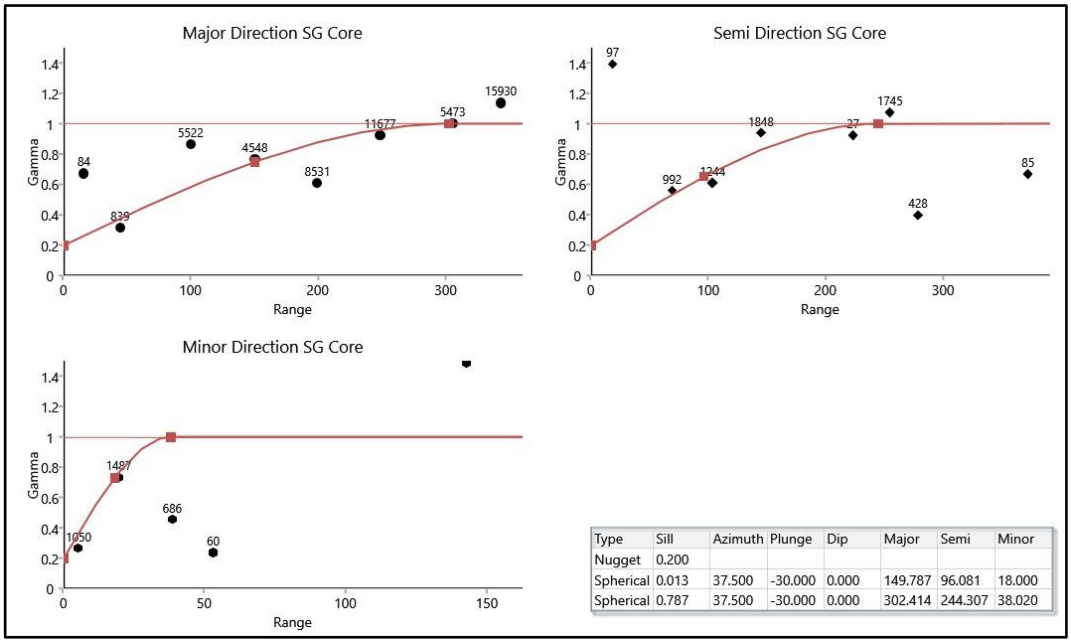


Figure B.9 Orthogonal semivariogram for SG in core zone.

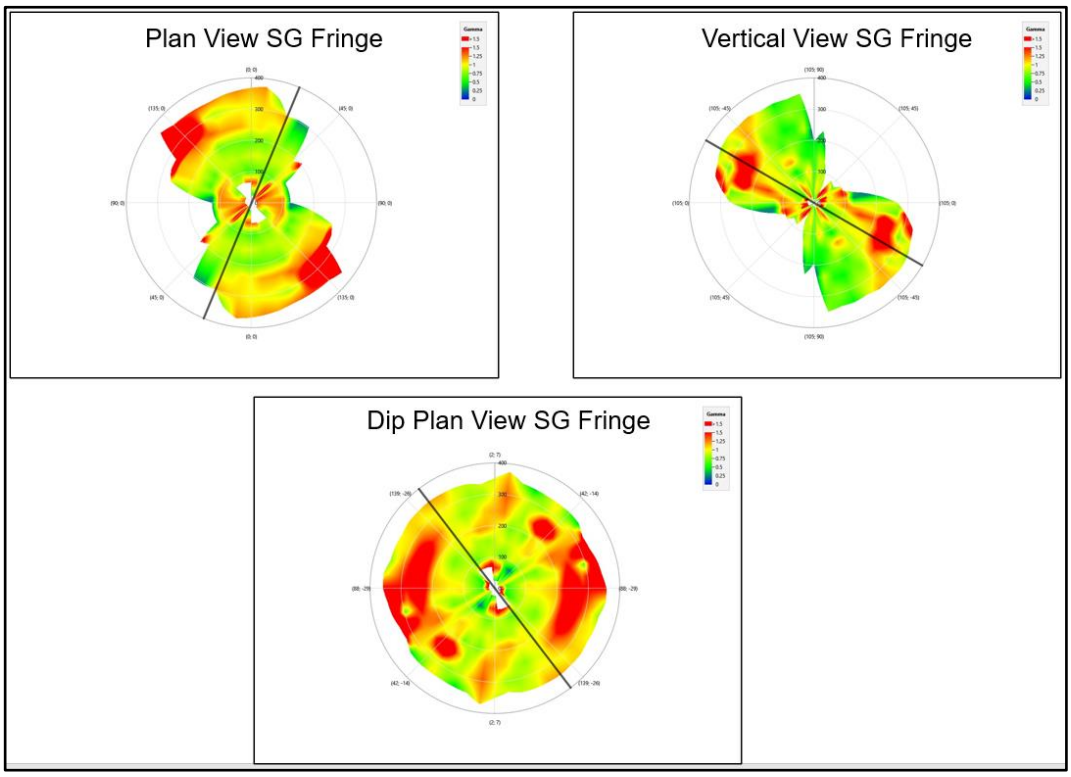


Figure B.10 Variogram maps for SG in fringe zone.

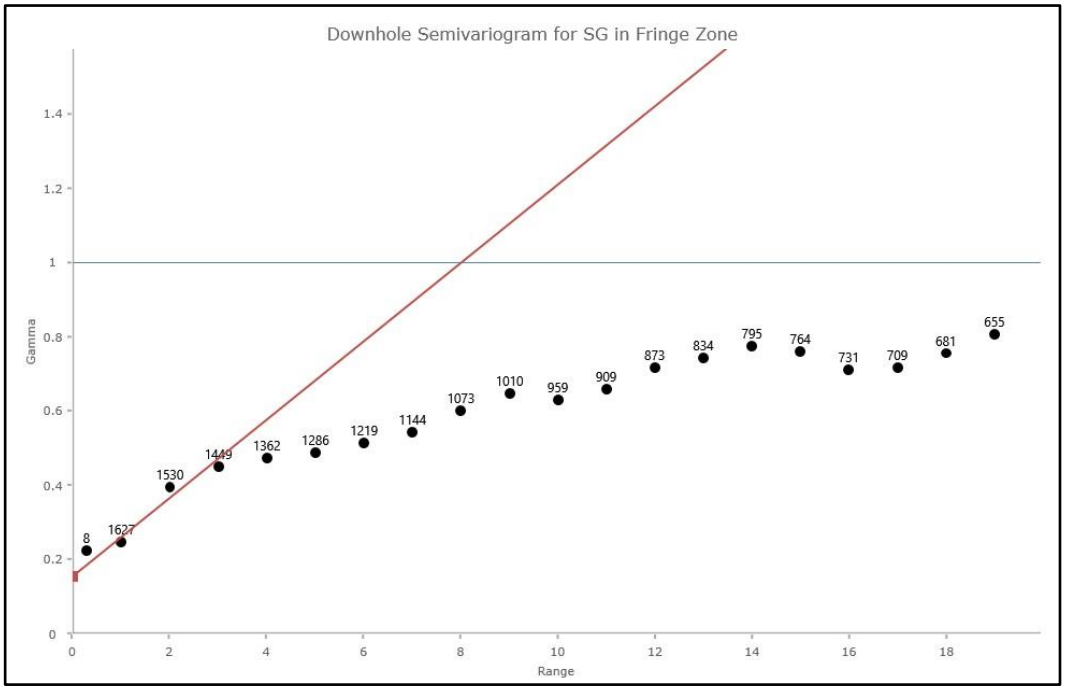


Figure B.11 Downhole semivariogram for SG in fringe zone.

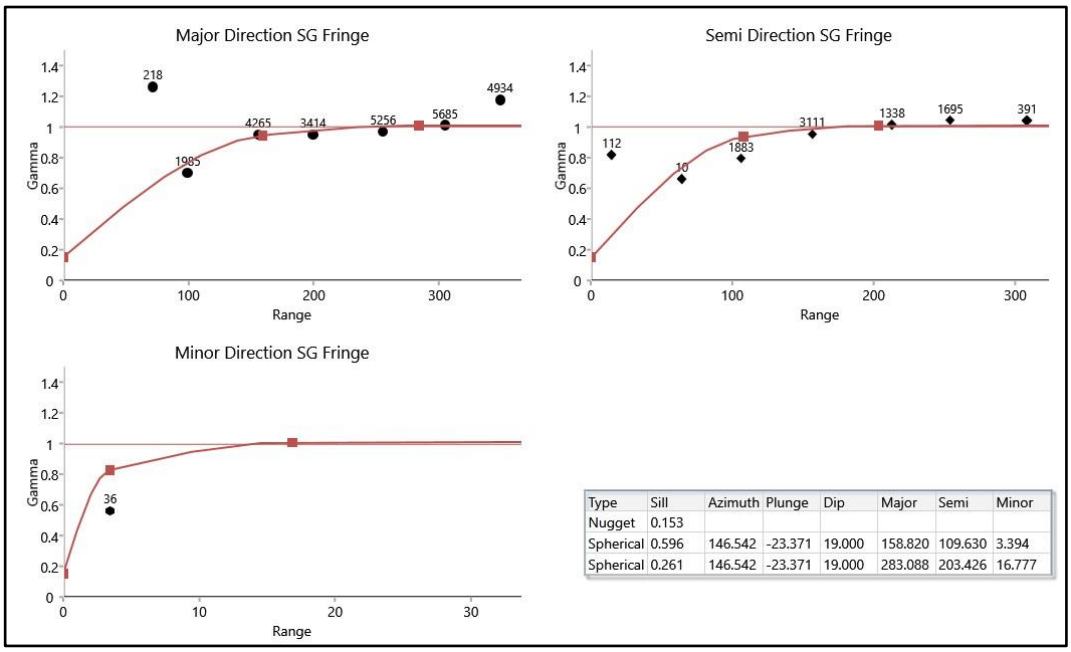


Figure B.12 Orthogonal semivariogram for SG in fringe zone.

APPENDIX C: ESTIMATION PARAMETERS FOR CORE AND FRINGE ZONE

Table C

Estimation ID	**Fringe Zn Pass 1**	**Fringe Zn Pass 2**	**Fringe Zn Pass 3**	**Core Zn Pass 1**	**Core Zn Pass 2**	**Core Zn Pass 3**
Estimation Type	ORDINARY KRIGING	ORDINARY KRIGING	ORDINARY KRIGING	ORDINARY KRIGING	ORDINARY KRIGING	ORDINARY KRIGING
Discretisation x	5	5	5	5	5	5
Discretisation y	5	5	5	5	5	5
Discretisation z	1	1	1	1	1	1
Standard Bearing	42	42	42	7.5	7.5	7.5
Standard Plunge	-34	-34	-34	0	0	0
Standard Dip	-23	-23	-23	-38	-38	-38
Major Axis	200	300	500	250	400	500
Semi Major Axis	180	270	400	180	300	600
Minor Axis	30	45	60	30	40	60
Min Samples	10	8	4	10	8	4
Max samples	25	25	25	25	25	25
Distance restriction on	ZN_PERC	ZN_PERC	ZN_PERC			
Threshold value	13.513	13.513	13.513	0	0	0
Major Axis Radius	100	100	100	50	50	50
Semi Major Axis Radius	100	100	100	50	50	50
Minor Axis radius	4	4	4	50	50	50
Soft Boundary	Yes	Yes	Yes			

APPENDIX D: SWATH PLOTS

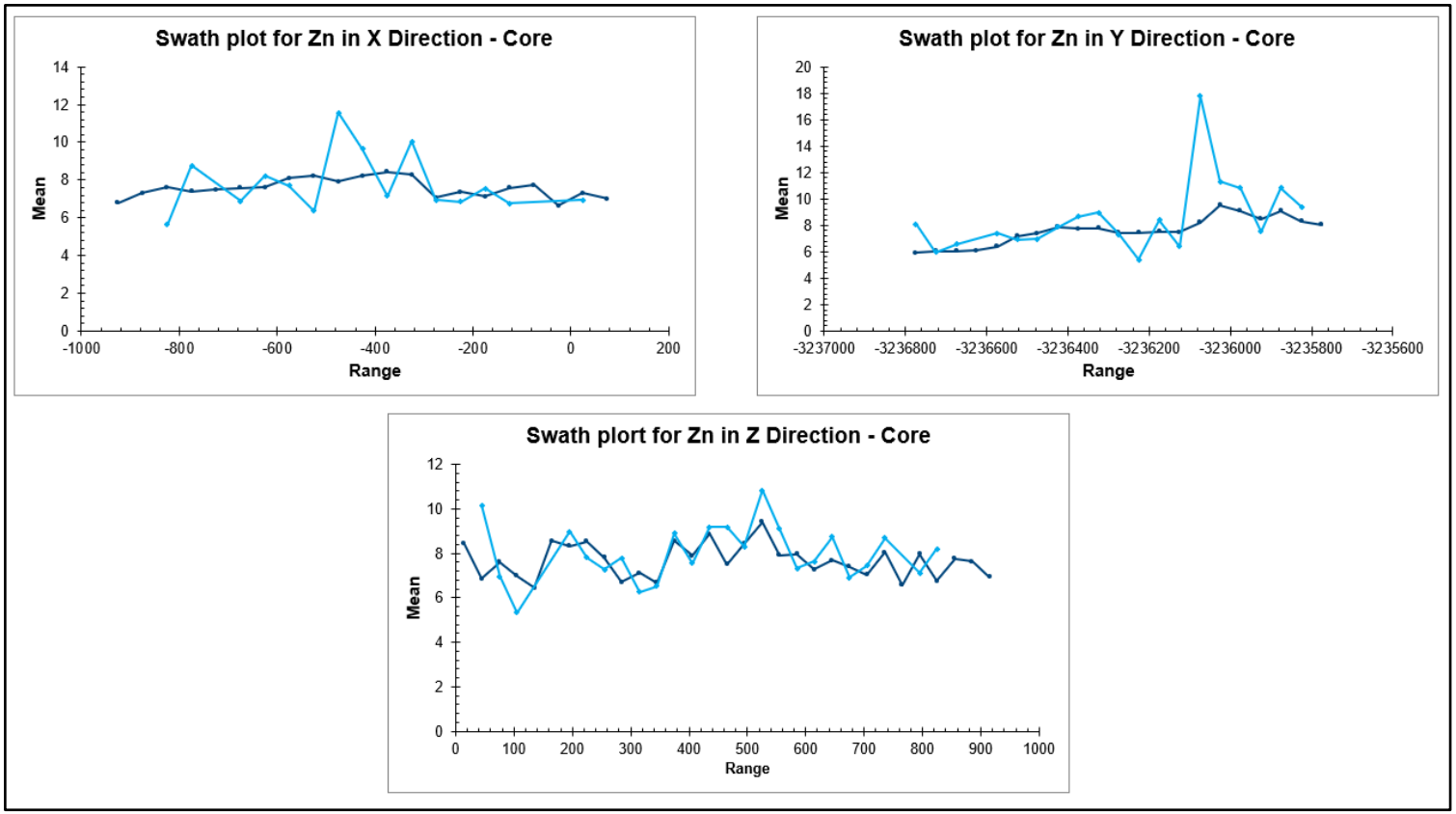


Figure D.1 Swath plots for Zn estimated grade in blocks (dark blue) and Zn grade in composites (light blue) for core zone. Step size is 50m in X, 50m in Y and 20m in Z directions.

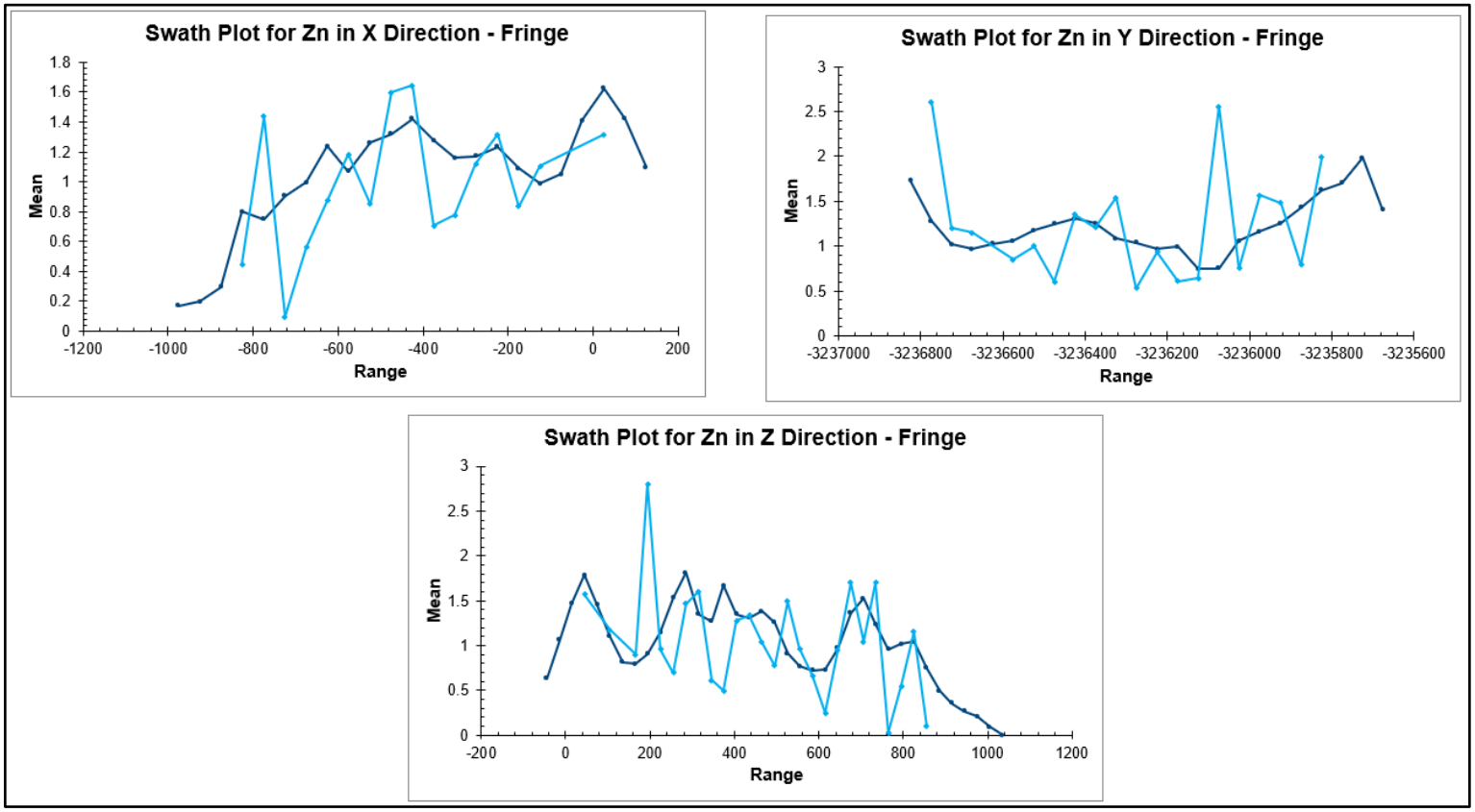


Figure D.2 Swath plots for Zn estimated grade in blocks (dark blue) and Zn grade in composites (light blue) for fringe zone. Step size is 50m in X, 50m in Y and 20m in Z directions.

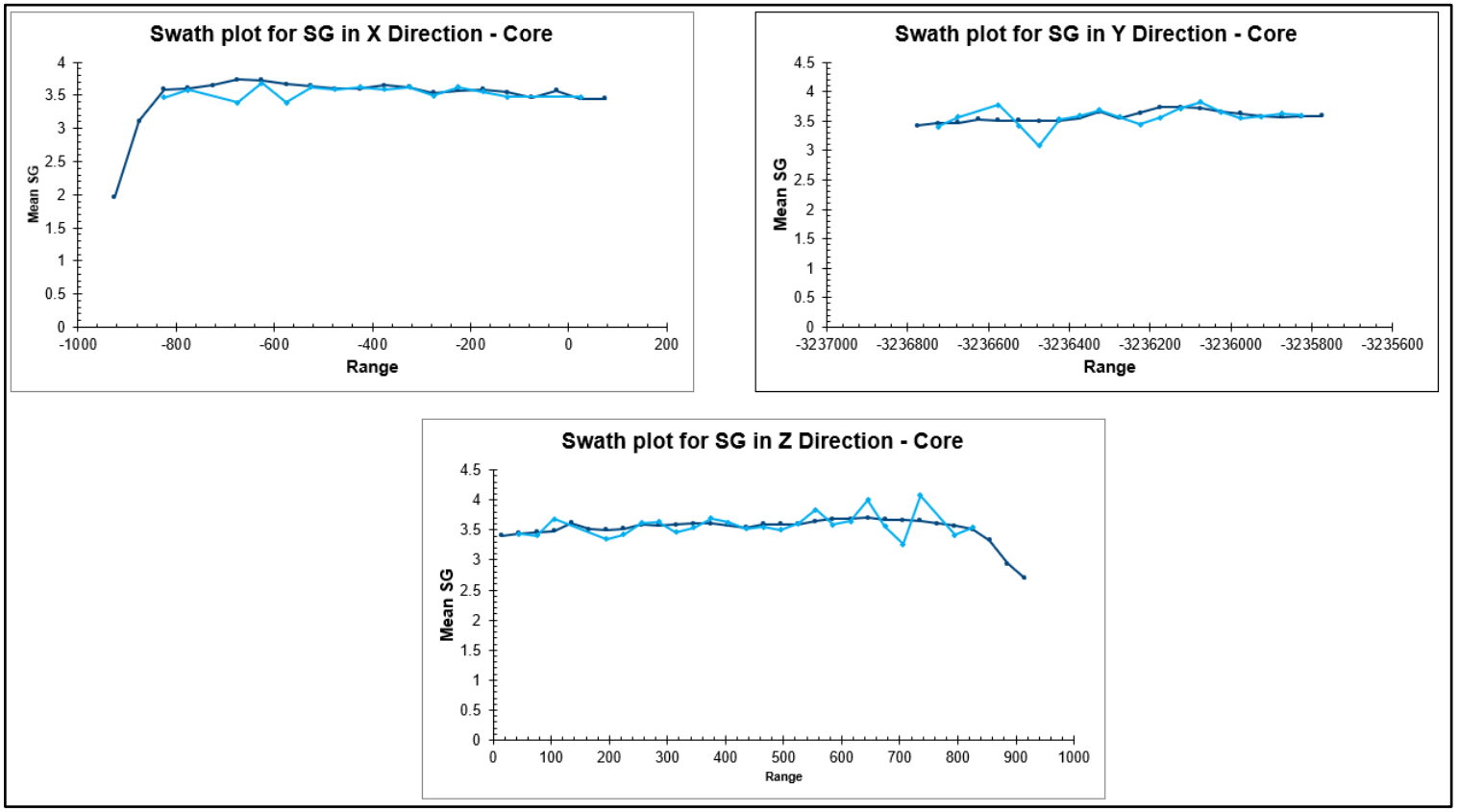


Figure D.3 Swath plots for SG estimated value in blocks (dark blue) and SG value in composites (light blue) for core zone. Step size is 50m in X, 50m in Y and 20m in Z directions.

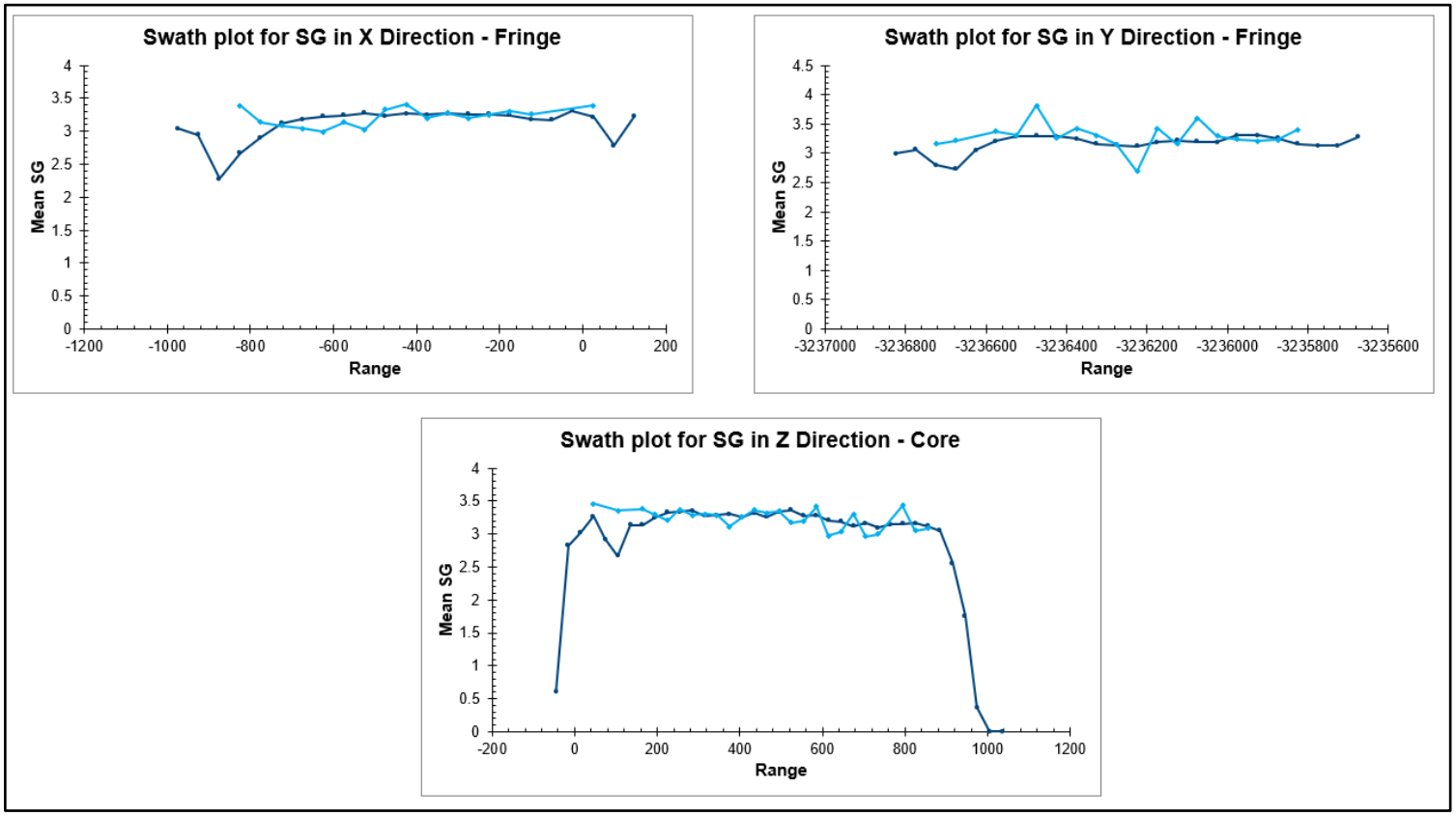


Figure D.4 Swath plots for SG estimated value in blocks (dark blue) and SG value in composites (light blue) for fringe zone. Step size is 50m in X, 50m in Y and 20m in Z directions.